

Statistical Size Effect in Steel Structure and Corresponding Influence on Structural Reliability

Von der Fakultät für Architektur, Bauingenieurwesen und Stadtplanung
der Brandenburgischen Technischen Universität Cottbus-Senftenberg
zur Erlangung des akademischen Grades eines
Doktor-Ingenieurs
genehmigte Dissertation

vorgelegt von

M. Eng. Zheng Li
aus Anhui, China

Gutachter: Prof. Dr.-Ing. habil. Hartmut Pasternak
Gutachter: Prof. Civ. Eng. Doncho Partov, PhD
Gutachter: Prof. Gang Shi, PhD

Tag der Disputation: 17.07.2018

Acknowledgement

The present thesis was created in the years 2014 - 2018 during my activity as a Ph.D. student at Chair of Steel and Timber Structures of the Brandenburg University of Technology.

I would like to express my sincerest gratitude to my supervisor Professor Dr.-Ing. habil. H. Pasternak for the support and professional advice. His wide knowledge has provided a good basis for the present thesis and his guidance, understanding, and encouraging helped me overcome all circumstances that I confronted during the past years.

I thank Prof. Dr.-Eng. Doncho Partov and Prof. Ph.D. Gang Shi for the interest in this work and the acceptance of the further assessment.

I am very grateful to my colleagues in the Chair of Steel and Timber Structures for all kinds of support and help.

Finally, I would also like to thank my wife and family for their extraordinary support during the preparation of this work.

Cottbus, 01.08.2018

Zheng Li

Abstract (EN)

This thesis aim to investigate the statistical size effect in the elasto-plastic material and the corresponding reliability of steel structures. The core idea is that the stochastic material properties are directly embedded in mechanical calculations to develop a more accurate and economical design method for steel structure. Moreover, the results of the experimental investigation with different specimen sizes, whose diameter is limit up to 32 mm, show that the statistical size effect exists in steel structures. This thesis demonstrates finally that the structural reliability is affected by the statistical size effect and the structural safety can be optimized by considering this effect.

Because of the uncertainty and non-uniformity of the microscopic imperfection distribution, the material strength in macroscale presents complex randomness. This study described the randomness of material properties through two different ways: developing a stochastic material model for elasto-plastic material and establishing a discrete random field with a general mathematical program. The proposed stochastic material model is extended to analyze the steel structure with multi-axial stress and is integrated into the commercial FEM software for analysis of the complex structures with stress gradient. The stochastic Finite Element Method is implemented to analyze the response of the 3D structures by a general-purpose FEM program when the random field file is imported into the finite element model.

The uniaxial tensile tests with different specimen sizes and different material are carried out to demonstrate the statistical size effect in steel structures. The results show that the variations of the yield and tensile strength increase with the decreasing specimen volume. Moreover, according to the bending tests, it is obvious that the structural component strength is not only related to the specimen volume, but also the stress distribution. These two proposed simulation methods, which are an extension and supplement to traditional simulation methods, can effectively simulate the statistical size effect for the tensile and flexural components in steel structures.

Finally, it is found by studying the influence of statistical size effect on structural reliability that the strength, which is obtained by small specimens through statistical analysis in the laboratory, is no more accurately applicable to large construction. The reliability theory for the structural safety which exists over the decades can be compared and validated or improved through the embedding the stochastic material properties in the numerical simulation.

Kurzfassung (DE)

Das Ziel dieser Arbeit ist es, den Einfluss des statistischen Maßstabeffekts auf die elasto-plastischen Werkstoffeigenschaften und die entsprechende Zuverlässigkeit im Stahlbau zu quantifizieren. Die stochastischen Materialeigenschaften werden direkt in die numerischen Berechnungen implementiert, um eine präzisere und wirtschaftlichere Methodik für die Bemessung von Stahlkonstruktionen zu entwickeln.

Darüber hinaus zeigen die Ergebnisse experimenteller Untersuchungen mit verschiedenen Probengrößen (max. Durchmesser bis zu 32 mm), dass der statistische Maßstabeffekt in Stählen existiert. Mittels numerischer Simulationen wird gezeigt, dass die Zuverlässigkeit der Bauteile durch den statistischen Maßstabeffekt beeinflusst wird und dass die strukturelle Sicherheit unter Berücksichtigung dieses Effekts optimiert werden kann.

Aufgrund der vorhandenen mikroskopischen Imperfektionen und der Unsicherheiten über deren Verteilung zeigen die mechanischen Eigenschaften des Werkstoffs Zufälligkeiten. Diese Arbeit beschreibt die Zufälligkeit des Werkstoffs auf zwei verschiedene Wege: die Erste ist die Entwicklung eines stochastischen Materialmodells mit elasto-plastischen Materialeigenschaften. Die zweite Möglichkeit ist der Aufbau eines diskreten Zufallfeldes mit einem allgemeinen mathematischen Programm. Das vorgeschlagene stochastische Materialmodell wird erweitert, um die Stahlkonstruktion unter multiaxialer Beanspruchung zu analysieren. Es wird in die kommerzielle FEM-Software integriert, um komplexe Bauwerke mit Spannungsgradienten zu analysieren. Die stochastische Finite-Elemente-Methode wird implementiert, um die Antworten der 3D-Konstruktion durch ein allgemeines FEM-Programm zu analysieren, nachdem die Zufallfelddatei in das Finite-Elemente-Modell importiert wurde.

Um den statistischen Maßstabeffekt im Stahlbau zu demonstrieren, werden uniaxialen Zugversuche mit unterschiedlichen Probengrößen und verschiedenen Werkstoffen durchgeführt. Die Ergebnisse zeigen, dass sich die Streuungen der Streckgrenze und die Zugfestigkeit mit zunehmenden Probenvolumen abnehmen. Darüber hinaus hängt die Festigkeit des Bauteils nicht nur vom Probenvolumen gemäß den Biegetests, sondern auch von der Spannungsverteilung ab. Sowohl die analytische Methode als auch die vorgeschlagene Simulationsmethode, die eine Erweiterung und Ergänzung zu traditionellen Simulationsverfahren sind, können den statistischen Maßstabeffekt für die Zug- und Biegekomponenten in Stahlkonstruktionen erfassen. Die Untersuchungen des Einflusses des statistischen Maßstabeffektes auf die strukturelle Zuverlässigkeit ergaben, dass die Festigkeiten, die an kleinen Proben durch statistische Analysen im Labor ermittelt werden, für größere Bauteile nicht mehr exakt zutreffen sind. Daher kann

die Zuverlässigkeitstheorie für die strukturelle Sicherheit mit der Simulation verglichen und validiert oder verbessert werden, indem die stochastischen Materialeigenschaften in das Simulationsmodell eingebettet werden.

Contents

Abstract (EN)	I
Kurzfassung (DE).....	II
Contents.....	IV
List of Figures	VII
List of Tables.....	XI
Nomenclature	XII
Formula symbols	XII
Abbreviations	XV
1 Introduction	1
1.1 Motivation	1
1.2 State of research.....	3
1.2.1 Statistical size effect.....	3
1.2.2 Uncertainty and modeling with random fields.....	5
1.2.3 Development and application of stochastic FEM	6
1.2.4 Reliability theory in civil engineering.....	8
1.3 Thesis structure.....	9
2 Analytical model for the statistical size effect	12
2.1 Overview	12
2.2 Stochastic material model.....	12
2.2.1 Weakest link model.....	12
2.2.2 Fiber bundle model.....	14
2.2.3 Real material properties	15
2.2.4 Chain of bundle model	18
2.2.5 Parameter study of the stochastic material model	22
2.3 Generalization of the chain of bundles model	25

2.3.1	Stress gradient and multi-axial stress state.....	25
2.3.2	Numerical methods to solve the statistical size effect coefficient	26
2.4	Conclusions	29
3	Uncertainty modeling and implementation of stochastic FEM.....	30
3.1	Introduction	30
3.2	Uncertainty modeling	31
3.2.1	Probability space and random variables.....	31
3.2.2	Random field in Hilbert spaces	32
3.2.3	Karhunen-Loève series expansion	34
3.2.4	Numerical solution of the K-L expansion.....	37
3.2.5	Simulation of pseudo random variables with Latin Hypercube sampling	41
3.2.6	Discretization error estimator and optimization.....	42
3.3	Connection between random field and finite element.....	46
3.4	The stochastic finite element method with Monte Carlo simulation.....	51
3.4.1	Formulation of the stochastic finite element matrix.....	52
3.4.2	Direct Monte Carlo simulation for stochastic FEM.....	54
3.4.3	Sample size for Monte Carlo simulation.....	55
3.5	Element types for stochastic FEM.....	56
3.6	Conclusions	58
4	Experimental and simulated investigation of tensile and flexural members.....	60
4.1	Introduction	60
4.2	Experimental investigation	60
4.2.1	Tensile testing with constant stress distribution.....	60
4.2.2	Bending tests with stress gradient	65
4.3	Simulation with stochastic material model.....	67
4.3.1	Models building.....	67
4.3.2	Material description of stochastic material model	68

4.3.3	Investigation of material parameters	70
4.3.4	Simulation of flexural members	72
4.4	Simulation by stochastic FEM.....	74
4.4.1	Random field of elasto-plastic material	74
4.4.2	Numerical simulation of tensile members.....	77
4.4.3	Numerical simulation of flexural members.....	81
4.5	Comparison of experiments and simulations results	83
4.6	Conclusions	86
5	Reliability assessment under considering material uncertainty	88
5.1	Introduction	88
5.2	Maximum Entropy fitting method.....	89
5.2.1	Information and Entropy	89
5.2.2	Maximum Entropy principle and maximum Entropy fitting method	90
5.3	Structural reliability analysis	94
5.3.1	Limit state of structure	94
5.3.2	Structural reliability and reliability index	95
5.3.3	Calculation of structural reliability	96
5.4	Structural reliability with statistical size effect	99
5.5	Probabilistic modeling of the ultimate bearing capacity of flexural members.....	101
5.5.1	Evolution of strength probability density function	103
5.6	Influence of statistical size effect on the structural safety.....	105
5.7	Conclusions	108
6	Overall conclusions	110
7	Recommendations for future works	113
	References	115

List of Figures

Figure 1.1: a) Relation between yield stress and material thickness, b) the probability distribution of the strength of the steel graded according to the thickness, from [8]..... 3

Figure 2.1: a) Weakest link model, b) Influence of the volume on the strength..... 13

Figure 2.2: Fiber bundle model..... 14

Figure 2.3: Post-peak behavior of material properties, a) ideal plastic, b) softening, c) brittle15

Figure 2.4: Upper and lower yield point of steel S235 16

Figure 2.5: Illustration of material under the stress 17

Figure 2.6: a) Chain of bundle model, b) bundle of chain model 17

Figure 2.7: Probability distributions with various volumes 18

Figure 2.8: Probability density function of the chain of bundle model with various volumes 19

Figure 2.9: Relationship of the proposed distribution and classical distribution, a) PDF, b) CDF 20

Figure 2.10: Numerical simulation of analytical model..... 21

Figure 2.11: Distribution of chain of bundle model with different volumes 22

Figure 2.12: Numerical approximation of the mean values of strength distribution 24

Figure 2.13: Relationship between coefficient of variation ω and variables V/V_{RVE} under different ξ values 24

Figure 2.14: Flowchart of UMAT-Subroutine 28

Figure 3.1: Comparison of different correlation functions $L_c = 20 \text{ mm}$ 36

Figure 3.2: Illustration of 2D random field aggregated by 1D random field..... 40

Figure 3.3: Random field, a) Two-dimensional, b) Three-dimensional..... 40

Figure 3.4: Gaussian random field samples generated by different methods, a) directly MCS, b) MCS with LHS..... 41

Figure 3.5: Point-wise estimator for variance error represented for different RF, a) 2D random field, b) 3D random field..... 43

Figure 3.6: Influence of RF mesh size and truncation order on global error of variance 44

Figure 3.7: Relationship of the discretization error and the truncated terms 46

Figure 3.8: Coordinate mapping representation of 3D 8-point FE mesh and 3D RF mesh..... 47

List of Figures

Figure 3.9: Flowchart of the mapping-interpolation method	48
Figure 3.10: a) 3D Gaussian RF, b) Random variables at integration points of I-section specimen, c) PDF of original RF, d) PDF of random variables at integration points	49
Figure 3.11: Different FE mesh and corresponding PDF of random variables at integration points, $LRF, b/LFE, b = 0.5$ in a) and c), $LRF, c/LFE, c = 4$ in b) and d)	50
Figure 3.12: Schematic of Monte Carlo simulation for SFEM with ABAQUS framework interfaced with MATLAB codes	55
Figure 3.13: Variation of stress response statistics with the number of samples	56
Figure 3.14: Illustration of mapping coordinates for beam a) and shell element b)	57
Figure 3.15: Random distributed yield strength for I-section beam	57
Figure 3.16: Response of plastic bearing capacity with different element types	58
Figure 4.1: Illustration of tensile specimens a) HEB 400; b) 40 mm thick plate	61
Figure 4.2: Extended geometry for big specimen a) the relationship between different specimen sizes, b) Specimen from 40 mm plate	61
Figure 4.3: a) Distribution of yield strength through flange with different specimen size, b) relationship between the coefficient of variation and specimen volume	62
Figure 4.4: Influence of the volume on the strength of specimens from HEB 400	63
Figure 4.5: a) The distribution of the strengths in the thickness direction, b) shape of the fracture surface	64
Figure 4.6: Relationship between the statistical results and the volume of the specimen, a) coefficient of variance, b) mean value	65
Figure 4.7: Illustration of flexural members for Waterjet cutting	65
Figure 4.8: a) 3-point bending tests, b) 4-point bending tests	66
Figure 4.9: Representation of the definition of the maximum elastic moment	67
Figure 4.10: Real and simulated tensile test specimen	68
Figure 4.11: Stress-strain curve, a) S235 from HEB400, b) S355 from 40 mm plate	69
Figure 4.12: Influence of two parameters on the yield strength	70
Figure 4.13: Monotonous relationship between yield stress and $VRVE$ -value	71
Figure 4.14: Experimental and numerical results of yield strength with various specimen volume, a) S235, b) S355	72
Figure 4.15: Illustration of the simulated 3-point a) and 4-point bending test b)	72

List of Figures

Figure 4.16: Influence of FE mesh on loads, a) 3-points bending simulation, b) 4-points bending simulation	73
Figure 4.17: Defined and true stress-strain curve in simulation and corresponding effective volume	74
Figure 4.18: Estimated assumptions of stochastic fluctuations of elasto-plastic material properties on stress-strain curve of steel	75
Figure 4.19: Random distributed Young's modulus, a) slices of RF, b) tensile specimen in RF	75
Figure 4.20: Random distributed yield strength, a) slices of RF, b) tensile specimen in RF...	76
Figure 4.21: Response of stress-strain curve, a) with RF of Young's modulus and yield strength, b) with RF of yield strength	77
Figure 4.22: PDF and CDF of the pre-defined random field and stochastic response of the yield stress	78
Figure 4.23: Relationships between the response of stress and volume of specimens	78
Figure 4.24: Coefficient of variation of random field and yield strength of specimen.....	79
Figure 4.25: Relationship between correlation length and reduction of yield stress with different specimen sizes	80
Figure 4.26: Comparison of experimental and simulated results with different correlation length	81
Figure 4.27: Random distributed yield strength in different specimens	82
Figure 4.28: Graphical representation of the equivalent yield stress	84
Figure 4.29: Moment-strain curves, a) 3-point test with small specimen, b) 4-point test with small specimen, c) 3-point tests with big specimen d) 4-point test with big specimen	85
Figure 5.1: Algorithm flowchart with Newton method for nonlinear equations	92
Figure 5.2: Theoretic distribution of the random variables and the maximum Entropy distribution under the first four moments constraints	92
Figure 5.3: Fitting lognormal distribution by MEFM with different statistical parameters	93
Figure 5.4: Flowchart of the proposed method for reliability assessment with structural response from SFEM.....	100
Figure 5.5: Distribution of yield stress in IPE-section beam, a) with 1 RF, b) with 3 divided RFs	102

List of Figures

Figure 5.6: a) ME PDFs with different sample sizes, b) K–S test results for different sample sizes	103
Figure 5.7: Evolution of strength probability density function for 3P and 4P flexural members, a) IPE100, b) IPE200, c) IPE300, d) IPE400, e) IPE500, f) IPE600	105
Figure 5.8: Reliability indices with increased sample sizes	106
Figure 5.9: Fluctuation of reliability indices considering statistical size effect.....	106
Figure 5.10: Influence of applied load distribution on the reliability analysis considering the statistical size effect, a) coefficient of variation of load distribution, b) distribution types of load	108

List of Tables

Table 3.1: Global error of discretization with various truncation order of K-L expansion 44

Table 3.2: Influence of FE size on the first fourth statistical moments 51

Table 4.1: Statistical results of tensile test from HEB 400 62

Table 4.2: Statistical results of tensile test from 40 mm thick plate 64

Table 4.3: Sketch and essential sizes for bending tests..... 66

Table 4.4: First four order statistical moments of structural response 82

Table 4.5: Comparison of maximum elastic moments from experiment and simulation 83

Table 5.1: Geometric parameters of the beams..... 101

Table 5.2: Computing time for discretization of different RFs and corresponding global error
..... 102

Nomenclature

Formula symbols

β	Reliability index
γ	Coefficient of statistic size effect
$\gamma(*)$	Skewness
ε	Tolerance
$\bar{\varepsilon}_{tar}(*)$	Target accuracy
$\varepsilon_{\sigma^2}(*)$	Global discretization error estimator of random field with respect to the variance
$\varepsilon_{Cov}(*)$	Global discretization error estimator of random field with respect to the covariance
θ	Primitive randomness
$k(*)$	Kurtosis
λ_i	i th eigenvalue
λ and μ	Lamé parameters
$\mu(*)$	Mean value
ν	Poisson's ratio
ξ	Material constant of stochastic material model
(ξ, η, ζ)	Local Cartesian coordinate system
ρ	Correlation coefficient
σ	Stress
σ_u	Lower limit of σ
σ_0	Scale parameter of σ
σ_v	Von Mises stress
σ_m	Tensile strength
σ_{eH}	Upper yield stress
σ_{eL}	Lower yield stress
σ^2	Standard deviation
τ	Shear stress
$\varphi_i(*)$	i th eigenfunction
Φ	Diameter of the tensile specimen
$\phi(*)$	Standard normal distribution function
$\phi_j(*)$	j th basic function of the eigenfunction
ω_i	i th weights of Gauss-Legendre integration

C	Constant
C_v	Coefficient of variation
$Cov(*)$	Covariance
d_{ij}	j th nodal value of the i th eigenfunction
$erf(*)$	Error function
$E(*)$	Expected value
E_t	Tangent modulus
$f_p(*)$	PDF for entire structure
f_y	Yield stress of steel
f_{y_eq}	Equivalent yield stress
$f^*(*)$	The PDF of a uniform distribution in a multidimensional rectangular domain
$F_i(*)$	CDF for the i th component
$F_p(*)$	CDF for entire structure
$g(*)$	Structural limit state function
$g_{ben}(*)$	The limit state function for bending members
$H(*)$	Random field
L_C	Correlation length
L_{RF}	Size of random field mesh
L_{FE}	Size of finite element mesh
m	Material constants of Weibull model
M	Truncated terms of K-L expansion
M_{re}	Maximum plastic moment of resistance
M_l	The applied moment
N_i	Shape functions of i th point of RF element
N_{ele}	Number of finite element
N_{IP}	Number of integration point per element
N_{sim}	Number of simulations
P_f	Failure probability
P_s	Reliability probability
s_{ij} and s_{kl}	Deviatoric stresses
V_0	The component volume
V	The entire structural component volume
V_{eff}	Effective volume
$V_{ELEM,i}$	Volume of i th finite element

V_{RVE}	Volume of representative volume elements
$Var(*)$	Variance
W_{pl}	Section moment
δ_{ij}	Kronecker delta
λ	Lagrange multiplier
Ω	Sample space
θ	Vector of statistical parameters
B_{ep}	Elasto-plastic strain matrix
D	Domain in the Hilbert space
D_{ep}	Elasto-plastic material constitutive matrix
$E(\mathbf{X}, \theta)$	Random field of Young's modulus
$f_y(\mathbf{X}, \theta)$	Random field of yield strength
F	Set of events
H	Entropy
J_e	Coefficient matrix mapping from local coordinates of RF element to global physical coordinates
K_e	Elastic stiffness matrix
K_p	Plastic stiffness matrix
P	Probability measure
X	Position vector
S	The action effect
R	The resistance
\bar{S}	Mean value of action effect
\bar{R}	Mean value of resistance
Z	The limit state

Abbreviations

SSE	S tatistical S ize E ffect
RVE	R epresentative V olume E lement
RF	R andom F ield
SFEM	S tochastic F inite E lement M ethod
3P	T hree- P oint bending
4P	F our- P oint bending
3D	T hree D imension
K-L	K arhunen- L oève expansion
MCS	M onte C arlo S imulation
TSFEM	T aylor expansion S tochastic F inite E lement M ethod
PSFEM	P erturbation S tochastic F inite E lement M ethod
NSFEM	N eumann expansion S tochastic F inite E lement M ethod
SSFEM	S pectral S tochastic F inite E lement M ethod
MEFM	M aximum E ntropy F itting M ethod
PDF	P robability D ensity F unction
CDF	C umulative D istribution F unction
FORM	F irst O der R eliability M ethod
SORM	S econd O der R eliability M ethod
LHS	L atin H ypercube S ampling
FE	F inite E lement
PHT	P lastic H inge T heory
SRCM	S tatistical R esponse C haracterization M ethod
IP	I mportance P ampling

1 Introduction

1.1 Motivation

Since the conditions of the occurrence of an event are not sufficiently known, there is no direct causal relationship between the condition and the result of an event, and thus the event exhibiting uncertainty. Practical experience of engineering shows that the uncertainty is not only in the load assessment, but also involves the engineering system of materials and geometric characteristics.

In general, the computational model and the numerical software usually are based on the deterministic method, which means that all geometries, materials, and loads of the structure must be deterministic values. However, many parameters of the structural engineering exhibit complex randomness, which cannot be completely captured and characterized by a deterministic model. The traditional approach is used to rationalize these uncertainties through probabilistic and statistical methods, and then the required determined values for the calculation model are obtained based on the extreme, minimum, maximum or mean values of system parameters. This approach contains the assumption that the results obtained by the deterministic analysis represent all possible situations of load and resistance in the structural components. In some cases, this assumption may be correct. However, it is definitely that the deterministic method cannot get the best solutions or optimum design for the structure.

In general, the safety factor has been used as an evaluation criterion of civil engineering. However, the safety factor is only a determined value obtained from known information, and it fails to account for any variability of parameters for structural design. In other words, the safety factor does not precisely characterize the safety of the structure, because the statistical parameters of the design variables are also variable with the change of external conditions.

With the continuous development of computational science, the precision of the structural calculation is continually increasing. Hence, the benefits obtained by the precise analysis of the structure are submerged by the traditional safety factor, if the variability of the statistical parameters of the random variables such as (material properties, geometries, etc.) is not considered. Thus, it has a great sign that the uncertain factors are introduced indirectly or directly into the mechanical calculation to analyze the structural mechanics and to evaluate the reliability of practical engineering.

As is well known, the elastic and plastic design in steel structure is widely used [1], since the steel has outstanding elasto-plastic material properties. It is certain that the yield strength of steel has variability because the uncertainties and spatial variability is inherently present in nature. The influence of this uncertainty of strength on the structure and corresponding safety is unclear. The statistical size effect phenomenon, which is originally used to describe the effect of the characteristic size on structural strength in the concrete structure, can explain the relationship between the volume of the similar structure and the material strength. The current elastic and elasto-plastic theory don't involve the statistical size effect and its influence. Whether the uncertainty of the steel strength can produce statistical size effect, is a problem that needs to be discussed, because the statistical size effect will change the strength of structural components and the corresponding safety level. Moreover, a question needs also to be raised, whether the material strength for steel with the small size of specimen applies to the practical large-scale structures.

In order to enable a more economical design method in future, this thesis mainly aims to investigate the influence of statistical size effect on the material strength and the corresponding reliability in steel structures. The implementation of the research process can be summarized as follows:

- Developing a stochastic material model with elasto-plastic material properties based on the known probability distribution model by mathematical methods. The proposed model will be embedded into the common structural analysis software to analyze complex structures with stress gradient.
- Establishing a discrete random field with a general mathematical program based on the randomness of the material properties. The structural response is obtained by stochastic finite element method (SFEM) after the random field file is imported into the finite element model.
- Implementing the uniaxial tensile test as well as three- and four-point bending tests to compare the above-mentioned theoretical analysis and to determine the corresponding parameters.
- Evaluating the influence of statistical size effect (SSE) on structural reliability by maximum Entropy fitting method based on the known information, which is the obtained structural response by the theoretical analysis.

1.2 State of research

In this section, the review of past and recent developments for statistical size effects, uncertainty modeling, generation and discretization of the random fields, development and application of stochastic FEM as well as application status and the challenge of reliability analysis in civil engineering will be briefly explained.

1.2.1 Statistical size effect

Referring to the reliability theory came in the past years to the question whether the strength of the material can be affected by the absolute volume of the structure [2–5]. From previous research, size effect can be described as two fundamentally different approaches, i.e., deterministic and statistical explanations. Most researchers focused on size effect on the energetic basis and this purely deterministic size effect is widely studied [6,7]. The SSE of steel structures was mentioned decades ago [3]. However, currently researches in this area are rare. This is due to the fact that the SSE in steel structures is not as prominent as in concrete since the strength variability of steel is relatively small. Moreover, most of the components in the steel structure are plate-type and not bulk-type, and some studies have focused on the relationship between strength and material thickness. For example, Figure 1.1 a) shows that the material yield strength decreases with increasing material thickness. Thus, the material strength is graded by thickness in Figure 1.1 b), but this method ignores the influence of the tensile specimen size. Hence, the graded material strength according to the thickness strength in the reference [8] and design code [1] covers the SSE phenomenon.

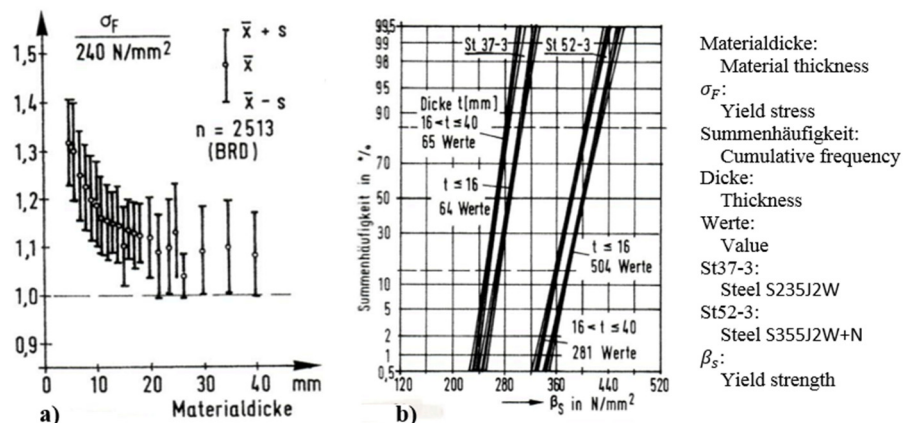


Figure 1.1: a) Relation between yield stress and material thickness, b) the probability distribution of the strength of the steel graded according to the thickness, from [8]

Theoretically, all materials are not perfect and have the defective structure on the microscopic scale. Currently, the prediction of failure of structural elements based on microstructural analysis, such as Gurson-Tvergaard-Needleman (GTN) material model [9], is widely mentioned

and studied. However, these researches did not deal with the link between the randomness of the underlying microstructure imperfections and the probability distribution of material properties at the macroscopic scale. The material properties are affected by the structural size since the size, quantity, and corresponding distribution of microstructure imperfections are changed as the structural volume increases. From a statistical point of view, increased defects can lead to a higher probability of failure under the same stress conditions; that is the strength decreases as the failure probability remains unchanged. Therefore, the distribution of the defects in microscale determines the material strength in macroscale. Because of the randomly distributed sliding surfaces and other mechanical defects in material, it is possible to study the size effect by statistical methods. The research method based on the strength of statistical theory avoids the difficulty to research microstructure of the material. According to some simplified assumption of the strength in microscale, the macroscopic strength can be obtained using a stochastic material model with probability and statistical method. Recently, the statistical size effect in the steel structure was demonstrated by experiment [10] and stochastic finite element method with random field [11].

The statistical size effect has been traditionally explained by Weibull-type statistical weakest link model [12]. The material strength depends on its weakest member. The underlying hypothesis is that the structure will fail as the stress exceeds the material strength at any point of the structure. Because of its simple form and relatively preciseness, Weibull distribution in brittle material has been widely applied [13,14]. However, Bažant found in the application of the classical Weibull-type approach with reinforced concrete structures that the structures with quasi-brittle materials are not only the existing statistical size effect but also strong deterministic statistical effect [15,16]. Moreover, some researchers show that Weibull size effect theory for rock, concrete and other quasi-brittle material needs to be corrected [17]. These researchers also attempt a new method to combine statistical and deterministic theories employing a nonlocal generalization of Weibull theory [18,19]. The other avenue of approach tries to amalgamate Weibull statistical weakest link model and Daniel's fiber bundle model to establish a new pure statistical analysis model [10,20,21]. Hence, it is necessary to propose a new model and formulas for approximation and prediction of the material strength under various conditions based on asymptotic mathematical matches.

The mathematical analysis of the statistical size effect is essentially based on the stochastic material model. The mathematical model, which is used to analyze the randomness of the material properties, can be roughly divided into three types: weakest link model, fiber bundle

model and the combination of both models. The weakest link model was proposed by mathematically first formulated by Fisher and Tippett [22] and used earliest to analyze the material strength by Weibull [12]. In the past decades, many researchers have conducted very in-depth studies [2,23]. The fiber bundle model was used to treat load-sharing among fibers by Daniel [24]. This model has been thoroughly investigated by S. Leigh Phoenix and other [25–28]. The combination of both classical models contains two different type, i.e., chain of bundle and bundle of chain models [17]. Morechovsky [21] shows the result in his doctoral thesis that the chain of bundles model provides a flexible selection of the generic probability distribution for different specimen size, which can result in different statistical size effect curves.

1.2.2 Uncertainty and modeling with random fields

From a mathematical point of view, the uncertainties in the structural Engineering can be divided into three categories: randomness, fuzzy and unascertainty. The unascertainty refers to the uncertainty resulting from incomplete information or data. The uncertainty involved in this thesis is specific to randomness because the stochastic problem in the engineering is to treat the distribution of random variables and the corresponding parameters.

The randomness is further divided into random variables, random processes and random fields. Random variables are used to describe the randomness of a single variable that is independent of time and space. The stochastic process is usually employed to deal with random parameters with varying properties [29]. For random parameters with spatial distribution characteristics, it is necessary to be treated with random field [30]. For a situation with defined coordinate position, the random field is degraded to random variables. It is obvious that the randomness of material properties is distributed in a three-dimensional (3D) space. Thus, it is necessary to describe the material properties by random fields. In some cases, the randomness may have the variability of time and spatial, for example, the random field with temperature in concrete. This situation can be seen as a four-dimensional random field, which is added a time dimension in the 3D random field. In this thesis, we mainly study the realization and dispersion of a 3D random field.

In fact, all the phenomena of uncertainty in nature can be attributed to the external manifestations of distributed disorder systems, which can be described as random distributions in spatially distributed or it depend on time. Vanmarcke studied the random field theory very early and systematically [31]. At the same time, he made an incisive exposition of the random field for the material properties of geotechnical engineering. A few decades ago, Shinozuka's researches were involved the random field characteristics of concrete materials [32]. From the

reference in the past times [33–36], it can be seen that the realization and discretization of all random fields revolve around two main categories, which is based on their probability distribution, namely Gaussian and non-Gaussian. According to the central limit theorem, a Gaussian random field is suitable using in lots of different situations. Because of the simplicity of the Gaussian random field and the lack of relevant experiments with random variables, it is often necessary to make Gaussian assumptions regarding these probabilistic characteristics.

Although the Gaussian random field is relatively simple and it has a wide range of applicability, several quantities arising in practical engineering exhibit non-Gaussian probabilistic characteristics [3]. There are two different approaches to implement the non-Gaussian random field. The first method is generating a sample function that matches the specified power spectral density function or the statistical moments of the target random field [37]. It is possible that the different marginal probability distributions have similar statistical moments even if the tails are dissimilar. The other approach is generating a sample function, which contains the probability information of the target function [38].

From the numerical calculation point of view, the random field must be discretized using a finite number of random variables. Some different random field discretization methods have been published in many references, for example, midpoint method [39], interpolation method [40], Karhunen-Loève (K-L) expansion [41] and the spectral representation method [42,43], etc. Recently, a general approach comprising spectral representation and K-L expansion is proposed for generating Gaussian random field simulations [44].

At present, most of random field theory and random field discrete method are limited to one-dimensional or two-dimensional. By the discretization of a random field with 3D domains, the main difficulty is to treat the problem that the solution of the eigenvalue function is included in the high dimensional integral. For this reason, the calculation of the corresponding matrix is very expensive or difficult to achieve. To speed up the assembly of a matrix with high-order integral, a method which approximates matrixes as a hierarchical matrix proposed [45].

1.2.3 Development and application of stochastic FEM

In recent decades, with the development of computer technology, the analysis and design of small- and large-scale engineering systems have been allowed to be performed in simulation software. Using the finite element method to analyze complex structure has become a numerical approach widely used in structural engineering practice. In addition, with the introduction of high-precision element, the deterministic finite element calculation is becoming more and more accurate. This approach applied in engineering practice can guarantee the structural reliability

with a reasonable safety factor, but is not an optimal design method [46]. However, with the increase of the structure complexity, there is a complex relationship between the response quantity of structure and the input quantity, which is often difficult to display with a function. By the traditional deterministic method, the mechanical problems with these uncertainties cannot be solved accurately by probability theory and statistics. The uncertainty and randomness of materials, boundary conditions and structure have been considered in the numerical model in recent years [47–52]. It is mentioned in [10,20] that the probability distribution of material uncertainties varies with the volume and stress gradient of the specimen and this phenomenon is difficult to be considered in the deterministic analysis. Therefore, the uncertainty can be embedded in the mechanical model with a random field (RF) to analyze the response of the mechanical properties and influence of reliability. This analysis will be gradually improved over the last few years. Because the strong capabilities and advantage of the stochastic finite element method (SFEM) are demonstrated in the probabilistic analysis of structures with uncertainties, the SFEM is considered as one of the best tools for these simulations.

The first ideal is direct to combine the finite element method with Monte Carlo method by Astill [47] and Shinozuka [48]. Because the direct Monte Carlo method is based on a large number of deterministic calculations, the computation of large structure is unacceptable, accordingly, some improved methods have also been proposed. Cambou [53] first studied the linearity problem by using a second order moment method. Then Baecher and Ingra [54] used a similar approach to solve the problem of uncertainty in geotechnical engineering. Due the process is carried out with the Taylor series expansion of the random variables, this method was called Taylor expansion stochastic finite element method (TSFEM). Hereafter, Hisada and Nakagiri [55] used the first-order and second-order perturbation techniques to consider the fluctuation of random variables and propose a more efficient perturbation stochastic finite element method (PSFEM). In the late of 1980s, Yamazaki and Shinozuka [49] creatively combine the Neumann expansion method with the Monte Carlo stochastic finite element method and propose a Neumann expansion stochastic finite element method (NSFEM) with high accuracy and efficiency. In 1991, Ghanem and Spanos [56] published the first monograph on the area of stochastic finite element method. This book is mainly discussed that the random processes are represented by discrete, independent random variables, which can be discretized and numerically solved in Hilbert space.

The SFEM can be considered as an extension of the classical deterministic finite element method and involves solving the problem of finite element with the randomness of material

properties and boundary conditions. From a mathematical point of view, the SFEM can be seen as a numerical solver for stochastic partial differential equations and calculates the statistics of the pre-defined randomness conditions for the system response. The SFEM makes possible to analyze the uncertainty with FEM, but the corresponding complexity of the numerical model and the computing resources are increased at the same time. Due to the iterative operations involved in the simulation of a nonlinear elasto-plastic material, the nonlinear constitutive relations are particularly difficult to analyze with uncertainty. Therefore, only the randomness of linear material is investigated in the most literature [50,57,58]. The simplification of nonlinear material using two fictitious bounding bodies is also employed to approximately satisfy the constitutive relations in [59,60]. More recent, the nonlinear problem can be solved by using the transformation of the stochastic elasto-plastic constitutive rate equation in the real space into a linear deterministic partial differential equation in the probability density space [61,62] and the stochastic Galerkin Method [63]. However, MCS is the most straightforward approach to implement SFEM in general simulation software, which is also easiest to program for the calculation of system response in the SFEM and probably the only general tool to solve the stochastic finite element problem with complex nonlinear elasto-plastic materials.

With the continuous improvement of the SFEM, the SFEM software, which can be used in the large-scale engineering design, is urgently needed. The current mainstream approach is to use general programming software to generate the random fields (such as MATLAB), and then the random field file will be inputted to the common commercial finite element software for further analysis. Finally, the results are returned to the mathematical software for analysis of statistical system response [64]. This approach is used to analyze the plane problem with the stochastic elastic material in [58]. Therefore, a general method needs to be developed to analyze three-dimensional bodies with a nonlinear elasto-plastic material.

1.2.4 Reliability theory in civil engineering

The basic theory and method of structural reliability were formed in the 1960s and 1970s, and its main application is structural safety design [65]. Nowadays, the reliability method has been widely applied to the design of new structures [66], the application of new material [67], the safety of infrastructure systems [68] and the assessment of existing structures [69], since the reliability-based design methods have dominated the development of current codes and standards. A recent reference [70] focuses on the review of the reliability-based performance criteria used to calibrate design and evaluation codes and standards for assessing the strength, serviceability, and fatigue resistance of structural components. Although there is a large difference in

the level of target reliability used for the strength of various structural members and materials, structural standards for reliability calibration are producing a good balance between safety and cost.

The structural reliability analysis is typically based on random variables of load and resistance. In principle, the reliability can be evaluated once the probability distribution of the load and resistance (or response) becomes available. However, the rationality of the reliability calculation is based on the fact that the random variables distribution model and the relevant statistical parameters are correct. For yield strength of the material, some studies [3,69,71] suggest that a lognormal distribution is appropriate. But the reference [72] shows that the goodness-of-fit tests suggest that the lognormal, Weibull and extreme value distribution are all equally valid choice for describing the yield strength of steel. Through a series of experiments, it was found that there was a correlation between the steel strength and the sizes of the specimen [10]. The statistical parameters of the strength vary with size. Hence, the key problem for steel structure safety is to obtain the suitable distribution under the consideration of the uncertainties of the material properties.

In recent decades, a more efficient approach, which is called the maximum entropy fitting method (MEFM) suggested by Jaynes [73], is to use a distribution free technique for estimating the probability density function of the samples of load and resistance or response. This method is employed to estimate the probability density function (PDF) of a random variable under specific moment constraints in the case of very little available data. This approach provides a minimum deviation probability distribution among all possible distributions consistent with the available data. An optimal probability distribution is constructed under the known information using this method. When the constraints are given, the maximum entropy principle can be derived from many well-known probability models. Therefore, the MEFM is widely used as an effective stochastic modeling tool for successful application in many problems [74–79] and the reliability analysis [69,80].

1.3 Thesis structure

This thesis is aimed to embed the randomness of material properties directly into mechanical methods to simulate the complex behavior and calculate the reliability of the actual structures. The structure of this thesis is shortly presented as follows.

Chapter 2 discusses the statistical size effect with stochastic material models in steel structures. The chain of bundle model is proposed based on two classical models, which is used to describe

the statistical size effect of steel, and the possibility to approximately determine the parameter of the model is given. Simultaneously, the proposed stochastic material model is extended to the multi-axial stress state with the von Mises yield criterion, and it will be applied to structural components with non-uniform stress distribution. Besides, the stochastic material model is integrated into the commercial FEM software ABAQUS by user subroutine UMAT.

Chapter 3 is focused on the implementation and application of stochastic finite element method. The SFEM is applied to the simulation for three-dimensional structure with the uncertainty of elasto-plastic material. The corresponding implementation is using the developed combination of general finite element software and mathematical software. The proposed approach combines K-L expansion and Galerkin techniques for computing the response variability of realistic structures. The uncertainty of Young's modulus and yield strength is described by the random field with Monte Carlo simulation enhanced by Latin Hypercube Sampling. Meanwhile, the random field and stress field can be arbitrarily separated and coupled by using the mapping interpolation method. Thus, this analysis is extended to be applied in a variety of element types in commercial FEM software.

Chapter 4 is assigned for the tensile and bending test to compare the results of the mathematical model and the simulation. The statistical size effect in steel structures is verified by uniaxial tensile tests, and the material parameters of the stochastic material model are determined by comparison of the experiment and simulation. Moreover, the bending tests are simulated with the stochastic material model. The results of bending tests show that the SSE also exists in the flexural member and the equivalent yield stress is closely related to the stress distribution and volume of structural component. The simulations with SFEM show that the statistical distribution of the entire structural response and the randomness of the input material properties are associated with the change of the effective volume and stress distribution of the structure.

Chapter 5 presents an efficient method based on SFEM for response variability and reliability analysis. The maximum entropy fitting method is employed to fit the distribution function of structural response. Furthermore, the reliability of steel structures with stress gradient was analyzed using this method. The results show that the material strength, which has been obtained from small specimens through statistical analysis in the laboratory, is no more accurately applicable to large construction considering the SSE in the reliability analysis. Simultaneously, the safety index is closely related to the effective volume and stress gradient of the structure.

The main conclusions of this thesis based on the results obtained in the previous chapter summarized in chapter 6.

Chapter 7 gives some recommendations for the future research activities and indicating future directions and addressing some open issues to be considered by the engineering.

2 Analytical model for the statistical size effect

2.1 Overview

According to the traditional approach, the imperfections of the microscopic structure and real stress distributions in the structural component cannot be considered since steel is regarded as an ideal body in the structural calculation. The classical material model does not treat the randomness of the material properties in mechanical analysis. For this reason, a method needs to be developed that it is possible to estimate the influence of the stress gradient and the stressed volume on the strength with the statistical size effect. Firstly, this chapter presents two classical stochastic material models. Based on the existing material models and the probability theory, a new stochastic material model is proposed to describe the statistical size effect. The developed model focus on the variations of the distribution functions, the mean value, the variance of the basic variables and the information of the probability function convergence. Besides, a method is put forward, which can estimate the parameters of a random material model. Afterward, this material model is extended with von Mises yield criterion to analyze the bending strength of the structure. The expanded model is programmed using User Subroutines in ABAQUS to describe the statistical size effect in complex structures.

2.2 Stochastic material model

2.2.1 Weakest link model

Ideal brittle materials are distinguished by the fact that no plastic deformations occur. There are neither sliding surfaces nor other mechanisms with which mechanical energy is dissipated. Assuming the homogeneous stress of the specimen, Weibull notes that the strength of an ideal brittle material depends on the specimen size and the concentration of the mechanical defects in the specimen [12]. The Weibull model is based on the weakest link to describe the ideal brittle materials. The statistical expected value of material fracture can be determined by the failure probability and depends directly on the specimen size. Usually, the smaller the specimen, the smaller the fracture probability under the same stress conditions [2,12].

It is assumed that the reference strengths σ_0 for the weakest link model are distributed by $F_i(\sigma)$ and the component volume V_0 for all members is same and very small compare to the entire structural component volume V . Furthermore, all elements are loaded under the same load F as shown in Figure 2.1 a). Thus, the probability of the weakest link model is written as follows:

$$P(X \leq \sigma) = F_p(\sigma) = 1 - (1 - F_i(\sigma))^m \quad (2.1)$$

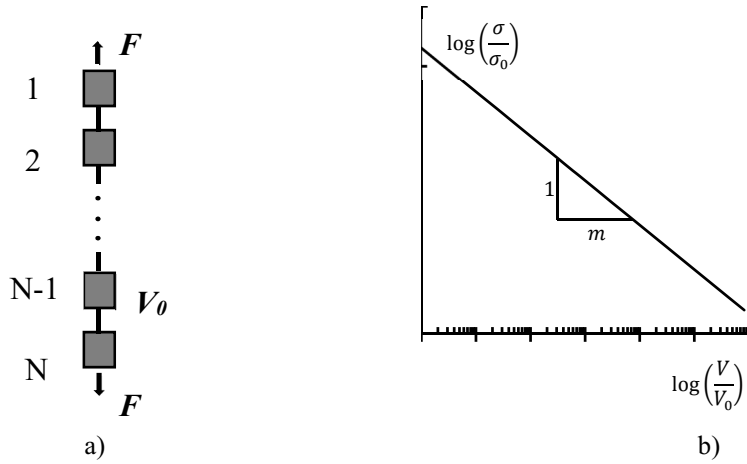


Figure 2.1: a) Weakest link model, b) Influence of the volume on the strength

With the reference volume V_0 and the reference strength distributed by $F_i(\sigma)$ the failure probability $F_p(\sigma)$ of the strength can be calculated using Eq. (2.1) for the ideal brittle material.

$$F_p(\sigma) = 1 - e^{\sum_{i=1}^N \ln(1 - F_i(\sigma))} \approx 1 - e^{-\frac{V}{V_0} F_i(\sigma)} \quad (2.2)$$

Based on experiments, Weibull had determined that the unique failure probability $F_i(\sigma)$ corresponds to the power law [12]. Due to the long chain, the unique failure probability must be very small, namely $F_i(\sigma) \ll 1$, therefore, $\ln(1 - F_i(\sigma))$ can be approximated as $-F_i(\sigma)$.

$$F_p(\sigma) = -e^{-\frac{V}{V_0} \int \left(\frac{\sigma}{\sigma_0}\right)^m dV} \quad (2.3)$$

where, σ_0 and m are two material constants which are determined based on the experiments. According to Figure 2.1 b), the smaller the material constants m , the more obvious the statistical size effect of the material.

The failure probability of this model is a monotonically increasing function based on the stress and the corresponding value range of this function is in the interval of $[0,1]$. According to the research from Karel [81], the following result for the mean value $\bar{\sigma}$, which is same with the expected value $E(\sigma)$, and the coefficient of variation C_v of the distribution function is given for the Weibull model in Eq. (2.4) and (2.5).

$$\bar{\sigma} = E(\sigma) = \int_0^\infty \sigma f_p(x) d\sigma = \Gamma\left(\frac{1+m}{m}\right) \sigma_0 \left(\frac{V}{V_0}\right)^{-\frac{1}{m}} \quad (2.4)$$

$$C_v = \sqrt{\frac{E(\sigma^2)}{(E(\sigma))^2} - 1} = \sqrt{\frac{\Gamma\left(\frac{2+m}{m}\right)}{\Gamma^2\left(\frac{1+m}{m}\right)} - 1} \quad (2.5)$$

It should be noted that the coefficient of variation of the statistical strength is independent of the total volume V and the reference volume V_0 . Thus, the material constant m can be obtained by the material strength coefficient of variation based on experiments. For most real material, such as steel, the C_v of material strength is also changed as the specimen volume increase [10]. Therefore, the Weibull statistical theory may be limited to use on ideal brittle materials or approximately on the brittle and quasi-brittle materials [13].

2.2.2 Fiber bundle model

Another classical stochastic material model, i.e., fiber bundle model was proposed by Daniel [24], which is formed of n parallel components, as shown in Figure 2.2. The stress-strain relationships are assumed to be identical for all n components of the bundle. Each component of the fiber bundle model is loaded by F/n and all components experience the same deformation. Compared to the weakest link model, the failure of a component no more definitely leads to the failure of the entire specimen. If j components fail, the stress on the bundle is taken over by the remaining $n - j$ intact components.

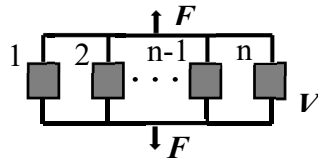


Figure 2.2: Fiber bundle model

If the system consists of similar components, it will be assumed that the reference strengths σ_0 of every components distributed by $F_i(\sigma)$ are statistically independent. The exact recursive formula of failure probability was developed by Daniels with the fiber bundles system as follows:

$$F_n(\sigma) = \sum_{k=1}^n (-1)^{k+1} \binom{n}{k} F_i^k(\sigma_0) F_{n-k} \left(\frac{n\sigma}{n-k} \right) \quad (2.6)$$

The probability function of the strength $F_n(\sigma)$ is numerically difficult to handle. Daniels has shown that the probability converges asymptotically to a Gaussian distribution for the case $n \rightarrow \infty$. Then,

$$F_n(\sigma) \approx \phi \left(\frac{\sigma - E(\sigma)}{D(\sigma)} \right) \quad (2.7)$$

where the expected value $E(\sigma)$ and the variance $Var(\sigma)$ can be expressed implicitly as follows:

$$E(\sigma) = \max(\sigma[1 - F_i(\sigma)]) \quad (2.8)$$

$$Var(\sigma) = \sigma^2 F_i(\sigma)[1 - F_i(\sigma)] \quad (2.9)$$

Hohenbichler and Rackwitz [82] expanded the theory of the fiber bundle model to reveal the component with complex stress-strain relationship for elastically brittle material. For the ideal elasto-plastic material, the failure probability can be approximated as a normal distribution according to the central limit theorem, if the stochastically strength is independent for each component.

2.2.3 Real material properties

The materials in reality are usually not ideal for brittleness and plasticity. Generally, one of several different post-peak behaviors of material properties, which are shown in Figure 2.3, will occur after the stress on the material exceeds the elastic limit. For the weakest link model, if the material reaches the maximum stress is defined as the failure; the post-peak behavior of material properties does not affect the analysis of the chain model. If the chain is long enough, the weakest link model is throughout following Weibull distribution regardless of whether the material has plasticity, brittleness or more realistic post-peak softening behavior. However, for satisfying this condition, it exists only in infinite structure volume.

The post-peak gradual softening behavior is difficult to analyze in the fiber bundle model because each fiber requires considering not only elasticity but also plasticity until it reaches the strength limit. Two other behaviors in fiber bundle model are relatively easy to study after reaching the strength limit, and it can be approximated by a normal distribution according to the central limit theorem for plastic material and recursive formula by Smith [26] for brittle material. Therefore, the two classical stochastic material models have some limitations, as well as it is not possible or difficult directly as a generic stochastic material model for elasto-plastic material.

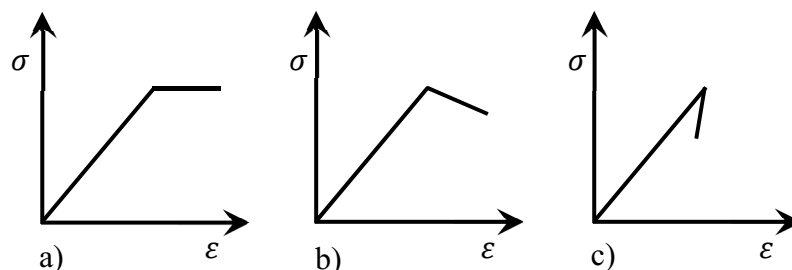


Figure 2.3: Post-peak behavior of material properties, a) ideal plastic, b) softening, c) brittle

It is well known that the steel is not an ideal elasto-plastic material. When the steel specimen is subjected to tensile test, it will experience several various stages before fracture. If this ductile material is stretched beyond the elastic point, the steel starts to show plastic behavior. The upper yield point is the point after which the plastic deformation starts. Moreover, a point at which minimum load or stress required to maintain the plastic behavior of material such a point is

called as lower yield point. The upper yield point is unstable; this is due to the fact that the dislocations in the crystalline structure start moving after this point. Normally, we use the lower yield point to determine the yield strength of the material being tested, because the upper yield point is momentary but lower yield point is stable.

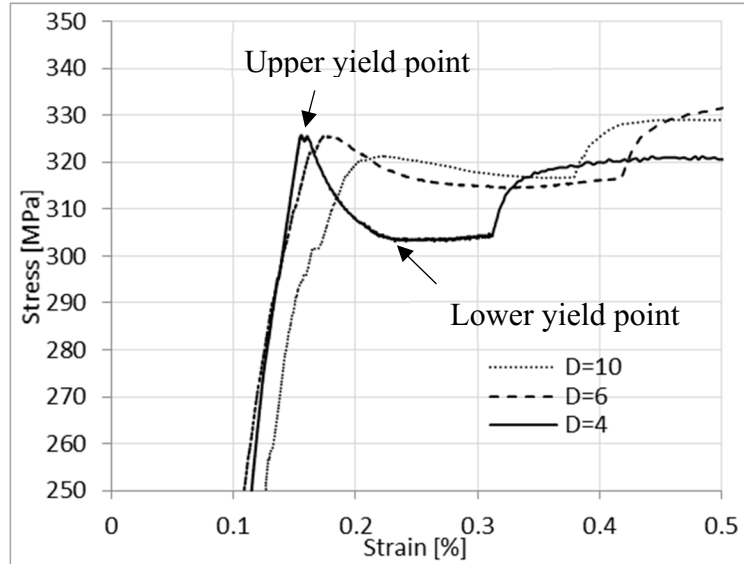


Figure 2.4: Upper and lower yield point of steel S235

Figure 2.4 shows the stress-strain curve of the steel S235 with different specimen diameters. It is clear that this kind of steel appears obvious upper and lower yield point. A very little change is remained in the upper yield strength for the different specimen sizes. However, the yield stress of a smaller specimen with diameter 4 mm is greater than the yield stress of another one with 10 mm diameter. Hence, it can be deduced that the steel with a relative small characteristic volume is not the ideal material and it reflects the more realistic post-peak behavior, which is gradually softening in Figure 2.3 b). Theoretically, the perfect plasticity and brittleness are just two extreme idealized models and the post-peak softening behavior should be between these two extremes. As well as it can more accurately describe the characteristics of the real materials. Theoretically, the artificially manufactured materials such as steel are not completely isotropic and inhomogeneous, which contain various structural imperfections. The material properties are influenced by the size and quantity of microstructural imperfections and the corresponding distribution. The material parameters distributed to $F_X(x|\theta)$ are given by the random variable (x_1, x_2, \dots, x_i) . θ is the vector of statistical parameters. The specimen can be simplified to the fiber bundle model only if the specimen size in the direction of the applied force is far smaller than the size transverse to the force in Figure 2.5 a). However, most of the situations in reality is similar to Figure 2.5 b), which cannot be described by the fiber bundle model. The structure in practice is obviously needed to be analyzed with more complex probability models.

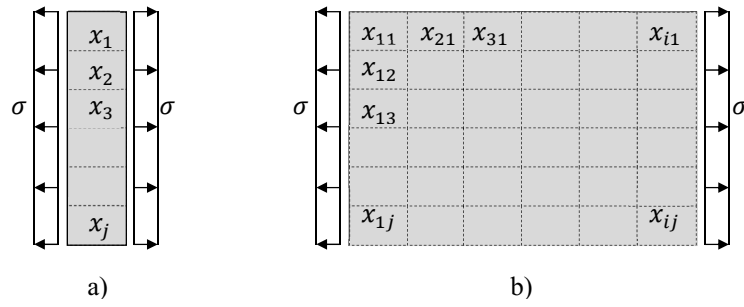


Figure 2.5: Illustration of material under the stress

From a probabilistic point of view, the relevant distribution of material properties is almost non-quantifiable, because the probability model of the structure is completely disordered. Hence, it is necessary to make reasonable assumptions and simplification of the stochastic material model. Theoretically, the failure mechanism can be modeled with a hybrid of series and parallel coupling. The chain of bundles model and the bundle of chain model can be used as a simplified form of complex models since the parallel model and the series model are the two basic probability models. The chain of bundle model is modeled as a chain of N representative volume elements (RVE), each of which is statistically represented by a model consisting of n bundles. On the other hand, the bundle of chain model is a series coupling of N RVE, but the RVE means a model consisting of a chain of basic members.

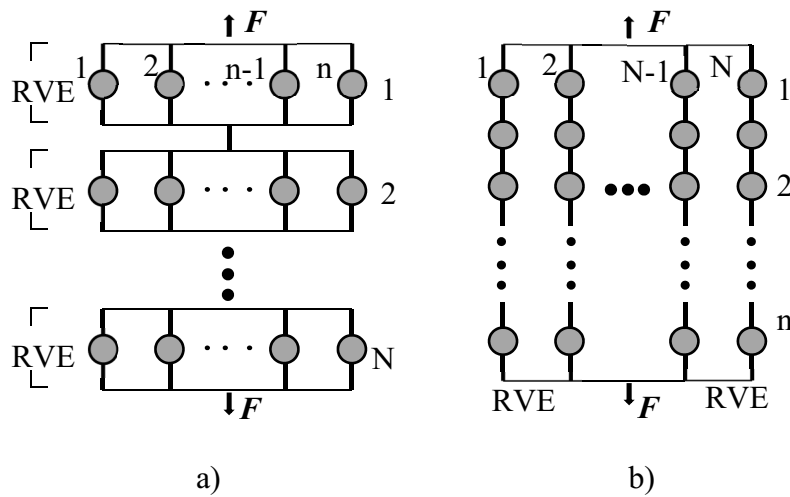


Figure 2.6: a) Chain of bundle model, b) bundle of chain model

Recently, a physical justification of the distribution of the structural strength was described based on the Maxwell-Boltzmann distribution of thermal energies of atoms in nanoscale by Bažant [83]. The number of the base element normally can be considered as infinite, and the number of RVE in a structure would be small. When the basic element is extremely small, it is assumed that the probability distribution function of element strength is a power law. Hence, the RVE, which is a chain composed of an infinite number of the fundamental element, obeys

the Weibull distribution. The mathematical significance of the bundle of chains model is calculating the probability of a parallel system with several Weibull distributions. However, the failure probability of this system could not be approximated accurately by simple analytical equations and be applied in the structural analysis, because the failure probability contains a complicated recursive formula. In summary, the chain of bundle model may be the only available probability model to analyze the statistical size effect for real materials. The RVE of the chain of bundle model is structured by a fiber bundle model with softening behavior material. Although there is no strict mathematical proof, it can be assumed that the real material with gradual softening behavior in the plastic stage is also close to normal distribution according to the central limit theorem when the number of fibers tends to infinity. The chain of bundles model offers an approach to fill the gap of the size effect between larger scale and small scale in Figure 2.7. Therefore, the focus in this chapter is on the analysis and application of chain of bundles model.

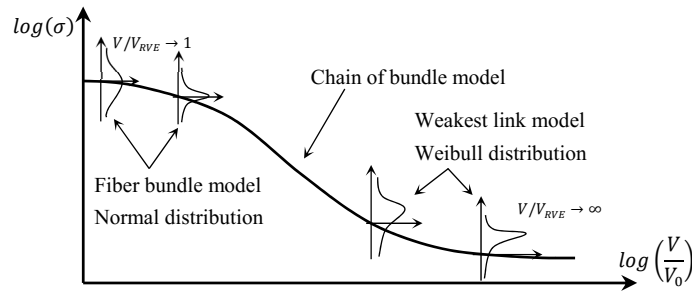


Figure 2.7: Probability distributions with various volumes

2.2.4 Chain of bundle model

As mentioned in section 2.2.3, the chain of bundle model is constituted by N RVE of n parallel reference element in a chain. The RVE is defined as the smallest volume of material, whose failure can cause the destruction of the whole structure. If the RVE can result in total failure, then the structure can be simplified as a chain of RVEs. In this case, the probability function of the respective parallel system can be analyzed and it obeys to a normal distribution, if the number of the parallel systems moves towards infinity. For a large coefficient of variation, the Gaussian distribution should be replaced with a logarithmic normal distribution to reduce the variance of heterogeneity of the material property and to prevent negative strengths. It is assumed that the failure probability of the RVE is statistically uncorrelated. For the chain of bundles model, the probability of failure is given as follows:

$$F_p(\sigma) = 1 - e^{-\frac{V}{V_{RVE}} \ln \left(1 - \Phi \left(\frac{\ln \left(\frac{\sigma - \sigma_u}{\sigma_0} \right)}{\xi} \right) \right)} \approx 1 - e^{-\frac{V}{V_{RVE}} \Phi \left(\frac{\ln \left(\frac{\sigma - \sigma_u}{\sigma_0} \right)}{\xi} \right)} \quad (2.10)$$

where $\Phi(\ast)$ is the distribution function of the standard normal distribution. ξ is the material constant. σ_u is the lower limit of σ and $\sigma > \sigma_u$. σ_0 is a scale parameter of strength.

According to the definition $F_p(\sigma) = \int_{-\infty}^{\sigma} f_p(\sigma) d\sigma$, the probability density function $f_p(\sigma)$ can be obtained by derivative of the cumulative distribution function $F_p(\sigma)$ of the continuous random variable σ in Eq.(2.11).

$$f_p(\sigma) = \frac{\sqrt{2} \frac{V}{V_{RVE}} e^{-\frac{\ln\left(\frac{\sigma-\sigma_u}{\sigma_0}\right)^2}{2\xi^2} \left(1 - \operatorname{erf}\left(\frac{\sqrt{2} \ln\left(\frac{\sigma-\sigma_u}{\sigma_0}\right)}{2\xi}\right)\right)^{\frac{V}{V_{RVE}}-1}}{\sqrt{\pi} \xi \left(\frac{\sigma-\sigma_u}{\sigma_0}\right)^2} \frac{V}{2^{\frac{V}{V_{RVE}}-1}} \quad (2.11)$$

Eq. (2.10) gives the continuous transition between Weibull weakest link model and Daniel's parallel bundle models. It is purely phenomenological and not based on any physical models. The failure probability approximates to a lognormal distribution, if the whole volume of the specimen is extremely small, i.e., $V/V_{RVE} \rightarrow 1$. On the other hand, according to [84], the failure probability of material strength converges to the Gumbel distribution rather than the Weibull distribution with the larger volume. But when the whole volume $V \rightarrow \infty$, the probability of strength converges to the Weibull distribution [83], i.e., the precise Weibull PDF would never be observed in practice.

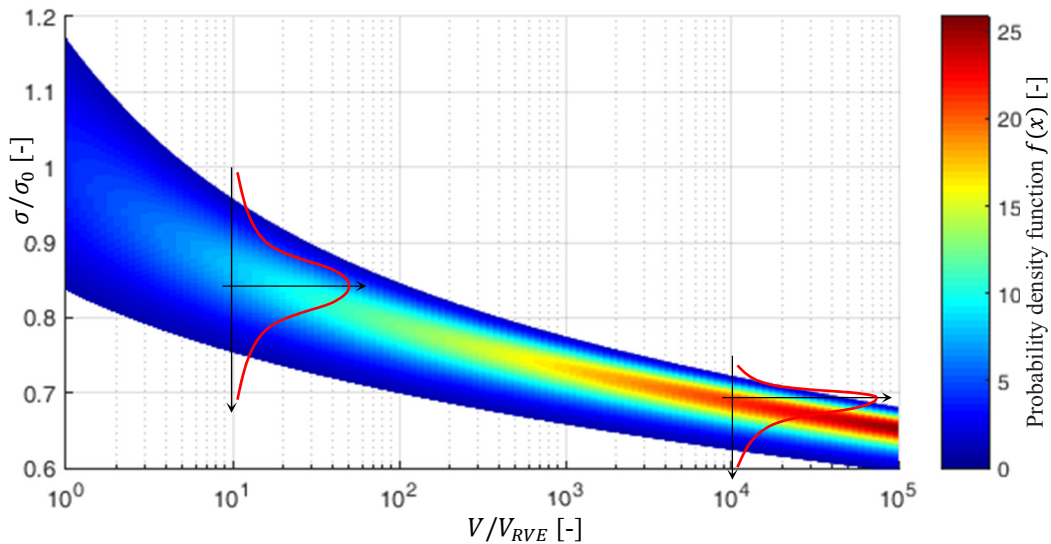


Figure 2.8: Probability density function of the chain of bundle model with various volumes

Figure 2.8 presents the PDF of the chain of bundles model with different σ/σ_0 -value and various numbers of RVEs, where the material constant ξ is assumed as 0.1. It is evident that the probability density distribution of σ/σ_0 is more concentrated with the increased the number of RVEs, i.e., the coefficient of variation of the distribution function decreases as the number of

RVEs increases. This phenomenon is consistent with the description of the statistical size effect in [21]. Furthermore, the mean value and skewness of the failure probability also vary with the number of RVEs. Therefore, the chain of bundle model provides a general probability distribution for the material strength and offers a flexibility choice through different ratios of structural component size and the RVE size. The Weibull, Gaussian and Lognormal distribution, which is suggested in the existing reference based on the tensile tests, can be obtained by proposed the probability distribution with different sizes of the structural component. Figure 2.9 shows the matching results of the recommended PDF and CDF and classical probability distribution of material strength.

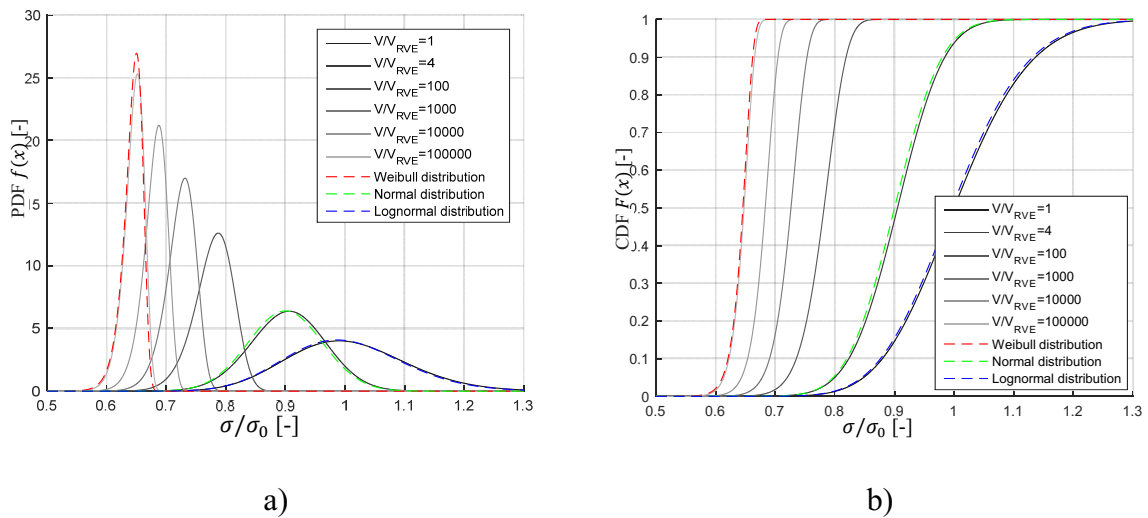


Figure 2.9: Relationship of the proposed distribution and classical distribution, a) PDF, b) CDF

In order to verify the distribution of the chain of bundles model, the numerical simulations are performed based on the pseudo-random number as in Figure 2.10. Firstly, it is assumed that the strength of all RVEs is subjected to lognormal distribution and each component are independent of each other in probability. Then the pseudo-random numbers will be produced through the computer simulation for different V/V_{RVE} -value ($\log(V/V_{RVE}) = 0, 1, 2, 3, 4, 5$).

In this simulation, the pseudo-random numbers represent the ration of the RVE strength σ_{RVE} and the scale parameter of strength σ_0 , i.e., σ_{RVE}/σ_0 . The corresponding mean value and coefficient of variation are assumed as 1 and 10%. Because the entire system is structured by a chain of the RVEs, the strength of the whole structure is equal to the minimum strength of all RVEs. Therefore, by repeating this process with a finite number n of times (10^4 in this simulation), discrete samples of the entire structural strength can be obtained.

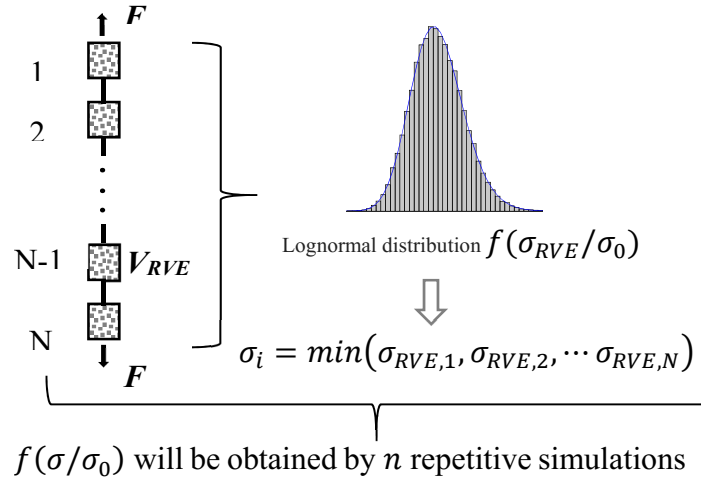
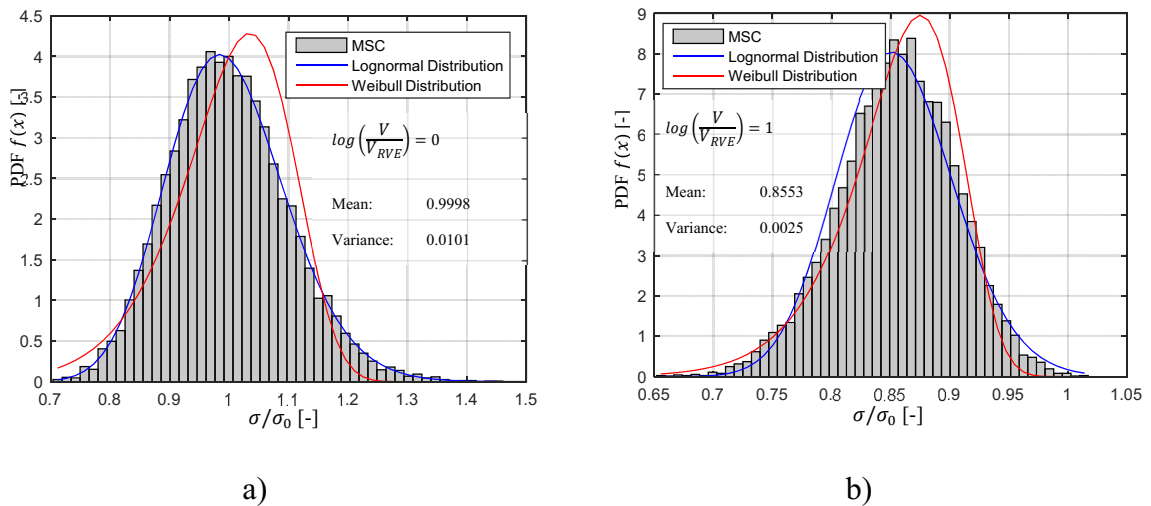


Figure 2.10: Numerical simulation of analytical model

Figure 2.11 shows the distribution of chain of bundles model with different volume of the structural component, i.e., different V/V_{RVE} -value. It is obvious that the distribution of strength is constantly changing with the increase of the V/V_{RVE} -value. It can be seen in Figure 2.11 a) that the strength distribution is consistent with the lognormal distribution as $\log(V/V_{RVE}) = 0$. The distribution of strength is very similar to Weibull distribution as $\log(V/V_{RVE}) = 5$. Furthermore, with increasing the $\log(V/V_{RVE})$ -value, the sample strength get closer to the Weibull distribution. These results are consistent with the conclusion from the Eq. (2.10). In addition, Figure 2.11 shows that the mean and variance value of the ratio σ/σ_0 are also reduced as the V/V_{RVE} -value increases. It is worth noting that the skewness of strength is a slow and continuous transition from positive to negative as the V/V_{RVE} -value increases.



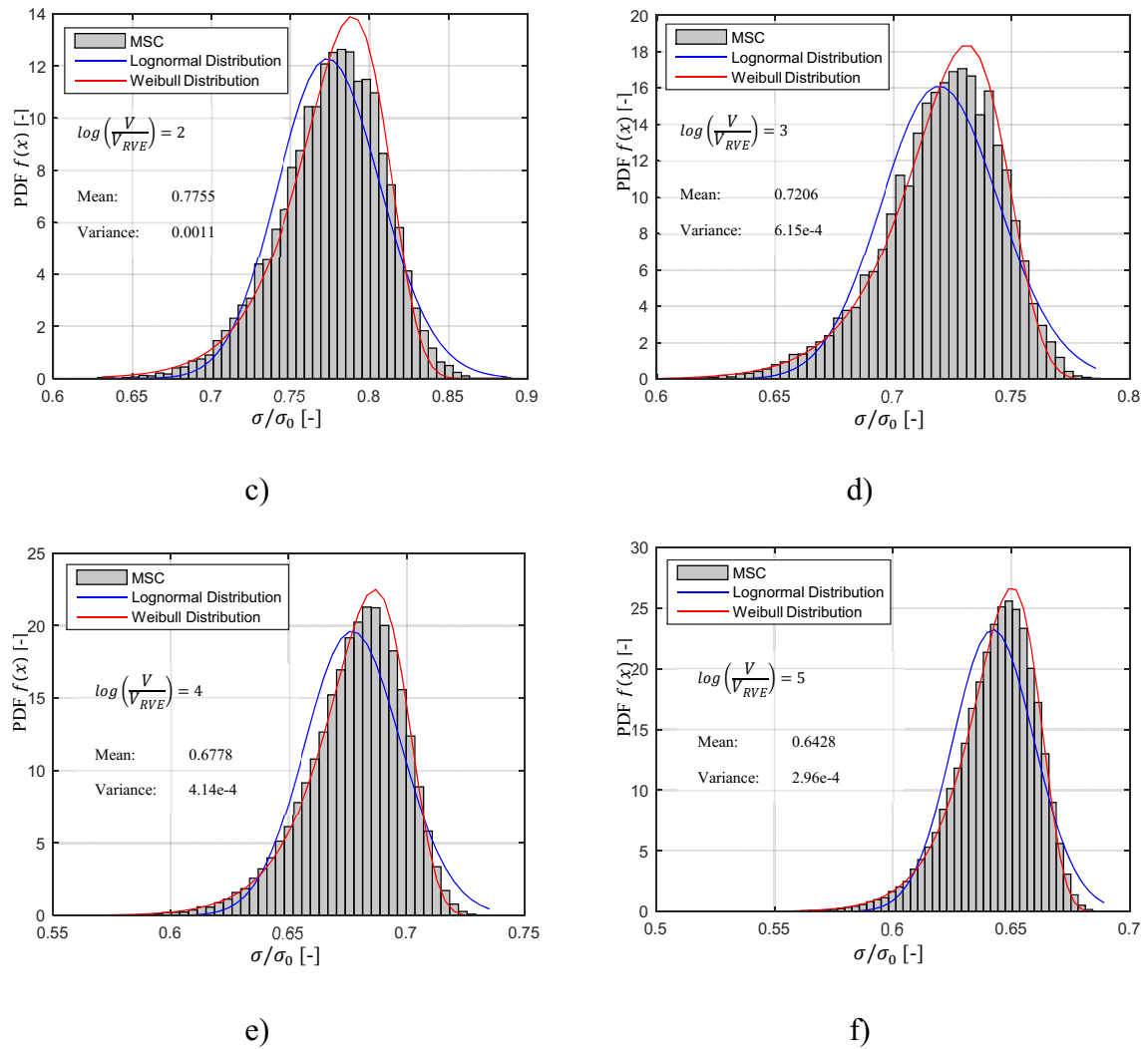


Figure 2.11: Distribution of chain of bundle model with different volumes

2.2.5 Parameter study of the stochastic material model

The probability density function $f_p(\sigma)$ in Eq. (2.11) is theoretically a distribution function with three parameters, i.e., σ_u , σ_0 and ξ . It should be mentioned, however, with the increase of the number of unknown parameters, the probability distribution parameter estimation becomes more difficult. For simplicity, it is assumed that the lower limit of σ is defined as $\sigma_u = 0$. This means that this CDF has a zero threshold and only two parameters need to be considered in this thesis. Because the material parameters are used to describe the randomness of the material properties with different volumes, the parameters cannot be obtained directly by measurement. The influence of the specimen size cannot be considered by tensile tests with a single volume, since the ratio of the specimen volume and RVE is normally unknown. According to the theoretical model, the PDF $f_p(\sigma)$ is related to the volume of the structural component and the CDF $F_p(\sigma)$ is monotonically decreasing as the volume increases. Hence, the statistical parameters could be obtained through a series of experiments, as well as the material parameters can

be determined reversely using the corresponding statistical results. For this purpose, the method of moments is employed, which is the most straightforward and intuitive approach to estimate the parameters of distribution.

For $\sigma_u = 0$, the mean values $\bar{\sigma}$ and the coefficient of variation C_v of the strength can be determined with:

$$\frac{\bar{\sigma}}{\sigma_0} = \frac{E(\sigma)}{\sigma_0} = \int_{\sigma_u}^{\infty} \sigma dF_p(\sigma) = \int_0^{\infty} \frac{\frac{V}{V_{RVE}} e^{-\frac{V}{V_{RVE}} \xi^2 \operatorname{erf}\left(\frac{\ln(\sigma)}{\sqrt{2}\xi}\right) + \ln^2(\sigma) + \frac{V}{V_{RVE}} \xi^2}}{2 * \xi^2} \frac{d\sigma}{\sqrt{2\pi}\xi} \quad (2.12)$$

$$C_v = \sqrt{\frac{E(\sigma^2)}{(E(\sigma))^2} - 1} = \sqrt{\frac{\int_0^{\infty} \frac{\frac{V}{V_{RVE}} e^{-\frac{V}{V_{RVE}} \xi^2 \operatorname{erf}\left(\frac{\ln(\sigma)}{\sqrt{2}\xi}\right) + \ln^2(\sigma) + \frac{V}{V_{RVE}} \xi^2}}{2 * \xi^2} \frac{d\sigma}{\sqrt{2\pi}\xi}}{\left(\int_0^{\infty} \frac{\frac{V}{V_{RVE}} e^{-\frac{V}{V_{RVE}} \xi^2 \operatorname{erf}\left(\frac{\ln(\sigma)}{\sqrt{2}\xi}\right) + \ln^2(\sigma) + \frac{V}{V_{RVE}} \xi^2}}{2 * \xi^2} \frac{d\sigma}{\sqrt{2\pi}\xi}\right)^2} - 1} \quad (2.13)$$

By Eq. (2.12) and (2.13), the ratio of mean values $\bar{\sigma}$ and the scale parameter of strength σ_0 are written as the integral formula, and the coefficient of variation C_v of the material strength is the function consisting of V/V_{RVE} and material constant ξ . This integral couldn't be directly calculated due to the error function $\operatorname{erf}(\cdot)$. Because some primitive functions of integral are usually difficult or impossible explicitly to specify, it can be expressed with discrete values in numerical mathematics. The numerical integration is the approximate calculation of certain integrals. Based on the function approximation by an interpolation polynomial, it is attempted to determine the approximate values, if the integral function satisfies the intermediate value theorem. From this, the approximate solution of definite integrals could be calculated with numerical integration.

It is easy to prove that the integral functions $\sigma * F_p(\sigma)$ and $\sigma^2 * F_p(\sigma)$ are integrable on an interval $[0, \infty]$. Using the mathematical software MATLAB, the mean value and the coefficient of variation are determined, as well as it is described as a graph in Figure 2.12. It is clearly obvious that the reduction of the mean value is proportional to the increase of V/V_{RVE} . The $E(\sigma)/\sigma_0$ -value is reduced with increasing ξ -value if V/V_{RVE} is relatively large. The opposite occurs when V/V_{RVE} strives to one. In general, the strength of the specimens in relation to the volume is monotonously decreasing when the material constant ξ is positive and V_{RVE} is constant.

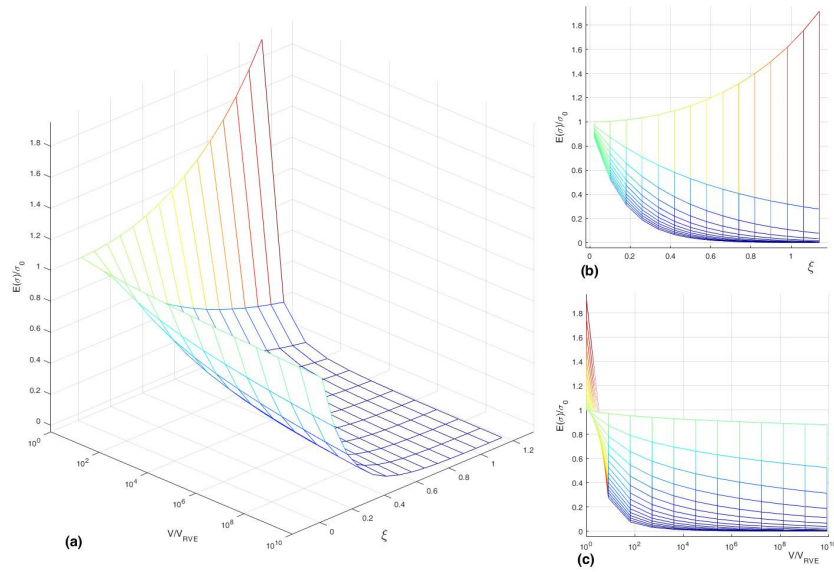
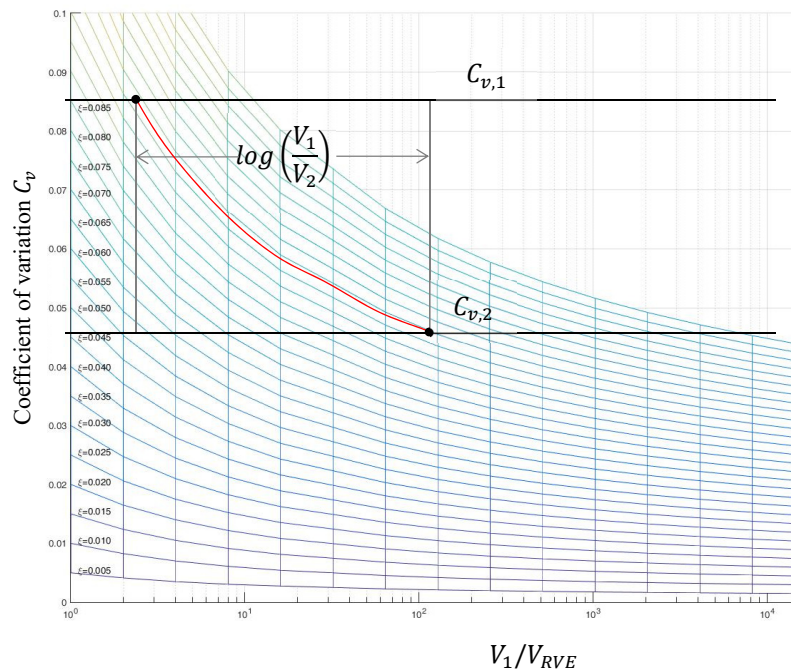


Figure 2.12: Numerical approximation of the mean values of strength distribution

In Figure 2.13, the coefficient of variation is represented by two variables V/V_{RVE} and ξ . The value decreases with increasing V/V_{RVE} . The coefficients of variation $C_{v,1}$ and $C_{v,2}$ can be determined by the tensile tests with two different specimens V_1 and V_2 . The parameter ξ is obtained with the help of Figure 2.13, where the ratio of volume is calculated according to Eq. (2.14). According to the approximation method, the material constant ξ will be determined with a certain proportion of volume, if the coefficient of variation locate on the interval $[C_{v,1}, C_{v,2}]$.

$$\log\left(\frac{V_1}{V_2}\right) = \log\left(\frac{V_1/V_{RVE}}{V_2/V_{RVE}}\right) = \log(V_1/V_{RVE}) - \log(V_2/V_{RVE}) \quad (2.14)$$


 Figure 2.13: Relationship between coefficient of variation ω and variables V/V_{RVE} under different ξ values

2.3 Generalization of the chain of bundles model

2.3.1 Stress gradient and multi-axial stress state

Since the chain of bundle model is a purely mathematical model, it can be used not only to accurately describe the relationship between strength and volume for the specimen with constant stress distribution, but also the specimen with stress gradient. The volume and stress of the specimen in the Eq. (2.10) cannot be treated as independent constant due to the existence of stress gradient. Therefore, the stress needs to be integrated on the interval of the entire specimen volume and the Eq. (2.10) is replaced by Eq. (2.15) as follows:

$$F_p(\sigma) = 1 - e^{-\frac{1}{V_{RVE}} \int_0^V \phi\left(\frac{\ln\left(\frac{\sigma - \sigma_u}{\xi}\right)}{\xi}\right) dV} = 1 - e^{-\frac{1}{V_{RVE}} \int_0^L \int_0^B \int_0^H \frac{1 + \operatorname{erf}\left[\frac{\ln(\sigma * f(x,y,z))}{\sqrt{2} * \xi}\right]}{2} dx dy dz} \quad (2.15)$$

where L , B and H represent respectively the length, width and height of the structural component, i.e., $V = L * B * H$. The $f(x, y, z)$ is the stress distribution function over the structure volume. The mean value of the material strength can usually be used to define the strength of the structure for arbitrary stress gradient and different volumes. The true strength of the material with the volume V can be expressed by Eq. (2.15).

$$\begin{aligned} \bar{\sigma}_V &= E(\sigma) = \sigma_0 * \int_{\sigma_u}^{\infty} \sigma dF_p(\sigma) \\ &= \sigma_0 * \int_0^{\infty} \frac{1}{V_{RVE}} * e^{-\frac{1}{V_{RVE}} * V * \alpha_1 * V * \alpha_2} \frac{1}{\sqrt{2\pi} * \xi} d\sigma \end{aligned} \quad (2.16)$$

where α_1 and α_2 are two reduction factors of effective volume and represented in Eq. (2.17) and (2.18).

$$\alpha_1 = \int_0^1 \int_0^1 \int_0^1 \frac{1 + \operatorname{erf}\left[\frac{\ln(\sigma * f(x,y,z))}{\sqrt{2} * \xi}\right]}{2} dx dy dz \quad (2.17)$$

$$\alpha_2 = \int_0^1 \int_0^1 \int_0^1 e^{-\frac{\ln^2(\sigma * f(x,y,z))}{2 * \xi^2}} dx dy dz \quad (2.18)$$

For simplicity, the SSE coefficient γ is defined as the ratio of mean value with volume V and V_0 of both the specimens under arbitrarily stress distribution.

$$\gamma = \frac{\bar{\sigma}_V}{\bar{\sigma}_{V_0}} = \frac{E(\sigma_V)/\sigma_0}{E(\sigma_{V_0})/\sigma_0} = \frac{\int_0^{\infty} \sigma_V dF_p(\sigma_V)}{\int_0^{\infty} \sigma_{V_0} dF_p(\sigma_{V_0})} = \int_0^{\infty} e^{-\frac{1}{V_{RVE}} * (\alpha_1 V - \alpha_{1,0} V_0)} * \frac{\alpha_2}{\alpha_{2,0}} d\sigma \quad (2.19)$$

It is assumed that the specimen strength $\bar{\sigma}_{V_0}$ with volume V_0 is obtained by uniaxial tensile test, which is carried out by a specimen with the circular cross-section. Therefore, the stress distribution function $f(x, y, z)$ is a constant and equal one, this two factors can be simplified as

$\alpha_{1,0} = (1 + \operatorname{erf}[\frac{\ln(\sigma)}{\sqrt{2}*\xi}])/2$ and $\alpha_{2,0} = \exp(-\frac{\ln^2(\sigma)}{2*\xi^2})$. At the same time, the material constant ξ and the volume of RVE V_{RVE} can be obtained by a series of tensile tests. Therefore, the strength of the structure with arbitrarily volume under arbitrarily form of load can be calculated with the SSE coefficient γ by the following equation.

$$\bar{\sigma}_V = \gamma * \bar{\sigma}_{V0} = \bar{\sigma}_{V0} * \int_0^\infty e^{-\frac{V}{V_{RVE}}*(\alpha_1 - \alpha_{1,0})} * \frac{\alpha_2}{\alpha_{2,0}} d\sigma \quad (2.20)$$

Since the tensile tests are loaded into one axis, the yield stress and the first main stress are equal ($\sigma = \sigma_I$). The above-described strength relationship is applicable when regarding the case of a uniaxial stress state. For the complex multi-axis stress situation, we need to make some assumptions. In order to consider the SSE in the multi-axial stress state, the following hypotheses are assumed:

- Maximum distortion energy theory (von Mises yield criterion) [85] is still applied within statistical size effect.
- The size effect coefficient in normal stress state and shear stress state are same ($\gamma = \gamma_\sigma = \gamma_\tau$).
- Steel is an isotropic material, i.e., the SSE coefficient γ in each direction is same.

With the help of these assumptions, the multi-axial stress state in a real structural component is replaced by fictional uniaxial stress, namely von Mises stress, as well as directly compared with the characteristic values from the tensile tests. The SSE with a non-constant stress state is considered by the SSE coefficient γ .

The yield strength of the material under specified volume can theoretically be obtained by the uniaxial tensile test. Therefore, the yield strength can be applied to any structural component with any size and any stress distribution over the volume by the reduction and amendment with the help of SSE coefficient γ . It is clear that the analysis of statistical size effect can be transformed into the calculation of the SSE coefficient. It is often difficult to determine the stress distribution function $f(x, y, z)$, since the stress distribution function is not only affected by the component geometry and the load types, but also constantly changing with the loading history of the structure. This means that the traditional analytical method cannot solve such problems. Therefore, the SSE coefficient γ is derived by numerical method in the following section.

2.3.2 Numerical methods to solve the statistical size effect coefficient

It is clear that the analytical integration cannot be solved if the primitive function is not explicit in a database. An approximation of integral calculation, which is based on the discretization of

the continues problem with the numerical method, could be employed to calculate the integral for the coefficient γ in Eq. (2.19). In this thesis, the coefficient γ will be determined by Subroutine UMAT in commercial FEM software ABAQUS. The yield strength of each integral point will be previously defined, and then it is reduced by multiplying the corresponding SSE coefficient. The User Subroutine in ABAQUS needs to be written with the efficient basic programming language FORTRAN [86]. The main effort of the calculation lies in the solution of the multiple integrals of α_1 in Eq. (2.17) and α_2 in Eq. (2.18) and solving the definite integral on the interval $[0, \infty]$.

For determination of the integral with an infinite upper limit, it is necessary that the integrand converted to a finite limit on the interval. A non-linear transformation of the integration variables is recommended in this thesis. The aim is to map the integration area to a standardized area, so that it is possible to use the integral formula in a limited area. By a substitution $t = 1/(1 + \sigma)$, the improper integral is replaced by an integrand with a bounded interval $[0, 1]$ in Eq. (2.21), where $t'dt$ is the required substitution for $d\sigma$.

$$\gamma = \frac{\sigma}{\sigma_0} = \int_0^\infty \frac{1}{\sqrt{V_{RVE}}} \frac{e^{-\frac{1}{\sqrt{V_{RVE}}} V \alpha_1 * V \alpha_2}}{\sqrt{2\pi\xi}} d\sigma = \int_0^1 \frac{1}{\sqrt{V_{RVE}}} \frac{e^{-\frac{1}{\sqrt{V_{RVE}}} V \alpha_{t,1} V * \alpha_{t,2}}}{\sqrt{2\pi\xi}} dt \quad (2.21)$$

To simplify the multiple integral, it is assumed that the stress distribution function $df(x, y, z)$ is constant, when $dV (dxdydz)$ is small relative to the entire component. According to Eq. (2.22) and (2.23), the coefficients $\alpha_{t,1}$ and $\alpha_{t,2}$ can be determined by the discretization of the continuous problem with the sum of the product of infinitesimal volume [87] and the corresponding stress, which can be solved very efficiently with the computer.

$$\alpha_{t,1} = \int_0^1 \int_0^1 \int_0^1 \frac{1 + \operatorname{erf}\left(\frac{\ln\left(\left(\frac{1}{t}-1\right)f(x,y,z)\right)}{\sqrt{2\xi}}\right)}{2} dxdydz \approx \sum_{i=1}^n \frac{V_i}{V} \frac{\operatorname{erf}\left(\frac{\ln\left(\left(\frac{1}{t}-1\right)f(x,y,z)\right)}{\sqrt{2\xi}}\right)}{2} \quad (2.22)$$

$$\alpha_{t,2} = \int_0^1 \int_0^1 \int_0^1 e^{-\frac{\ln^2\left(\left(\frac{1}{t}-1\right)f(x,y,z)\right)}{2\xi^2}} dxdydz \approx \sum_{i=1}^n \frac{V_i}{V} e^{-\frac{\ln^2\left(\left(\frac{1}{t}-1\right)f(v_i)\right)}{2\xi^2}} \quad (2.23)$$

After the algebraic substitution, the coefficient α_1 and α_2 will be resulted in exponentially decaying integrand [87], which is efficiently applicable to the trapezoid rule. Because of the simplification of the stress in the infinitesimal volume, the finite element mesh generation is defined preferably finely. In contrast, the mesh in the modeling of FEM is as coarse as possible for the reason that the simulations with the iteration of non-linear material properties need to consume significant computational resources. Hence, using the stochastic material model for

the analysis of structures need to find the balance between computational accuracy and computational efficiency, especially for the structures with stress gradient. The more detailed discussion will be presented in section 4.3.4.

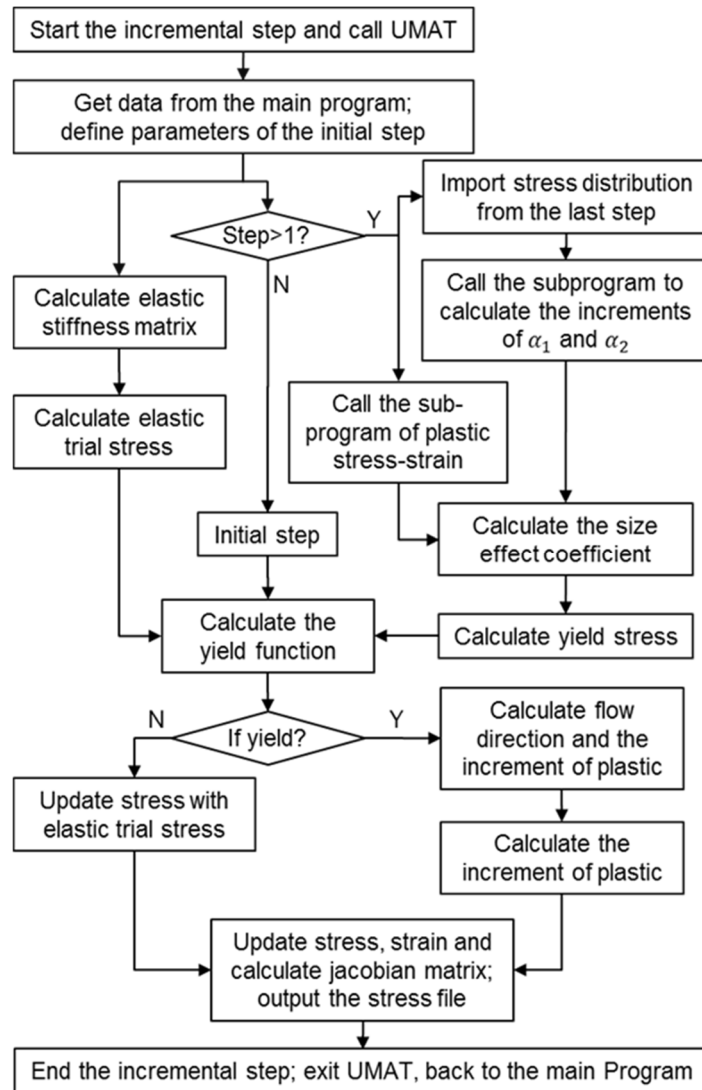


Figure 2.14: Flowchart of UMAT-Subroutine

Because the stress distribution changes nonlinearly in the plastic phase, an iterative method in every substep is applied to solve the nonlinear elasto-plastic problem. Firstly, it is assumed that the deviation of the two adjacent iteration steps is negligible, when the increment of iteration step is small. Because the stress distribution of current iteration step is unknown, the stress distribution function $f(x, y, z)$ will be replaced by the distribution of the previous iteration step. Therefore, the SSE coefficient γ can be calculated for each iteration steps. After determination of the yield criterion, the Jacobi matrix and updated stresses are determined. Simultaneously, the Jacobi matrix is transferred back to a whole stiffness to the main program. To illustrate the implementation of Subroutine, the flowchart for UMAT is shown in Figure 2.14.

2.4 Conclusions

In this chapter, a new stochastic material model for the elasto-plastic material was proposed. This model can be used to analyze the statistical size effect. Firstly, the classical stochastic material model has been briefly described, as well as the modeling and application scope of the two most fundamental models are discussed in detail. By analyzing the real material properties, it is generally considered that the two classical random material models are not able to describe the material properties very accurately, namely a new material model needs to be developed. Subsequently, the chain of bundle model based on two classical models was proposed and employed to describe the statistical size effect for steel. According to the mathematical analysis, the probability distribution function of this chain of bundle model is not constant, i.e., this probability distribution was skewed to the left with a small volume of the structural component and to the right with big specimen size. Besides, a numerical simulation proves the correctness of this model. Finally, the proposed model was extended to analyze the steel structure with multi-axial stress state using the von Mises yield criterion. This model was also applied to structural components with non-uniform stress distribution.

Furthermore, the stochastic material model was integrated into the commercial FEM software ABAQUS by user subroutine. In the following chapters, the statistical size effect of steel will be verified by uniaxial tensile tests and bending tests, and the parameters of statistical size effect will be determined by experimental results and simulations. The simulation with the chain of bundle model will be carried out in section 4.3 and the results of simulation will be compared with results of the experiment and stochastic finite element method.

3 Uncertainty modeling and implementation of stochastic FEM

3.1 Introduction

Essentially, the uncertainties of the material properties are necessarily presented in the entire volume of the structural component, because the mechanical defects of the material are randomly distributed in the whole structure. Nowadays, it is widely recognized that the material properties are characterized by intrinsic randomness and uncertainty, as well as these properties exhibit stochastic variation in space. The conventional method, where the structure is modeled by the reduced mean value of basic random variables, is not adequate since it is not able to reproduce the point-to-point variability. The random field is a useful mathematical model that can describe the properties of spatial variability accurately in the structural component. However, the numerical method used in structure analysis cannot directly deal with continuous models; thus the discretization of the random field is required. The purpose of discretization is to approximate the random field by the finite set of random variables. Nevertheless, if the discretization of the random fields used to describe the performance of the structure is not accurate enough, the investigation of reliability analysis could be misleading. Moreover, obtaining the approximate random field with the correct statistical parameters is a prerequisite for the study of SFEM.

The statistical size effect based on the mathematical model can be obtained the results, which are the phenomenon by a variety of assumptions and simplifications. The SSE based on the uncertainty of the material properties can be theoretically described with the FEM simulation, when the material randomness can be defined with the mathematical model. A powerful approach to solve this kind of problem is the stochastic FEM. The SFEM is treated as an extension of the classical deterministic FE approach in numerous studies. Recently, Stefanou provided a state-of-the-art review of past and recent developments in the area of SFEM and given some open issues to be studied and solved [46]. One of the most urgent needs for applications of SFEM in engineering problems is to develop a robust and efficient framework that can interact with powerful third-party codes [58].

In this chapter, the Kahunen-Loève expansion is used to implement the random field, and the acceptable approximated random field is obtained by truncating the series expansion. Afterwards, the material properties in the random field are assigned to the integrations point by the

3D interpolation function with the proposed mapping-interpolation method. The error of discretization and interpolation is formulated for each step with corresponding error estimator. The constitutive equation of elasto-plastic material is decomposed into deterministic and stochastic parts in the finite element software, as well as it will be solved by Monte Carlo simulation. Besides, this method will be developed to analyze three-dimensional bodies with nonlinear elasto-plastic material and to apply in a variety of element types in commercial FEM software.

3.2 Uncertainty modeling

3.2.1 Probability space and random variables

The observation of random phenomena is traditionally called the experiment. A probability space is constructed with a specific kind of situation or experiment in mind. All the possible outcomes of an experiment form the sample space, usually represented by Ω . The probability theory aims at associating numbers to events, i.e., their probability of occurrence. Let P denote this so-called probability measure. The collection of possible events having well-defined probabilities is called the σ -algebra associated with Ω , indicated here by F . Finally, the probability space constructed utilizing this notion is denoted by (Ω, F, P) . In probability theory, a probability space consists of three parts:

- Ω : Sample space, which is the set of all possible outcomes.
- F : Set of events, which is a collection of some subset of Ω and where each event can be a set containing zero or more outcomes.
- P : Probability measure, which can describe the possibility of all the events included in F in a random experiment.

Intuitive understanding, the sample space Ω is the range of all possible outcomes before the experiment has been predictable. The set of events F specifies which subset of Ω can be called an Event, thus avoiding the paradox caused by unpredictable sets. The probability measure P is a function returning an event's probability. A probability is a real number between zero and one. The probability measure function must satisfy two simple requirements: the probability of a countable union of mutually exclusive events must be equal to the countable sum of the probabilities of each of these events and the measure of entire sample space is equal to one. It is clear that the probability measure P can determine the probability of each event.

Due to the accidental factors, some variables may take a variety of different values with uncertainty and randomness under different conditions, but these values fall within a certain range of probability is certain. These variables are called random variables. A real random variable X is

a mapping $X: (\boldsymbol{\Omega}, \mathbf{F}, \mathbf{P}) \rightarrow \mathbb{R}$. The probability of outcomes measurable is given by a set of all event, but a single random variable does not return the probability. For the continuous random variables, the PDF and CDF are represented respectively by $f_X(x)$ and $F_X(x)$. Some random phenomena need to be described by multiple random variables at the same time. A random vector \mathbf{X} is a collection of random variables. The probability distribution of random variables is often characterized by a small number of parameters, which also have a practical interpretation. The mathematical concept of expected value of the continuous random variable denoted by $E(*)$. The mean value, variance and n -th moment of random variable X are shown as following:

$$\mu = E[X] = \int_{-\infty}^{\infty} x f_X(x) dx \quad (3.1)$$

$$\sigma^2 = E[(X - \mu)^2] = \int_{-\infty}^{\infty} (x - \mu)^2 f_X(x) dx \quad (3.2)$$

$$E(X^n) = \int_{-\infty}^{\infty} x^n f_X(x) dx \quad (3.3)$$

In probability theory and statistics, the covariance is used to measure the global error of two variables. The variance is a special case of covariance, i.e., when two variables are the same. The covariance $Cov(X, Y)$ between two real random variables X and Y of $E[X]$ and $E[Y]$ is defined as:

$$\begin{aligned} Cov(X, Y) &= E[(X - E[X])(Y - E[Y])] = E[XY] - E[X]E[Y] \\ &= \iint_{-\infty}^{\infty} (x - \mu_X)(y - \mu_Y) f_{X,Y}(X, Y) dx dy \end{aligned} \quad (3.4)$$

As a measure of correlation between X and Y , The covariance is effective for the situation with the same physical dimension. However, the covariance of two variables shows great differences when the two variables are used in the different dimensions. Therefore, the following concepts, namely correlation coefficient $\rho_{X,Y}$, are introduced to describe the correlation of random variables.

$$\rho_{X,Y} = Corr(X, Y) = \frac{Cov(X,Y)}{\sigma_X \sigma_Y} \quad (3.5)$$

3.2.2 Random field in Hilbert spaces

Many of physical phenomena in nature can be attributed to the external manifestations under the influence of distributed of disorder system. This system can be described as a random field in probability space or a random process based on time. Vanmarcke [30] illustrates the origin and establishment of the random field, as well as suppose that the establishment of the random

field is a passive process. This is because all aspects of the system cannot be known, and can only obtain the information of the parts by collecting part of the sample. Finally, the random field is established using the estimated approach.

The random field is the generalization of the random process in the spatial domain. The basic parameters of the random field $H(\mathbf{X})$ are the position vector $\mathbf{X} = (x, y, z)$. The random field is not a conventional engineering problem, because it involves a somewhat abstract and mathematical concept. Therefore, it is necessary to keep the degree of abstraction at the minimum to avoid obscuring the engineering aspects of the problem. In this section, the mathematical description of the random field will be elaborated in the simplest way.

A random field $H(\mathbf{X}, \theta)$ is defined in the Hilbert space over a domain \mathbf{D} with values on the real line \mathbb{R} . The probability space of real random variables with the finite second moment ($E(X^2) < \infty$) is denoted by $L(\Omega, \mathcal{F}, \mathbf{P})$. $H(\mathbf{X}, \theta)$ is a collection of random variables indexed by a continuous parameter $\mathbf{X} \in \mathbf{D}$, where θ is an element of Ω . This means that the random field $H(\mathbf{X}_0, \theta)$ is a random variable if the position vector \mathbf{X}_0 is given. In other hands, $H(\mathbf{X}, \theta_0)$ is a realization of the field function for a given outcome θ_0 .

It is assumed that each element of $H(\mathbf{X}, \theta)$ in the Hilbert space is integrable functions over \mathbf{D} . If the inner product of two elements in the Hilbert space and the probability space vanishes, the two elements of the Hilbert space is orthogonal [56]. Then, the random field can be defined as a curve in the Hilbert space. Hilbert spaces have beneficial properties to develop approximate solutions of boundary value problems, such as the Galerkin procedure.

Although most of the uncertainties present in practice are essentially non-Gaussian, the Gaussian assumption is often used, due to its simplicity and lack of relevant experimental data. In addition, from the central limit theorem and the maximum entropy principle with the information on the second-order moments, the Gaussian stochastic random field assumption is reasonable. If the all element $\{H(\mathbf{X}_1, \theta), H(\mathbf{X}_2, \theta) \cdots H(\mathbf{X}_n, \theta)\}$ is Gaussian, the corresponding random field $H(\mathbf{X}, \theta)$ is Gaussian. A Gaussian random field is completely defined by the mean $\mu(\mathbf{X})$, variance $\sigma^2(\mathbf{X})$ and correlations coefficient function $\rho_{\mathbf{X}, \mathbf{X}'}$. The corresponding correlations length is normally a characteristic parameter.

The main difficulty is to describe the abstract measure space in a limited physical intuitive space when the random field is associated with the numerical finite element analysis. This is because, it involves the treatment of functions defined on these abstract spaces and the random variables defined on the σ -field of random events. The widely used method is the Monte Carlo simulation with the sampling and random selection of random variables. However, if a good approximation

wants to be achieved, this approach needs to sample a considerable number of points. Generally, it gives two most often used and more appealing methods developed for the simulation of Gaussian random processes and fields: the spectral representation method and the Karhunen–Loève expansion. In this thesis, the K-L expansion will be mainly used.

A random field is called one- or multi-dimensional RF depending on whether the dimension d of \mathbf{X} is $d = 1$ or $d > 1$. It is uni- or multi-variate according to the quantity $H(\mathbf{X})$ attached to position \mathbf{X} , that is a random variable or a random vector. The multi-dimensional random field will be considered and this thesis will focus on the three-dimensional random field in the following. In a practical situation, the mechanical properties of the material are a random field with multi-variate, such as Poisson’s ration, Young’s modulus, yield stress and tensile strength. It is assumed that these parameters are statistically independent, and for the sake of simplicity, it can be described by numerous random field with uni-variate. Therefore, in chapter uni-variate multidimensional random field will be considered and simulated.

3.2.3 Karhunen-Loève series expansion

The Kahunen-Loève series expansion is a series expansion method for the representation of the random field. This approach is based on the spectral decomposition of the covariance function $C_{HH}(\mathbf{X}_1, \mathbf{X}_2)$ of the field. In this thesis, K-L expansion is used for discretization of spatially varying random field in the three-dimensional domain. The 3D random field $H(\mathbf{X}, \theta)$ with non-zero means and Gaussian (or non-Gaussian) distributions are decomposed into a deterministic part and a stochastic part as follows:

$$H(\mathbf{X}, \theta) = \mu(\mathbf{X}) + \sum_{i=1}^{\infty} \sqrt{\lambda_i} \xi_i(\theta) \varphi_i(\mathbf{X}) \quad (3.6)$$

where $H(\mathbf{X}, \theta)$ is a random field on a probability space; \mathbf{X} represents the position vector defined over the space domain D and θ is primitive randomness that belongs to the space of random event; $\mu(\mathbf{X})$ is the mean function of the field, however $\mu(\mathbf{X})$ is defined as a constant and does not vary over the domain D ; $\xi_i(\theta)$ is a statistically uncorrelated random variable with zero mean; λ_i and $\varphi_i(\mathbf{X})$ are the eigenvalue and the eigenfunction of the covariance kernel, which are the solution to the homogeneous Fredholm integral equation of second kind [88]:

$$\int_D C_{HH}(\mathbf{X}_1, \mathbf{X}_2) \varphi_i(\mathbf{X}_2) d\mathbf{X}_2 = \lambda_i \varphi_i(\mathbf{X}_1) \quad (3.7)$$

In this chapter, the covariance function $C_{HH}(\mathbf{X}_1, \mathbf{X}_2)$ is considered as the kernel function. By definition, the covariance function is a bounded, symmetric and positive semi-definite kernel. The eigenfunctions are continuous and orthogonal to each other in accordance with Mercer’s

theorem, when the corresponding eigenvalues are nonnegative [89]. Therefore, it can be written as the follows:

$$C_{HH}(\mathbf{X}_1, \mathbf{X}_2) = \sum_{i=1}^{\infty} \lambda_i \varphi_i(\mathbf{X}_1) \varphi_i(\mathbf{X}_2) \quad (3.8)$$

Because the symmetry and the positive definiteness of the covariance kernel, the eigenfunctions are orthogonal and form a complete set. It can be normalized according to the following criterion.

$$\int_D \varphi_i(\mathbf{X}) \varphi_j(\mathbf{X}) d\mathbf{X} = \delta_{ij} \quad (3.9)$$

where δ_{ij} is the Kronecker delta. In most of the civil engineering applications, the random fields are assumed to be weakly homogeneous. Compared to other materials, the steel is more consistent with the isotropic properties. Therefore, the random field of steel strength is seen as purely homogeneous and they are determined by the marginal distribution, i.e. the corresponding mean value and variance, and the covariance function. In the Gaussian random field, the covariance function depends on the distance $d = \mathbf{X}_2 - \mathbf{X}_1$ between two points in the 3D space, as well as it can be expressed by the autocorrelation function $\rho_{HH}(\mathbf{X}_1, \mathbf{X}_2)$, i.e., $C_{HH}(\mathbf{X}_1, \mathbf{X}_2) = \sigma(\mathbf{X}_1) \cdot \sigma(\mathbf{X}_2) \cdot \rho_{HH}(\mathbf{X}_1, \mathbf{X}_2)$, where σ is the standard deviation of random field. In research [30,90], isotropic exponential in Eq. (3.10), squared exponential in Eq. (3.11) and sine functions in Eq. (3.12) are defined as autocorrelation coefficient function for numerical analysis in most multidimensional homogenous and isotropic random fields in Figure 3.1.

$$\rho_{HH,1}(\mathbf{X}_1, \mathbf{X}_2) = \exp\left(-\frac{|\mathbf{X}_1 - \mathbf{X}_2|}{L_c}\right) = \exp\left(-\frac{|x_1 - x_2|}{l_x} - \frac{|y_1 - y_2|}{l_y} - \frac{|z_1 - z_2|}{l_z}\right) \quad (3.10)$$

$$\rho_{HH,2}(\mathbf{X}_1, \mathbf{X}_2) = \exp\left[\left(-\frac{|\mathbf{X}_1 - \mathbf{X}_2|}{L}\right)^2\right] \quad (3.11)$$

$$\rho_{HH,3}(\mathbf{X}_1, \mathbf{X}_2) = \frac{\sin\left(\frac{2.2|\mathbf{X}_1 - \mathbf{X}_2|}{L_c}\right)}{\frac{2.2|\mathbf{X}_1 - \mathbf{X}_2|}{L_c}} \quad (3.12)$$

where L_c is the correlation length of the random field; $|x_1 - x_2|$, $|y_1 - y_2|$ and $|z_1 - z_2|$ are the distances of two points in different directions; l_x , l_y and l_z are the physical correlation lengths in different directions. In this analysis, the most common forms will be selected and used, but the method can be applied to arbitrary types of autocorrelation coefficient function. The correlation length and distance of two points are considered separately in different directions. Therefore, the analysis can be applied without modification for the problem with different correlation lengths in different directions, namely anisotropic.

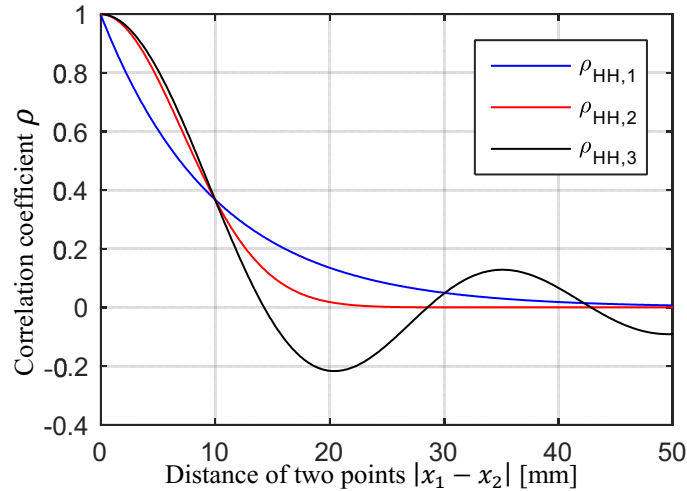


Figure 3.1: Comparison of different correlation functions $L_c = 20 \text{ mm}$

The small probability events in the random field, which are sensitive to the tail regions of probability distributions, are often very important for SFEM and structural reliability. Because of the central limit theorem, an arbitrary distribution would be nearly or approach to Gaussian in most cases. Hence, the non-Gaussian random field can be transformed using the preceding discretization method of random field so that the distribution information is accurately represented. Usually, the discretization of the Gaussian random field with K-L series expansion not only accurately represent the first two moments, but also the behavior of the field in the far tail of the underlying distribution [91]. This discretization is a linear expansion of the Gaussian distribution and the Gaussian distribution remains closed in the linear transformation. If the random field $H(\mathbf{X}, \theta)$ is Gaussian distribution, then $\xi_i(\theta)$ in Eq. (3.6) are uncorrelated random variables of standard normal distribution. In other cases, the non-Gaussian distribution of $\xi_i(\theta)$ is difficult to be employed. The K-L expansion is widely used to the discretization of the Gaussian random field. However, a direct application of these methods cannot provide accuracy for a non-Gaussian distribution.

For non-Gaussian random field, it is not feasible directly to apply these methods even if the first two moments are accurately expressed since it is not able to provide the accuracy in the tail probability. A classical way is using a translations processes to extend the non-Gaussian [92], where the non-Gaussian random field will be transformed to a Gaussian field with a nonlinear function. If a non-Gaussian random field is classified as translation field, it can be defined as a nonlinear function of a Gaussian field through a mapping method in Eq. (3.13).

$$H_{tran}(\mathbf{X}, \theta) = g[H(\mathbf{X}, \theta)] \quad (3.13)$$

where $H_{tran}(\mathbf{X}, \theta)$ is the non-Gaussian random field after the nonlinear translation; $g[*]$ represents a nonlinear function. The lognormal distribution can be obtained with Gaussian distribution through the Eq. (3.14) [58]. Simultaneously, the standard deviation σ_N and mean value μ_N in Gaussian distribution are used as in Eq. (3.15) and (3.16) for variance σ_L^2 and mean value μ_L of the uncertainties of material properties with the lognormal distribution.

$$H_{tran}(\mathbf{X}, \theta) = \exp\left[\mu_N(\mathbf{X}) + \sum_{i=1}^{\infty} \sqrt{\lambda_i} \xi_i(\theta) \varphi_i(\mathbf{X})\right] \quad (3.14)$$

$$\sigma_N = \sqrt{\ln\left[\left(\frac{\sigma_L}{\mu_L}\right)^2 + 1\right]} \quad (3.15)$$

$$\mu_N = \ln\mu_L - \frac{1}{2}\sigma_N^2 \quad (3.16)$$

Theoretically, the correlation coefficient function $\rho_{HH}(\mathbf{X}_1, \mathbf{X}_2)$ needs to be translated as $\rho_{HH}^{tran}(\mathbf{X}_1, \mathbf{X}_2)$ of the desired non-Gaussian random field through an integral equation in [91]. In general, $\rho_{HH}^{tran}(\mathbf{X}_1, \mathbf{X}_2) \leq \rho_{HH}(\mathbf{X}_1, \mathbf{X}_2)$ and for the most cases $\rho_{HH}^{tran}(\mathbf{X}_1, \mathbf{X}_2) \approx \rho_{HH}(\mathbf{X}_1, \mathbf{X}_2)$ [93]. Therefore, the correlation coefficient function $\rho_{HH}^{tran}(\mathbf{X}_1, \mathbf{X}_2)$ of the non-Gaussian random field is usually estimated directly with $\rho_{HH}(\mathbf{X}_1, \mathbf{X}_2)$. If the coefficient of variance C_v is small, the distortion of the correlation structure caused by the nonlinear transformation will be small [94]. Consequently, the K-L expansion can be used for the non-Gaussian random field in the case of small C_v .

3.2.4 Numerical solution of the K-L expansion

The sum of the infinite number of terms in Eq. (3.6) is impossible to achieve in the discretization with the numerical method. Hence, the K-L expansion can be approximated using truncated expansion after M terms:

$$\hat{H}(\mathbf{X}, \theta) = \mu(\mathbf{X}) + \sum_{i=1}^M \sqrt{\hat{\lambda}_i} \hat{\xi}_i(\theta) \hat{\varphi}_i(\mathbf{X}) \quad (3.17)$$

The approximation $\hat{H}(\mathbf{X}, \theta)$ of the continuous series expansion by finite M set of random variables is called as discretization of the random field. Because the analytical solution of the Fredholm integral equation only exists for a limited set of covariance function, the Galerkin finite element approach is more suitable to solve the random field with K-L expansion problem. In Galerkin finite element approach, the eigenfunction is approximated by discretizing to a combination of basic functions $\phi_j(\mathbf{X})$. It can be expressed as follows,

$$\hat{\varphi}_i(\mathbf{X}) = \sum_{j=1}^n d_{ij} \phi_j(\mathbf{X}) \quad (3.18)$$

where d_{ij} is the j th nodal value of the i th eigenfunctions; n is the number of nodes per random field element.

The basic functions can be defined as any orthogonal polynomial in the Hilbert space. The choice of the basic functions is variable and uncertain, such as piecewise polynomials in [56], Legendre orthogonal polynomials in [95], Hierarchic Gegenbauer polynomials in [89] and Lagrange interpolation polynomials in [58], etc. In this thesis, the Lagrange interpolation polynomials from shape function of eight nodes in 3D linear finite element have been selected as the basic functions, so that the random field of material properties and stress field can be better mapped with each other in commercial finite element software. The 3D element is obtained by the expansion of the 1D linear element with two points in the Cartesian coordinate system [96]. In order to ensure continuity between the elemental domains, one-dimensional local basis functions are chosen as the following piecewise linear polynomials,

$$l_1^{1D} = \frac{1-\eta}{2} \quad (3.19)$$

$$l_2^{1D} = \frac{1+\eta}{2} \quad (3.20)$$

where η is the local coordinate that runs on the standard interval $[-1,1]$.

In Galerkin method, by substituting Eq. (3.18) to the eigenfunctions of Eq. (3.7) and applying Galerkin procedure to the corresponding residual, a generalized algebraic eigenvalue problem is obtained,

$$\mathbf{AD} = \mathbf{ABD} \quad (3.21)$$

where the different matrices are defined as follows,

$$\mathbf{A}_{ij} = \int_{\mathbf{D}} \int_{\mathbf{D}} C_{HH}(\mathbf{X}_1, \mathbf{X}_2) \phi_i(\mathbf{X}_1) \phi_j(\mathbf{X}_2)^T \mathbf{J}_e^2 d\mathbf{X}_1 d\mathbf{X}_2 \quad (3.22)$$

$$\mathbf{B}_{ij} = \int_{\mathbf{D}} \phi_i(\mathbf{X}) \phi_j(\mathbf{X})^T \mathbf{J}_e d\mathbf{X} \quad (3.23)$$

$$\mathbf{D}_{ij} = \mathbf{d}_{ij} \quad (3.24)$$

$$\mathbf{\Lambda}_{ij} = \delta_{ij} \lambda_{ij} \quad (3.25)$$

where \mathbf{J}_e is coefficient matrix mapping from local coordinates of RF element to global physical coordinates; δ_{ij} is the Kronecker symbol, so that the eigenvalues λ_{ij} are located on the diagonal of the matrix $\mathbf{\Lambda}$.

On three-dimensional domains, the position vector can be decomposed into three orthogonal components. This means that Eq. (3.22) and (3.23) constitute respectively a three-fold and a

six-fold integral. This will require unacceptable computational resources in 3D random field problem. Following Ghanem and Spanos in [56], the solution of the multi-dimensional eigenvalue and eigenfunction problem is obtained by products of one-dimensional solutions in the orthogonal coordinate system. For three dimensional element, the eigenfunction can be written in a product of components of different dimensions as follows,

$$\hat{\phi}_i(\mathbf{X}) = \hat{\phi}_i(x, y, z) = \hat{\phi}_i(x) \cdot \hat{\phi}_i(y) \cdot \hat{\phi}_i(z) \quad (3.26)$$

In Eq. (3.26), the shape function for an arbitrary Lagrangian hexahedral element can be obtained by multiplying the one-dimensional Lagrangian polynomials in each direction. The isotropic exponential covariance function in Eq. (3.10) can be determined by the product of autocorrelation functions in different orthogonal axes. It can be written as follows:

$$\phi_i(\mathbf{X}) = \phi_i(x, y, z) = \phi_i(x)\phi_i(y)\phi_i(z) \quad (3.27)$$

$$\begin{aligned} C_{HH}(\mathbf{X}_1, \mathbf{X}_2) &= \sigma^2 \exp\left(-\frac{|\mathbf{X}_1 - \mathbf{X}_2|}{L_c}\right) \\ &= \sigma^2 \exp\left(-\frac{|x_1 - x_2|}{l_x}\right) \exp\left(-\frac{|y_1 - y_2|}{l_y}\right) \exp\left(-\frac{|z_1 - z_2|}{l_z}\right) \end{aligned} \quad (3.28)$$

Hence, the Matrix \mathbf{A}_{ij} containing the sixth-order integral will be aggregated by three matrices which are derived from a one-dimensional element and have low-order integration. This composition of the matrix is determined by the position or coordinate of the three-dimensional element in each direction. The operation of Matrix \mathbf{A}_{ij} is expressed as in Eq. (3.29).

$$\mathbf{A}_{ij} = \sigma^2 \begin{bmatrix} \mathbf{A}_{111} & \cdots & \mathbf{A}_{1n} \\ \vdots & \ddots & \vdots \\ \mathbf{A}_{n1} & \cdots & \mathbf{A}_{nn} \end{bmatrix} = \sigma^2 \begin{bmatrix} \mathbf{A}_{111}^x \mathbf{A}_{111}^y \mathbf{A}_{111}^z & \cdots & \mathbf{A}_{1nx}^x \mathbf{A}_{1ny}^y \mathbf{A}_{1nz}^z \\ \vdots & \ddots & \vdots \\ \mathbf{A}_{nx1}^x \mathbf{A}_{ny1}^y \mathbf{A}_{nz1}^z & \cdots & \mathbf{A}_{nxx}^x \mathbf{A}_{nyy}^y \mathbf{A}_{nzz}^z \end{bmatrix} \quad (3.29)$$

$$\mathbf{A}_{ij}^x = \int_{x_1} \int_{x_2} \exp\left(-\frac{|x_1 - x_2|}{l_x}\right) \phi_i(x_1) \phi_j(x_2)^T \mathbf{J}_x^2 d x_1 d x_2 \quad (3.30)$$

$$\mathbf{A}_{ij}^y = \int_{y_1} \int_{y_2} \exp\left(-\frac{|y_1 - y_2|}{l_y}\right) \phi_i(y_1) \phi_j(y_2)^T \mathbf{J}_y^2 d y_1 d y_2 \quad (3.31)$$

$$\mathbf{A}_{ij}^z = \int_{z_1} \int_{z_2} \exp\left(-\frac{|z_1 - z_2|}{l_z}\right) \phi_i(z_1) \phi_j(z_2)^T \mathbf{J}_z^2 d z_1 d z_2 \quad (3.32)$$

where \mathbf{A}_{ij}^x , \mathbf{A}_{ij}^y and \mathbf{A}_{ij}^z are the components of matrix \mathbf{A}_{ij} from the one-dimensional element in x , y and z direction; n represent the n th element in 3D and nx , ny and nz are the number of element in each dimension, i.e., $n = nx \cdot ny \cdot nz$. Thus, the matrix \mathbf{B}_{ij} will also be using the decomposition and composition of the matrix in the various directions. By this method, the matrix \mathbf{B}_{ij} will be transformed from a three-order integral to a first-order integral. Therefore, it

is possible to discretize the 3D random field by using this method and the computational resources consumption is acceptable.

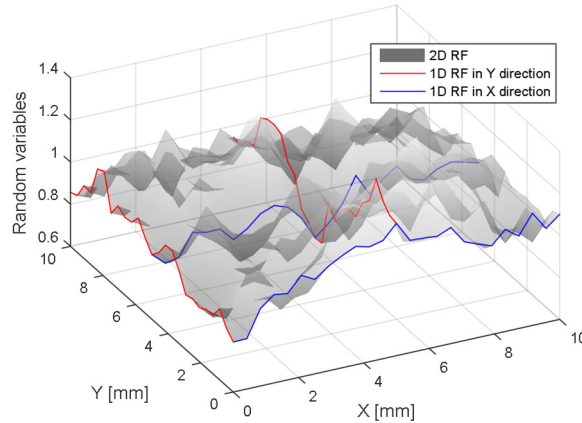


Figure 3.2: Illustration of 2D random field aggregated by 1D random field

The multidimensional expansion of 2D random field is illustrated in the Figure 3.2. It is obvious that the approach can accelerate the generation of multidimensional random field and use in in higher-dimensional RF. Figure 3.3 shows the different dimensional Random fields realized by the proposed approach based on the 1D random field. A virtual structure with length in every direction 10 mm was simulated. The corresponding length was divided into 20 discretization points associated with finite elements. This means that the random field has total 20^d discretization points, where d is a number of dimensions. These illustrations are the univariate Gaussian random field with mean $\mu_N = 1$, variance $\sigma_N^2 = 0.01$. The correlation properties of the structure were used the exponential function in Eq. (3.10) and the corresponding correlation length is 5 mm, i.e., $L_c = 5mm$.

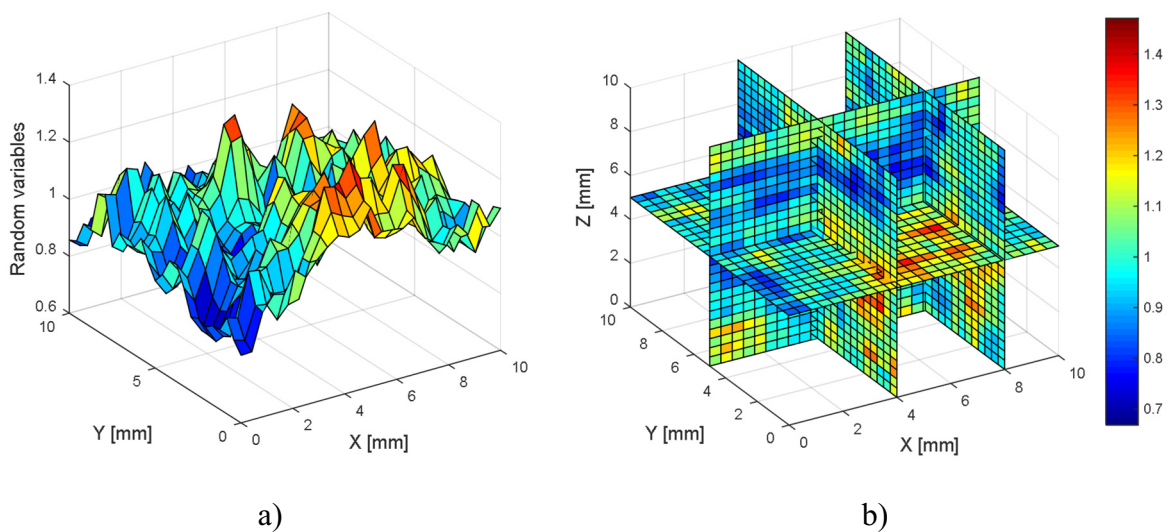


Figure 3.3: Random field, a) Two-dimensional, b) Three-dimensional

3.2.5 Simulation of pseudo random variables with Latin Hypercube sampling

Monte Carlo simulation is a widely used purely mathematical computer algorithm. In SFEM, this approach is employed to simulate the structural response with uncertain by using a very large number of similar random samples. To consider the uncertainties of material, a zero-mean and unit-variance independent Gaussian random variables $\xi_i(\theta)$ in the K-L series expansion need to be generated. A set of random variables can be described as realizations, observations or samples in MCS, so that a stochastic problem is transformed to a larger number of deterministic problems. However, the random variables $\xi_i(\theta)$ requires a sufficient number to describe the random field accurately. To reduce the computational time in the MCS, an efficient sampling method need to be used.

Due to the small number of iterations, Latin Hypercube Sampling, as a more efficient sampling method, has enormous advantages in terms of sampling efficiency and computational runtime [97]. In particular, LHS is also useful for the analysis of the situation where the probability distribution contains low probability events [98]. LHS ensures that off-center events are accurately represented during simulation through mandatory simulations. When the low probability results are very important, the LHS technique can efficiently simulate the effect of low probability events on the output distribution. This method can isolate low probability results and directly analyze the results response. With the help of the LHS method, the statistical properties of random field and low probability events of each simulated variable will be precisely presented with a small number of samples.

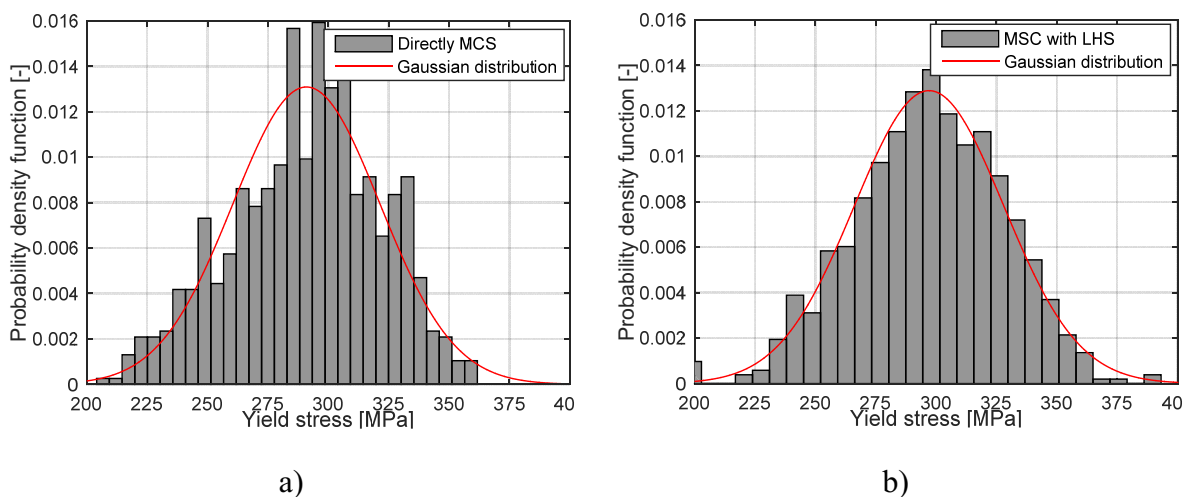


Figure 3.4: Gaussian random field samples generated by different methods, a) directly MCS, b) MCS with LHS

The LHS can provide an accurate representation of the random field only with a few random variables, as well as a quite small number of simulations is necessary for the simulations with SEFM. Figure 3.4 shows the stochastic samples of a 3D Gaussian random field with different

methods. Obviously, the samples obtained using the LHS technique are more in line with the target distribution density function than the directly MSC, where it is calculated with the same number of sampling for the uncorrelated random variables. Usually, the basic information of the random field is captured by the first second moment, i.e., mean value and variance, and the covariance function. However, the moment, correlation and spectral characteristics of the random variables cannot absolute accuracy be generated. Therefore, the statistical characteristics of the required field should be as close as possible to the target statistical parameters.

3.2.6 Discretization error estimator and optimization

The variance and the covariance functions of the truncated K-L expansion in Eq. (3.17) can be written as follows [99]:

$$Var[\hat{H}(\mathbf{X}, \theta)] = \hat{C}_{HH}(\mathbf{X}, \mathbf{X}) = \sum_{i=1}^M \lambda_i \varphi_i^2(\mathbf{X}) \quad (3.33)$$

$$Cov[\hat{H}(\mathbf{X}_1, \theta), \hat{H}(\mathbf{X}_2, \theta)] = \hat{C}_{HH}(\mathbf{X}_1, \mathbf{X}_2) = \sum_{i=1}^M \lambda_i \varphi_i(\mathbf{X}_1) \varphi_i(\mathbf{X}_2) \quad (3.34)$$

Because the truncated K-L expansion is approximated by a sum of infinitesimal terms as the sum of M terms. This means that this approximate calculation ignores the high order terms in the tail. Hence, it can be seen that the truncated K-L expansion underestimates the pointwise variance of the random field. In mathematical form can be written as in Eq. (3.35).

$$Var[\hat{H}(\mathbf{X}, \theta)] < Var[H(\mathbf{X}, \theta)] \quad (3.35)$$

where $Var[H(\mathbf{X}, \theta)]$ represents the target variance of the random field. The truncation of the K-L expansion means that the discretization of the random field is inevitable to produce errors. Therefore, the accuracy of the discretization can be expressed by reference to the variance and covariance function of the random field. The error measure for the discretization can be stated using the variance of the approximation and continuous random field. It is can be defined as follows [91],

$$\epsilon_{\sigma^2}(\mathbf{X}) = \frac{Var[H(\mathbf{X}, \theta) - \hat{H}(\mathbf{X}, \theta)]}{Var[H(\mathbf{X}, \theta)]} \quad (3.36)$$

$$\epsilon_{Cov}(\mathbf{X}_1, \mathbf{X}_2) = \frac{|Cov[H(\mathbf{X}_1, \theta), H(\mathbf{X}_2, \theta)] - Cov[\hat{H}(\mathbf{X}_1, \theta), \hat{H}(\mathbf{X}_2, \theta)]|}{Var[H(\mathbf{X}, \theta)]} \quad (3.37)$$

In the Eq. (3.36) and (3.37), the fraction is always positive since the truncated K-L expansion underestimates the variance and the covariance of the random field. A spatial 3D domain is presented in the following example, and the representation shows the numerically reproduced error of variance with 2D in Figure 3.5 a) and 3D in b). The covariance function presented in Eq. (3.28) is used. The physical sizes are $L_x = L_y = L_z = 10 \text{ mm}$, and the correlation length

is defined to be equal in all directions $L_{C,x} = L_{C,y} = L_{C,z} = 2 \text{ mm}$. The ratio of random field mesh and correlation length is $L_{RF}/L_c = 0.25$. The truncated K-L expansion will be discretized with $M = 1000$ terms. It is clearly in Figure 3.5 that the error of variance in the mostly positions are relatively small, i.e., $\epsilon_{\sigma^2}(\mathbf{X}) < 0.1$, but the error at the edge position is generally large, especially at the vertex.

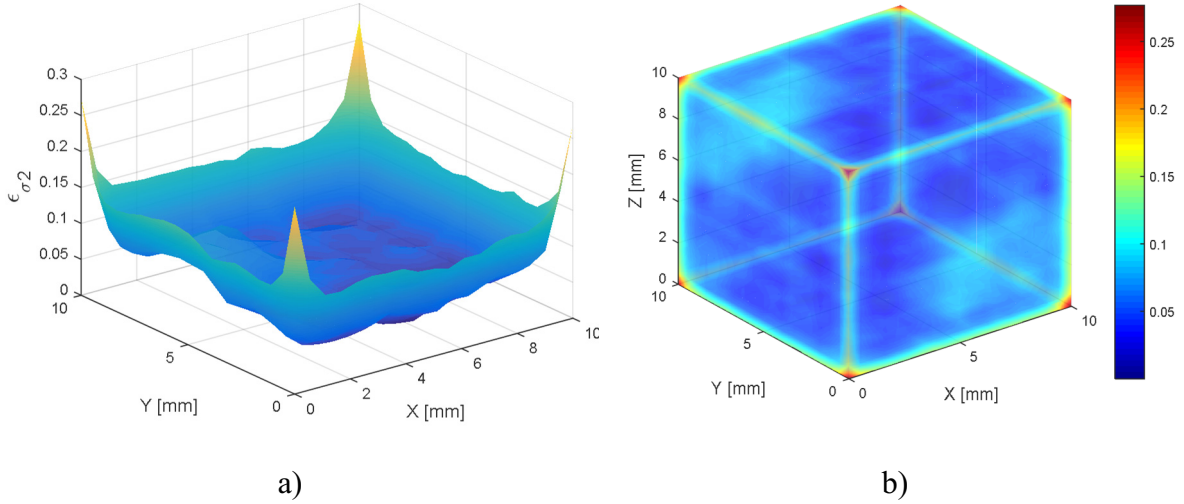


Figure 3.5: Point-wise estimator for variance error represented for different RF, a) 2D random field, b) 3D random field

Usually, the global error measures are applied to compare random field discretization methods and to quantify the overall quality of a random field approximation. The corresponding global error measures are defined as the weighted integral in reference [90]. It is reasonable to consider that the global error estimator is obtained as the integrals of the error variance $\epsilon_{\sigma}(\mathbf{X})$ and the error covariance $\bar{\epsilon}_{Cov}(\mathbf{X}_1, \mathbf{X}_2)$ over the space domain D as following,

$$\bar{\epsilon}_{\sigma^2}(\mathbf{X}) = \frac{1}{|D|} \int_D \epsilon_{\sigma}(\mathbf{X}) d\mathbf{X} = \frac{1}{|D|} \int_D \epsilon_{\sigma}(x, y, z) dx dy dz \quad (3.38)$$

$$\bar{\epsilon}_{Cov}(\mathbf{X}_1, \mathbf{X}_2) = \frac{1}{D^2} \int_D \int_D \epsilon_{Cov}(\mathbf{X}_1, \mathbf{X}_2) d\mathbf{X}_1 d\mathbf{X}_2 \quad (3.39)$$

where $|D| = \int_D dx dy dz$. The following Table 3.1 shows the error variance $\bar{\epsilon}_{\sigma^2}(\mathbf{X})$ and the error covariance $\bar{\epsilon}_{Cov}(\mathbf{X}_1, \mathbf{X}_2)$ by the truncated expansion after different M terms. The parameters of the random field are same with the random field in Figure 3.5 b). For the error of covariance $\bar{\epsilon}_{Cov}(\mathbf{X}_1, \mathbf{X}_2)$, the point \mathbf{X}_1 represent the all point in the random field and the \mathbf{X}_2 is defined as a specified point, i.e., $\mathbf{X}_2 = (x_2 = 0, y_2 = 0, z_2 = 0)$. The global error of variance is several orders of magnitude larger than the global error of variance covariance. Furthermore, the global error is reduced with the increased truncated expansion terms M .

Table 3.1: Global error of discretization with various truncation order of K-L expansion

M terms	40	200	400	600	800	1000	1200
$\bar{\epsilon}_{\sigma^2}(\mathbf{X})$	0.610	0.323	0.188	0.110	0.060	0.039	0.017
$\bar{\epsilon}_{Cov}(\mathbf{X}_1, \mathbf{X}_2)$	1.04E-05	9.43E-06	8.76E-06	8.61E-06	7.18E-06	7.68E-06	6.08E-06

The global error of variance is not the only accuracy criterion of the discretization. Some other error measure has been proposed for the discretization of the random field in [91], for example the supremum norm of the error variance and the error in the covariance function. Because the global error of variance is larger than the others [95], it will be considered to evaluate and optimize the random field approximation in this thesis.

The size of the RF L_{RF} mesh should be chosen to adequately capture the essential features of the stochastic spatial variability of the material properties. On the other hand, the RF mesh size needs to be as coarse as possible to reduce the discrete calculations of the random field. The size of RF mesh strongly affect the efficiency of calculation since the matrix size of the eigenvalue vector depends only on the discrete points of RF. Figure 3.6 shows the changes of the global error of variance with the truncated M items and the size of RF mesh. In general, the global error is reduced with the truncated M increases. It is worth mentioning that the global error and truncated items is not a strict monotonous relationship and the error will fluctuate, when the size of the mesh is very small, namely, $L_{RF}/L_C \leq 0.2$. With the refinement of the mesh, the global error is noticeably decreasing, when the truncated M items are relatively small ($M < 500$). Therefore, it is necessary to determine the appropriate the size of RF mesh.

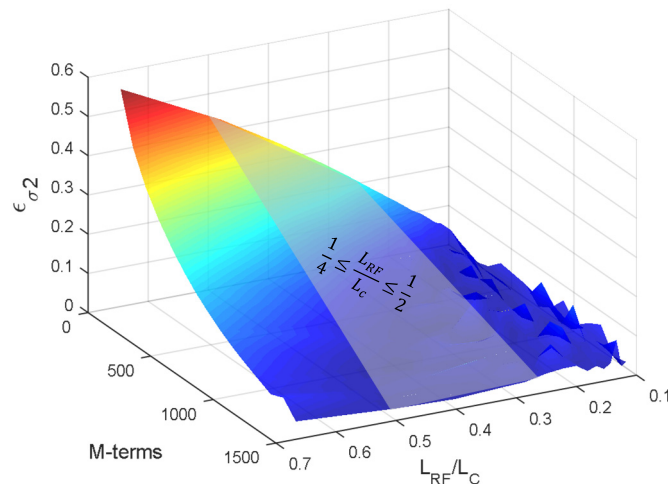


Figure 3.6: Influence of RF mesh size and truncation order on global error of variance

The strategy used to select the number or the size of the element by the discretization of RF is comprehensively studied in some reference. A genetic algorithm is employed in the optimization of the 2D random field in [99]. The results show that a suitable RF mesh and the smallest truncation order M can be obtained with the genetic algorithm using smaller computing resources. For the 3D random field, this optimization may not be very useful, because a single discrete calculation of random field is already very computationally expensive. Thus, it is proposed in this thesis that the size of RF mesh needs to be previously selected and defined.

$$\frac{1}{4} \leq \frac{L_{RF}}{L_C} \leq \frac{1}{2} \quad (3.40)$$

The Inequation (3.40) was used in the case of a one-dimensional random field with the EOLE method in [90]. According to the Figure 3.6, the global error can be satisfied by increasing the truncation order M to meet the accuracy requirements when the L_{RF}/L_C -value is between 0.25 and 0.5. Thus, this condition will be extended to a 3D random field with K-L series expansion in the following analysis. The boundary conditions in Inequation (3.40) is not a necessary constraint for discretization of the random field. It only represents a recommended choice to achieve a satisfactory discretization. Theoretically, the discrete size of the random field can be infinitely small, but it has an upper limit. The correlation properties of the random field will be partially missing if the size of RF mesh is larger than the correlation length L_C . Hence, for the K-L expansion method, the selection of the number of elements must be satisfied the following condition.

$$L_{RF} \leq L_C \quad (3.41)$$

The efficiency of the discretization method is expressed as the ability to accurately represent the random variables of the random field as few as possible. Therefore, it is clear that the computational efficiency is strictly dependent on the choice of the statistical characteristics and the requirements for proper accuracy or the discretization error. The different discrete methods also have a significant effect on discrete efficiency. Usually, the K-L series expansion is the most efficient method in the case of the exponential correlation function, where the eigenvalues and the eigenfunctions of the covariance function are available in closed form [91,99]. In this work, it is decided to discretize the random field with the K-L series expansion. This means that it needs the least amount of computational resources to obtain the required discrete accuracy. Therefore, the discretization of a random field can be formulated as an optimization problem and a simple, accurate and versatile numerical approach is necessary for the formulation of the optimization problem.

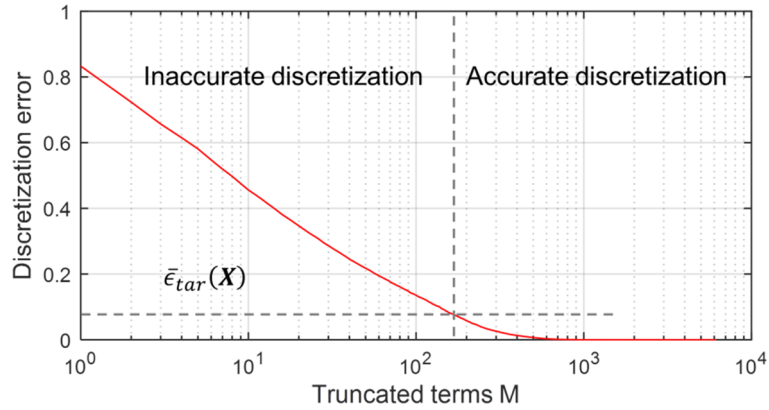


Figure 3.7: Relationship of the discretization error and the truncated terms

In the numerical approximation, smaller truncation order M can reduce the computational resources, but for mathematical precision, it is desirable to use larger value. Hence, the optimization of a random field discretization is to find the smallest truncation terms M , so that the discretization error $\bar{\epsilon}_\sigma(\mathbf{X})$ is less than the target accuracy $\bar{\epsilon}_{tar}(\mathbf{X})$. The relationship between the global error of discretization and the truncation order is shown in Figure 3.7. Mathematically, the truncation order M exists, and it is unique, due to the monotonic decreasing behavior of discretization error. Consequently, binary search algorithm [100] is applied to the optimization for the random field.

3.3 Connection between random field and finite element

From the above description, it is known that the size of RF mesh usually depends on the randomness of material properties, such as correlation length L_c . However, the division of FE mesh is based on the stress gradient distribution and the complexity of the geometry. Thus, it is possible to make the two meshes with the application of different criteria to achieve reasonable accuracy by separating the RF mesh from the FE mesh. In the reference [58], a general mapping-interpolation method between random field and finite element meshes was proposed for implementation of the stochastic finite element in a general simulation program in two dimensions. This reasonable interpolation method will be extended to the three-dimensional problem in this thesis. Essentially, the discrete value of the random field must be eventually mapped to the integration points of the finite element, because the elemental stiffness matrix is obtained from the Gaussian integration by using the material properties defined at the integration point. According to the relationship between the coordinates of the discrete value of the RF and the coordinates of the corresponding Gaussian integration points, the material properties of the Gaussian integration points are carried out using the eight-node shape function of RF mesh in three dimensions. Because the material properties at the integration point depend on the position

of the integration point and the position of the RF element, there is no necessary correlation between RF mesh and FE mesh. Form the point of view of discrete precision it is preferable that the FE mesh is smaller than the RF mesh since the large FE mesh will cause the lack of uncertainties information of random field.

The Illustration of mapping-interpolation method in Figure 3.8 shows the relationship between one random field element and eight finite elements. The green point is the integration point of the finite element. The (ξ, η, ζ) is a local Cartesian coordinate system with the RF element center as the origin of the coordinates. The length of the RF element in each direction is assumed as two, and the coordinate of the corresponding point in RF element is presented in Figure 3.8.

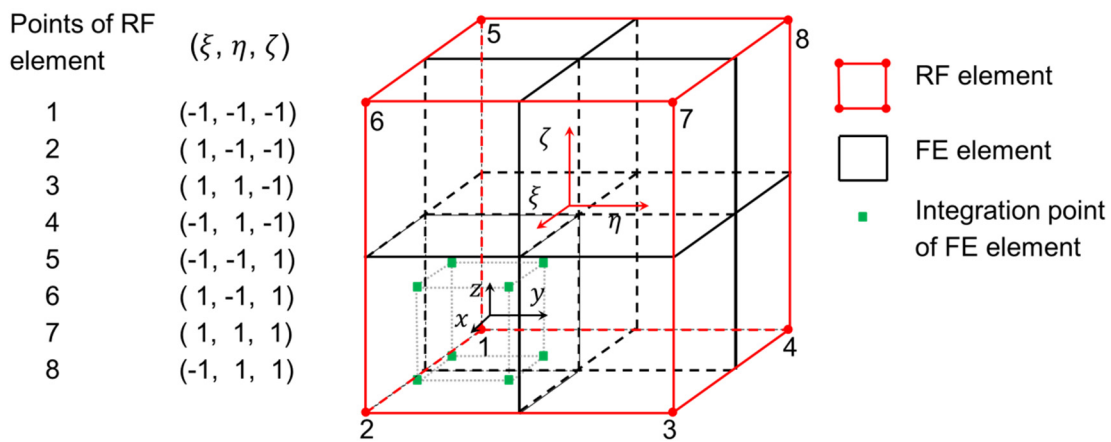


Figure 3.8: Coordinate mapping representation of 3D 8-point FE mesh and 3D RF mesh

Firstly, the coordinates of the integration point p need to be exported from the element of FE mesh, and the RF element will be determined, which the point p is located. By using a nonlinear equation (9.1) in [96], the coordinate (x_p, y_p, z_p) of point p in the global coordinate system is mapped as (ξ_p, η_p, ζ_p) to the local coordinate system of RF element. After solving the nonlinear mapping problem, the random values \hat{H}_p of material properties in the integration point p is obtained from the random values \hat{H}_i of the RF using the Eq. (3.42) with the eight-node shape function of RF mesh in Eq. (3.43).

$$\hat{H}_p = \sum_{i=1}^8 N_i \hat{H}_i \quad (3.42)$$

$$N_i = \frac{1}{8} (1 + \xi_i \xi) (1 + \eta_i \eta) (1 + \zeta_i \zeta) \quad (3.43)$$

where N_i are the shape functions of i th point of RF element ($i = 1 \sim 8$); ξ, η and ζ are equal to 1 or -1 and represents the quadrant of the i th point of RF element.

Figure 3.9 shows the flowchart of the mapping-interpolation method for the 3D solid element, where the N_{ele} and N_{IP} are respectively the numbers of the total finite element and the integration point per element. This algorithm is easy to implement in the general finite element program, for example, with ABAQUS User Subroutine UMAT or USDFLD.

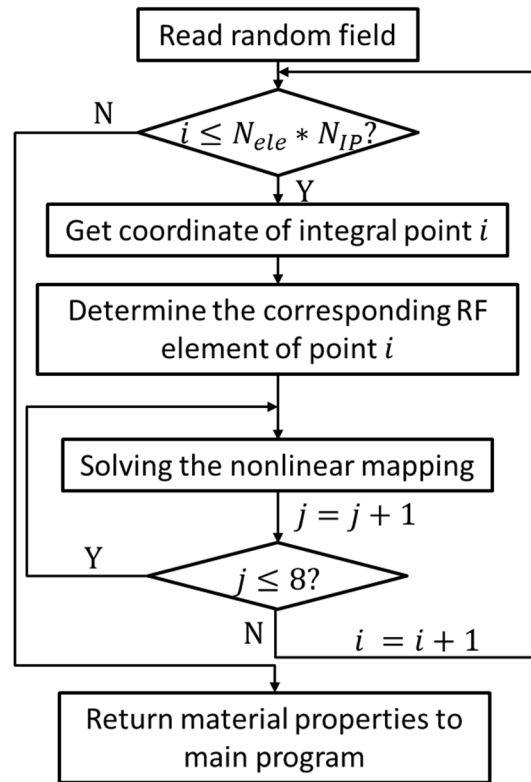


Figure 3.9: Flowchart of the mapping-interpolation method

The proposed method is to map the discrete random field to the FE mesh, and then the material properties will be interpolated to the integration points of the finite element by the coordinate relationship of the two meshes. The mapping-interpolation error can be divided into the mapping error and the interpolation error. Theoretically, the mapping process don't produce errors since the total size of the two meshes is the same. However, for the modeling convenience, it can be chosen that the domain of RF and FE are not exactly coinciding. Figure 3.10 shows the original random field with the size $10 \times 10 \times 10$ mm in a) and the random variables at integration points of an I-section specimen in the same space in b). According to the probability distribution function of corresponding random variables in Figure 3.10 c) and d), mapping the larger random field to the smaller finite element will make the information of the original RF missing, but the mapping distortion of random field is in an acceptable range. When the difference between the RF and the FE size is large, it is necessary to reduce the mapping error by increasing the sample size in the random field.

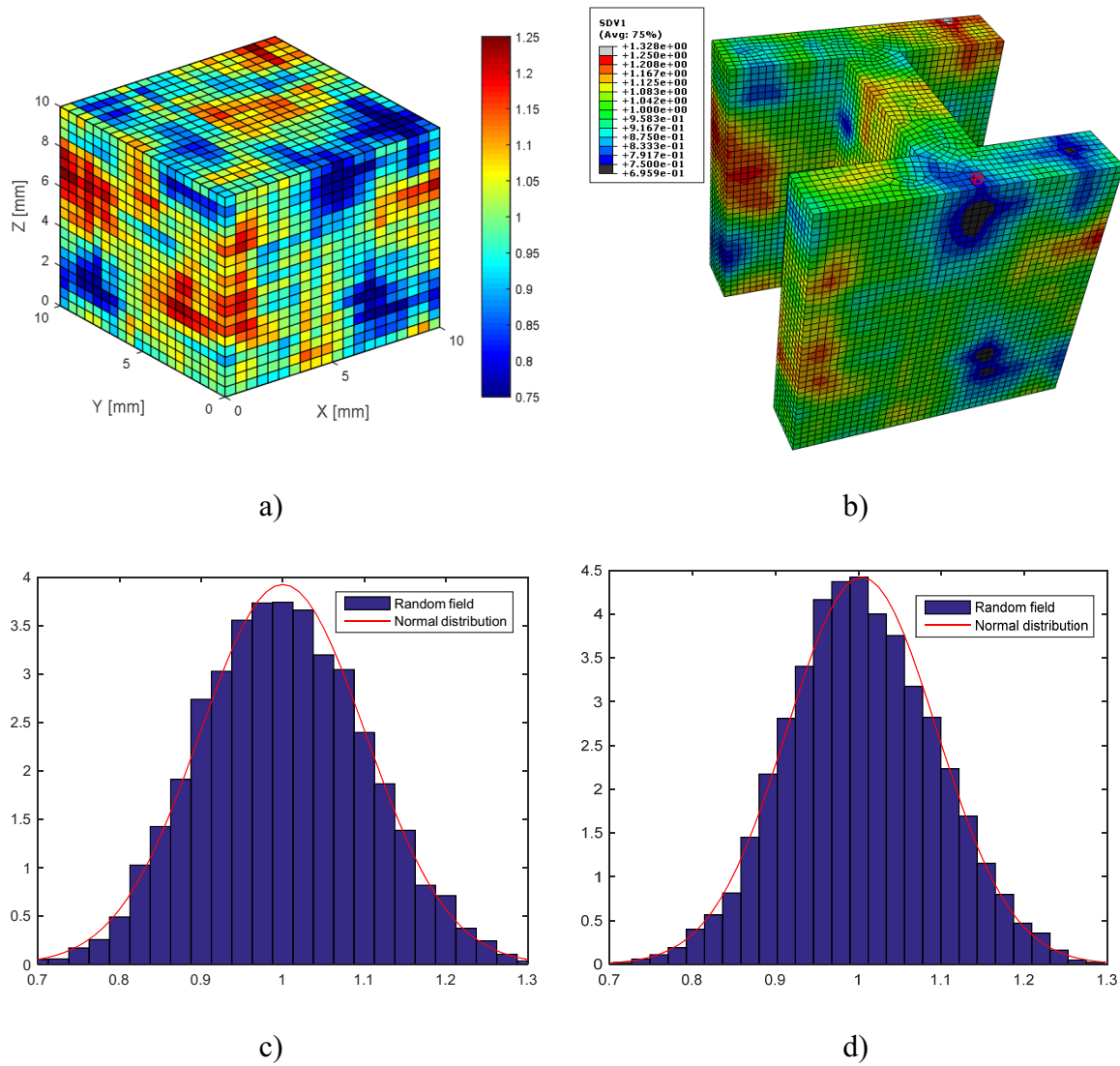


Figure 3.10: a) 3D Gaussian RF, b) Random variables at integration points of I-section specimen, c) PDF of original RF, d) PDF of random variables at integration points

Usually, the error caused by 3D interpolation process can distort the original random field, because the finite element type and the number of element and integration point are variable. To demonstrate the interpolation error evaluation, the random field which is the same physical domain used in section 3.2.6 will be mapped and interpolated into the finite element in ABAQUS with difference FE mesh size. The 8-node brick element C3D8 is employed in ABAQUS for this example. The random variables, which are obtained by mapping and interpolation on the finite element from RF, can be referred to Figure 3.11 a) and b), where the mesh of FE in a) is finer than in b), namely $L_{RF,b}/L_{FE,b} = 0.5$ and $L_{RF,c}/L_{FE,c} = 4$. The corresponding PDFs of random variables at the integration points are shown in Figure 3.11 c) and d). The information of original random field is not fully expressed in the model with big FE size, due to the small number of the integration points. It can be seen from the corresponding PDFs of

the random variables that the coarse mesh of FE in Figure 3.11 b) will lead to the lack of RF details and the distribution of random numbers has a significant error with the original random field. The PDF of random variables with fine FE mesh in Figure 3.11 c) is consistent with the distribution of the random variables of the target distribution, which is generated in MATLAB to represent the discrete random field.

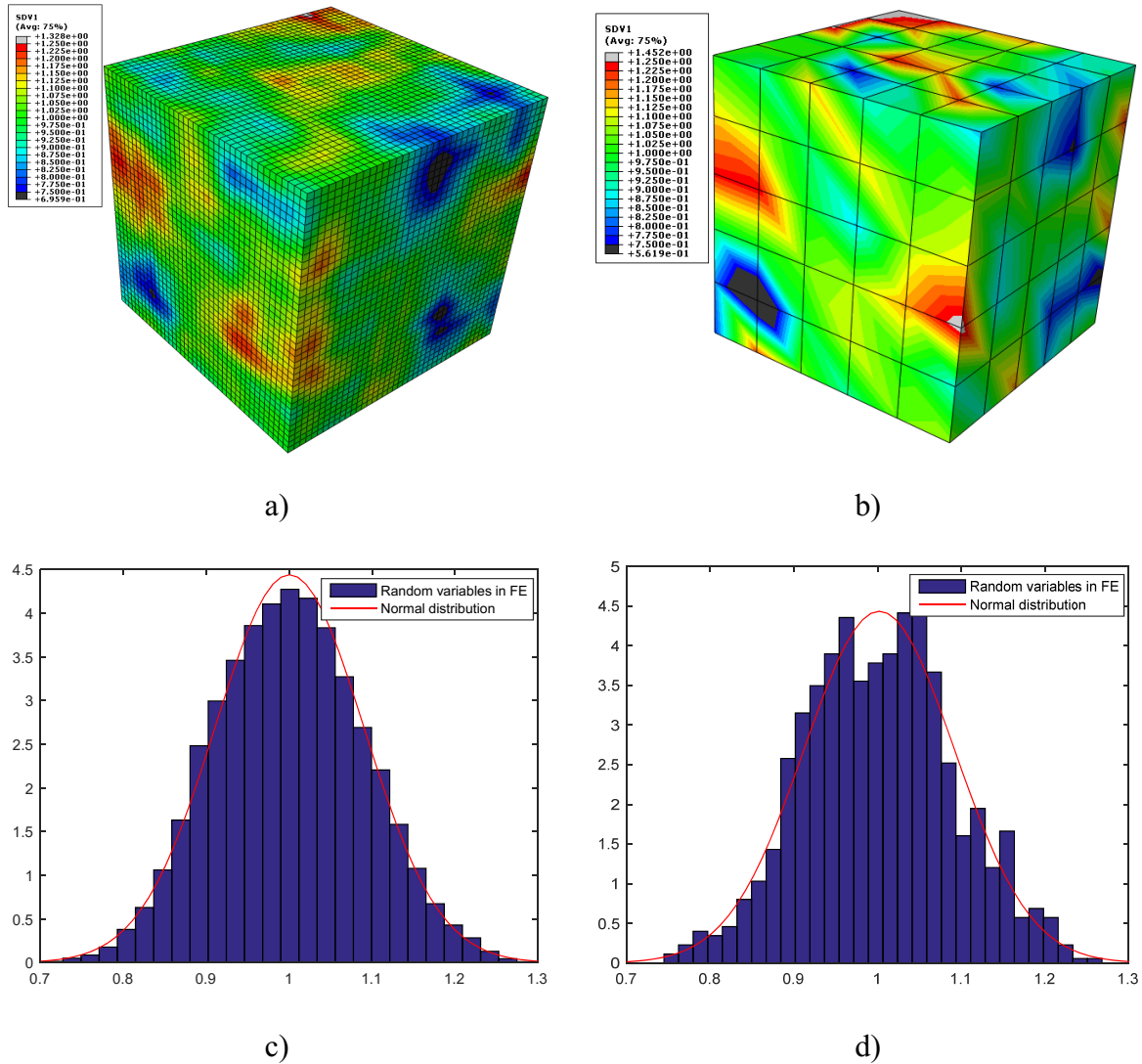


Figure 3.11: Different FE mesh and corresponding PDF of random variables at integration points, $L_{RF,b}/L_{FE,b} = 0.5$ in a) and c), $L_{RF,c}/L_{FE,c} = 4$ in b) and d)

Table 3.2 shows the first 4th moments of the original random field and the material properties in the integration point, which is obtained by the mapping-interpolation method. The size of the FE mesh (or the ratio of RF size and FE size L_{RF}/L_{FE}) has a few influences on the 4th moment of material properties at the integration point in spite of the relatively significant impact of FE size on PDF. It is worth noting that the variance on the finite element is always less than the

original variance. According to the description in section 3.2.6, this error is caused by the discretization of the random field.

Table 3.2: Influence of FE size on the first fourth statistical moments

Statistical moments		Mean value	Variance	Skewness	Kurtosis
Random Field		1.0000	0.0100	0.0844	2.8416
$\frac{RF\ Mesh}{FE\ Mesh}$	0.50	1.0002	0.0081	0.0642	2.7715
	0.75	1.0002	0.0080	0.0740	2.7899
	1.00	1.0002	0.0081	0.0583	2.7714
	1.25	1.0008	0.0081	0.0642	2.7484
	1.50	0.9981	0.0080	0.0690	2.6767
	2.00	1.0000	0.0081	0.0309	2.7745
	4.00	1.0020	0.0081	0.0684	2.7710

From the perspective of computational efficiency and computational accuracy, it is recommended to choose the size of finite elements satisfying the following condition.

$$L_{FE} \leq L_{RF} \quad (3.44)$$

Therefore, it is possible to avoid the error caused by the lack of the random field information and to reduce the computational complexity of the SFEM in this way. It is obvious that the recommended FE size offers a good balance between accuracy and computational efficiency of SFEM.

3.4 The stochastic finite element method with Monte Carlo simulation

In the analysis of the uncertain system, it is a very important step to study the uncertainty of the system and its stochastic response. In the framework of the stochastic finite element method, the problem with randomness, which is difficult to solve using the classical deterministic method, studied very well. The SFEM comprises three basic steps:

- Discretization of the random field representing the uncertain system properties;
- Formulation of the stochastic stiffness matrix;
- Calculation of the structural response.

The first step is the discretization of random field and the connection with the stress or strain field and this step have been studied and described in detail in section 3.2 and 3.3. The discretized random fields are used for the stochastic stiffness matrix of each integration point in every finite element. The construction of random stiffness matrix and the calculation of the structural response will be described in the following sections.

3.4.1 Formulation of the stochastic finite element matrix

Due to the inherent randomness of the material properties, the stress σ , strain ε and stiffness matrix C of element are also become stochastic. The stochastic quantities can be described by the corresponding probability distributions. The relationship between the pre-defined probability distribution of material properties and the unknown distribution of these variables will be defined by the constitutive equation of deterministic analysis as follows [96],

$$\dot{\sigma}_{ij}(\mathbf{X}, \theta) = C_{ijkl}^{ep}(\mathbf{X}, \theta) \dot{\varepsilon}_{kl}(\mathbf{X}, \theta) \quad (3.45)$$

In order to clarify the formula, the stochastic element stiffness matrix for a homogeneous elastoplastic material will be presented. It is assumed that the distributions of yield strength and the tensile strength are the same, then the tangent modulus E_t is a determine quantity. Therefore, the field variable $C_{ijkl}^{ep}(\mathbf{X}, \theta)$ contains the other two random field variables, i.e. Young's modulus $E(\mathbf{X}, \theta)$ and yield strength $f_y(\mathbf{X}, \theta)$. The specific form of stiffness matrix at the integration points is obtained as follows,

$$\begin{aligned} C_{ijkl}^{ep}(\mathbf{X}, \theta) &= C_{ijkl}^e - \frac{9\mu^2 s_{ij} s_{kl}}{(3\mu + E_t) \sigma_f^2} \\ &= \lambda \delta_{ij} \delta_{kl} + \mu (\delta_{ik} \delta_{jl} + \delta_{il} \delta_{jk}) - \frac{9\mu^2 s_{ij} s_{kl}}{(3\mu + E_t) f_y^2} \\ &= E(\mathbf{X}, \theta) \left(\frac{\nu}{(1+\nu)(1-2\nu)} \delta_{ij} \delta_{kl} + \frac{\nu}{2(1+\nu)} (\delta_{ik} \delta_{jl} + \delta_{il} \delta_{jk}) \right) - \frac{E(\mathbf{X}, \theta)}{f_y(\mathbf{X}, \theta)^2} * \\ &\quad \frac{1}{E(\mathbf{X}, \theta) 3\nu + 2(1+\nu) E_t} * \frac{9\nu^2}{2(1+\nu)} s_{ij} s_{kl} \\ &= E(\mathbf{X}, \theta) * \mathbf{K}_e - \frac{E(\mathbf{X}, \theta)}{f_y(\mathbf{X}, \theta)^2} * \frac{1}{E(\mathbf{X}, \theta) 3\nu + 2(1+\nu) E_t} * \mathbf{K}_p \end{aligned} \quad (3.46)$$

where λ and μ are Lamé parameters; s_{ij} and s_{kl} are deviatoric stresses; ν is Poisson's ratio; \mathbf{K}_e and \mathbf{K}_p represents two tensors or matrices with determine quantities.

The stiffness matrix of an element can be obtained by integrating the constitutive matrix of the integration points in the element. The stochastic stiffness matrix for an 8-points hexahedral element will be calculated by the following equations,

$$\begin{aligned} [K_{ep}]_e &= \iiint_{-1}^1 [\mathbf{B}_{ep}]^T [\mathbf{D}_{ep}] [\mathbf{B}_{ep}] |J| d\xi d\eta d\zeta \\ &= \sum_{i=1}^2 \sum_{j=1}^2 \sum_{k=1}^2 \omega_i \omega_j \omega_k [\mathbf{B}_{ep}]^T [\mathbf{D}_{ep}] [\mathbf{B}_{ep}] |J| \end{aligned} \quad (3.47)$$

$$[\mathbf{D}_{ep}] = E(\xi_i, \eta_j, \zeta_k, \theta) [\mathbf{K}_e] - \frac{E(\xi_i, \eta_j, \zeta_k, \theta)}{f_y(\xi_i, \eta_j, \zeta_k, \theta)^2} * \frac{1}{E(\xi_i, \eta_j, \zeta_k, \theta)^{3\nu+2(1+\nu)} E_t} [\mathbf{K}_p] \quad (3.48)$$

$$E(\xi_i, \eta_j, \zeta_k, \theta) = \sum_{n=1}^8 N_n(\xi_i, \eta_j, \zeta_k) E(\mathbf{X}, \theta) \quad (3.49)$$

$$f_y(\xi_i, \eta_j, \zeta_k, \theta) = \sum_{n=1}^8 N_n(\xi_i, \eta_j, \zeta_k) f_y(\mathbf{X}, \theta) \quad (3.50)$$

where ω_i , ω_j and ω_k are defined as weights of Gauss-Legendre integration; $[\mathbf{B}_{ep}]$ is elasto-plastic strain matrix and $[\mathbf{D}_{ep}]$ is the elasto-plastic material constitutive matrix. $E(\xi_i, \eta_j, \zeta_k, \theta)$ and $f_y(\xi_i, \eta_j, \zeta_k, \theta)$ are respectively randomly distributed Young's modulus and yield strength at integral points, which are calculated by using the Mapping-interpolation method from the pre-defined random field $E(\mathbf{X}, \theta)$ and $f_y(\mathbf{X}, \theta)$.

The iteration of the elasto-plastic constitutive matrix at each integration point of each element can be performed using the ABAQUS subroutine UMAT, and the random fields $E(\mathbf{X}, \theta)$ and $f_y(\mathbf{X}, \theta)$ generated by MATLAB will be obtained in the subroutine UMAT. Then the elasto-plastic element stiffness matrix will be assembled into a global stiffness matrix and this matrix will be delivered to a numerical solver with pre-defined boundary conditions.

Since the stochastic finite element method with elasto-plastic materials involves nonlinear iterative calculation at integration points, some stochastic finite element methods (such as Neumann SFEM and spectral SFEM) cannot be applied to solve such problems. From a mathematical point of view, the solution of the stochastic stiffness matrix is essentially to solve non-linear stochastic partial differential equations. The mostly application of SFEM is practically limited to linear problems. Currently, some researches have tried to solve the problem of elasticity by introducing some simplified assumptions. For example, a stochastic response surface approach has been proposed for solving nonlinear mechanical problems [101,102].

More recently, a new method relies upon a stochastic Galerkin formulation based on a nonlocal Fokker-Planck-Kolmogorov equation at the constitutive level has been presented [62], where the stiffness random field is decomposed using a multidimensional polynomial chaos expansion. However, there is no universal and efficient method has been proposed. Considering the current situation, direct Monte Carlo simulation is the only universal tool for treating such complex SFEM problems at the expense of a prohibitive computational cost. Furthermore, the direct MCS is the simplest method to simulate the response of structures with uncertain material properties by using a very large number of similar random samples. Therefore, this thesis focus on the calculation of the structural response with direct MCS.

3.4.2 Direct Monte Carlo simulation for stochastic FEM

In the past decades, direct MCS is not widely used in SFEM, because the direct MCS requires a lot of computational resource and time, especially for the nonlinear problem in 3D space. Especially for the efficient solution of reliability problems, where the calculation of small failure probabilities requires a very large number of samples, the direct MCS is hard or not possible for large-scale practical problems in a few years ago due to its excessive computational cost. However, the direct Monte Carlo Simulation is the simplest approach to calculate the structural response with random properties under the SFEM framework; especially it is one or only one general method for treating the elasto-plastic problems.

The main idea in this method is that the samples of random properties are generated and discretized using K-L expansion, and then the samples of the response vector are obtained by repeating the deterministic finite element calculations. Based on the obtained samples of the response, the response variability of the structure is determined using the statistical relationships. In general, the evaluation of structural response and the analysis of the reliability of the structure are carried out with the first n -th moments of the statistics. It is obvious that the structural analysis accuracy increases with the increased the order of the statistical moments. In this work, we will analyze the first fourth moments of the structural response, i.e., mean value $\mu(R)$, variance $\sigma^2(R)$, skewness $\gamma(R)$ and kurtosis $k(R)$. The first fourth moments of the discrete samples can be determined by the following equations.

$$\mu(R) = \frac{1}{N_{sim}} \sum_{i=1}^{N_{sim}} R_i \quad (3.51)$$

$$\sigma^2(R) = \frac{1}{N_{sim}} \left[\sum_{i=1}^{N_{sim}} R_i^2 - N_{sim} * \mu^2(R) \right] \quad (3.52)$$

$$\gamma(R) = \frac{\frac{1}{N_{sim}} \sum_{i=1}^{N_{sim}} (R_i - \mu(R))^3}{\left(\frac{1}{N_{sim}} \sum_{i=1}^{N_{sim}} (R_i - \mu(R))^2 \right)^{3/2}} \quad (3.53)$$

$$k(R) = \frac{\frac{1}{N_{sim}} \sum_{i=1}^{N_{sim}} (R_i - \mu(R))^4}{\left(\frac{1}{N_{sim}} \sum_{i=1}^{N_{sim}} (R_i - \mu(R))^2 \right)^2} - 3 \quad (3.54)$$

It is worth noting that the estimated accuracy and the number of samples are closely related. The results of the following section 3.4.3 are shown that the accuracy of the statistics can be achieved when the sample size is sufficient. Therefore, the distribution function of the structural response can be obtained based on the stable first 4-th order statistical moments by using the

maximum entropy distribution principle. In chapter 5, the reliability analysis combined with the maximum entropy principle distribution will be described in detail.

With the development of computer technology and the applicability of direct MCS method to parallel processing with excellent efficiency, the direct MCS makes it possible to consider the material uncertainty and randomness in the 3D space, by combining the common finite element software ABAQUS and the general-purpose mathematical software MATLAB. Hence, the direct MCS can be seen as the only available universal tool to solve the problem of SFEM relatively exactly with elasto-plastic non-Gaussian random material properties [46]. In addition, the flowchart showing the process of the SFEM analyze with MCS is depicted in Figure 3.12.

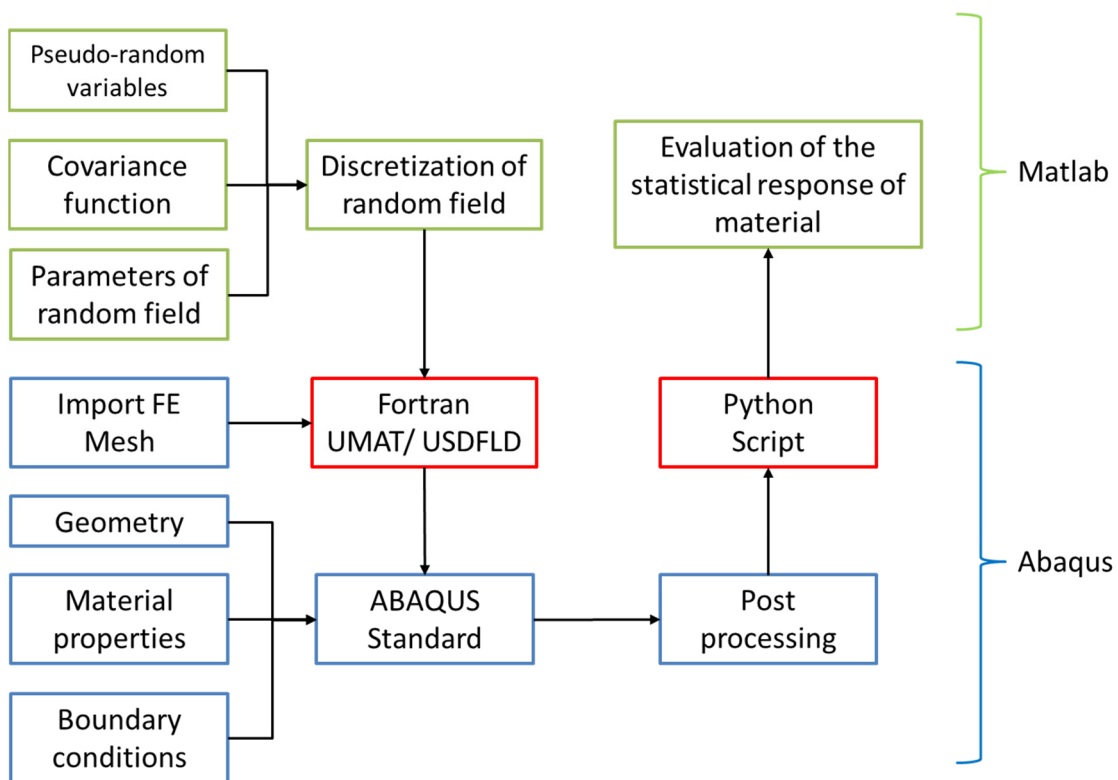


Figure 3.12: Schematic of Monte Carlo simulation for SFEM with ABAQUS framework interfaced with MATLAB codes

3.4.3 Sample size for Monte Carlo simulation

In the direct MCS method, the number of nonlinear analysis is consistent with the number of samples generated by discretization of the random field. As the number of samples increases, the consumed computational resources are proportionally increased. Obviously, the accuracy of the estimation depends on the number of samples. Furthermore, the estimate of statistical moments of the response, namely, the mean value and standard deviation is inversely proportional to the number of samples. Therefore, this analysis requires using the minimal computational resource to obtain results, which satisfy reasonable accuracy. It is possible to estimate

the PDF or CDF of the response with at least 500 samples of the random field for elastic material [46]. For the estimation of the mean value and standard deviation, the required minimum samples are less than the number of samples for the approximation of the PDF and [103] shows that the sample size with 30-100 already has reliable accuracy.

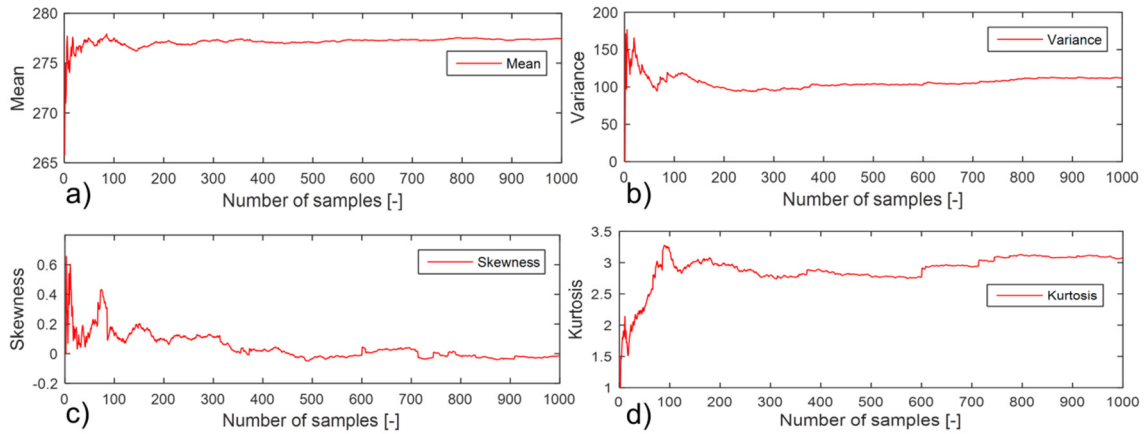


Figure 3.13: Variation of stress response statistics with the number of samples

Figure 3.13 shows that a numerical example of tensile test simulation with the spatially varying yield strength in chapter 4 has to be implemented for different number of samples. If the number of samples reaches or exceeds 200, the mean in Figure 2.13 a) and variance in b) of the response of stress for entire specimen will tend to be stable. However, the third- and fourth central moments namely skewness and kurtosis of the stress response have still a large fluctuation at this situation, and more than 1000 samples may be required to reduce this instability to infinitesimal. The number of the required sample for MCS is difficult to be accepted by the analysis of structural reliability in practice when the structural reliability coefficient is relatively large. As an alternative, the probabilistic description of response will be obtained by the fitting techniques of the probability distribution function and then used in the reliability assessment [80].

3.5 Element types for stochastic FEM

From the computational perspective, all the discrete values of material properties will be finally calculated at the integration points. Theoretically, the different element types do not change the results of calculation of SFEM with the random field for the uncertainty of material properties. Therefore, this mapping-interpolation method can also be employed for the beam and shell element in Figure 3.14. However, the accuracy of response results with the mapping-interpolation approach in SFEM will be significantly affected by element types, because the different elements have an unequal number of the integration points. It is clear that the randomness of the material cannot be accurately represented in the entire model if fewer integration points are

defined. Specifically, it is difficult to add integration points in the thickness direction of web and flanges for the beam element with open section such as I-section. This means that the beam element may not be used for I-section with thicker web or flanges for FEM with the random field.

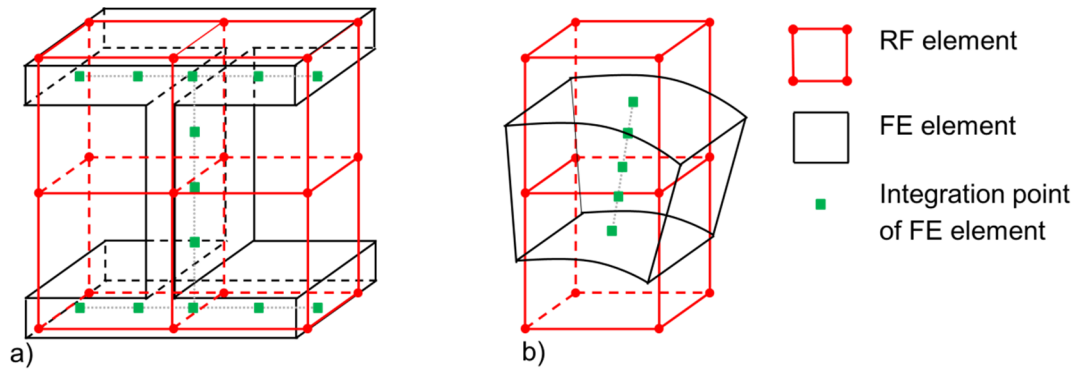


Figure 3.14: Illustration of mapping coordinates for beam a) and shell element b)

In order to combine random field with a variety of element types and verify their applicability, a three-point bending simulation of an I-section beam with the random field of yield strength will be performed using the beam, shell and solid element in Figure 3.15 and the corresponding plastic bearing capacity of the beam are compared with each other. The I-section beam is a HEA100 regardless of the radius with a length of 1000 mm. Three models with different element type were simulated based on MSC respectively with 500 RF samples, i.e., a) the beam with 50 B31OS beam element, b) the beam with 480 S4 shell element, c) the beam with 3700 C3D8 solid element. The discrete random field will be defined as a 3D rectangular space of $100 \times 100 \times 1000$ mm. The length of RF mesh and the correlation length of the random field are respectively assumed as 10 and 40 mm. The target accuracy of discretization of random field is set equal to 1%. The lognormal distribution with constant mean value 300 MPa and standard deviation 30 MPa will be treated as a distribution of random field for the three-point bending simulation.

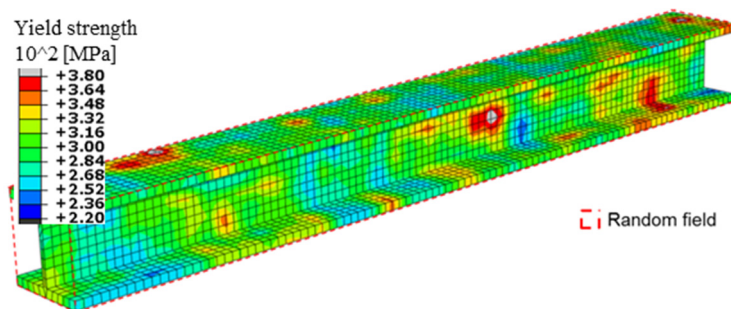


Figure 3.15: Random distributed yield strength for I-section beam

After 500 times of MCS, the statistical response results of the plastic bearing capacity of 3P bending simulation are shown in Figure 3.16. The error of mean value for each element types is less than 1%. The variance and coefficient of variation C_v in the beam element are 10% larger than in other elements since the beam element has relatively fewer integration points. Therefore, the beam element is limited to analyze the response of structure which is needed to consider the I-section beam with a thick web and flange by using SFEM considering the randomness of material properties in ABAQUS.

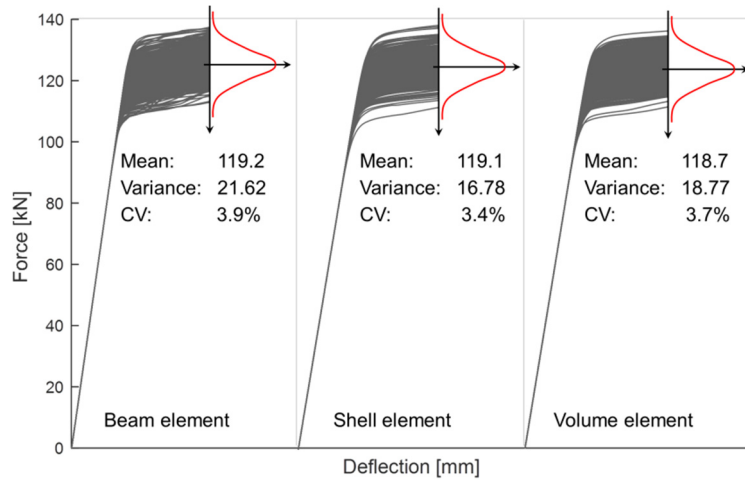


Figure 3.16: Response of plastic bearing capacity with different element types

3.6 Conclusions

In this chapter, the stochastic FEM was implemented to analyze the response of the 3D structures by interactively applying FEM program ABAQUS and mathematical program MATLAB with uncertainty and randomness of nonlinear elasto-plastic materials. Firstly, the uncertainty modeling and the random field in Hilbert space were briefly introduced. Then, the discretization of the 3D random field was realized by the truncated Karhunen-Loève expansion. For the matter, the Galerkin finite element techniques was used to solve the Eigenvalue analysis, which is the main task of calculating Karhunen-Loève expansion. After that, the modeling of the 3D random field was achieved by the proposed approach with an acceptable amount of computation. The cost to solve the homogeneous Fredholm integral equation was reduced by decomposing the 3D eigenfunction problem in orthogonal coordinate axes as well as composing the matrixes again with the coordinates of elements. Besides, the discretization errors were discussed in detail. Since the calculation of the small probability events needs a larger number of samples and the Latin Hypercube sampling is efficient for the generation of a random field by a small number of basic random variables, the Latin Hypercube sampling was employed to treat the sampling for the stochastic variables of the random field. Besides this, the non-Gaussian random

field, which has a relatively small coefficient of variance with non-zero mean, was expressed in terms of a Gaussian random field through a nonlinear mapping transformation. Simultaneously, the binary search algorithm was employed to optimize the computational accuracy and efficiency of the truncated Karhunen-Loève expansion.

In the second part of this chapter, a general mapping-interpolation method was proposed to connect the 3D random field and the finite element mesh. The mentioned mapping-interpolation approach will be not only applied in different criteria for two different meshes, but also be employed for different element types. For the stochastic nonlinear material, the constitutive matrix at each integration points of the elements was computed using the user Subroutine in ABAQUS. The interpolation error shows that the mapping-interpolation method does not engender an unacceptable deviation with a coarse mesh of random field and smaller finite elements. Thus, the distortion of a random field from mapping and interpolation can be avoided, if it meets the requirements the recommended mesh size of a finite element.

The formulation of the stochastic finite element matrix, which is the key point of this method, is then presented. Essentially, the primary task of stochastic FEM is to solve a stochastic differential equations contains elasto-plastic material. The most general and straightforward Monte Carlo simulation was employed to obtain the structural response. The probability distribution function of structural response and the reliability analysis will be studied with fitting techniques in chapter 5.

4 Experimental and simulated investigation of tensile and flexural members

4.1 Introduction

In spite of the existence of statistical size effect in all materials, the use of these material properties in the structural engineering needs to be validated, as well as the randomness of material properties also needs to be determined according to the experiments. To assess the effects of statistical size effect, the tests with tensile and flexural members need to be performed under different load types. By demonstrating that the uncertainty of material properties can affect the bearing capacity of the structure, the structure design can be able to consider the SSE in the practical engineering.

The statistical size effect is subjected to the spatial correlation of materials such as the correlation length and correlation coefficient. The assessment of the SSE is not simple when considering all conditions together. Therefore, the sample tests and the specimens with clear stress distribution are preferred to analyze the relationship between the material strengths and specimen sizes. By a series of tensile test (max. specimen diameter 32 mm) with various sizes of the specimen, the statistical results of each kind of specimen needs to be analyzed.

The relevant parameters which are required in numerical simulations with the stochastic material model and SFEM, can be obtained in the inverse analysis that is capable of identifying and characterizing the uncertainty in material properties on the basis of experimental tests. In this chapter, the parameters for the stochastic material model and the random field of material properties will be investigated, and these will be applied to consider the effects of SSE on the bearing capacity in the flexural members.

4.2 Experimental investigation

4.2.1 Tensile testing with constant stress distribution

The tensile tests were carried out with the specimens from HEB400 rolled profile and a 40 mm thick plate in Figure 4.1. All specimens are accordance with the request of DIN 50125 [104], the speed of the tensile tests is taken from DIN EN ISO 6892-1 [105]. To compare the results of all specimens with each other, the geometric sizes of all specimens are maintained in a constant ratio. Because the stress distribution in the circular cross-section is constant, this section

is used for all tested specimens. In tensile tests, the testing machine is position-controlled with a very small test speed, so that the influences of the test speed become negligible.

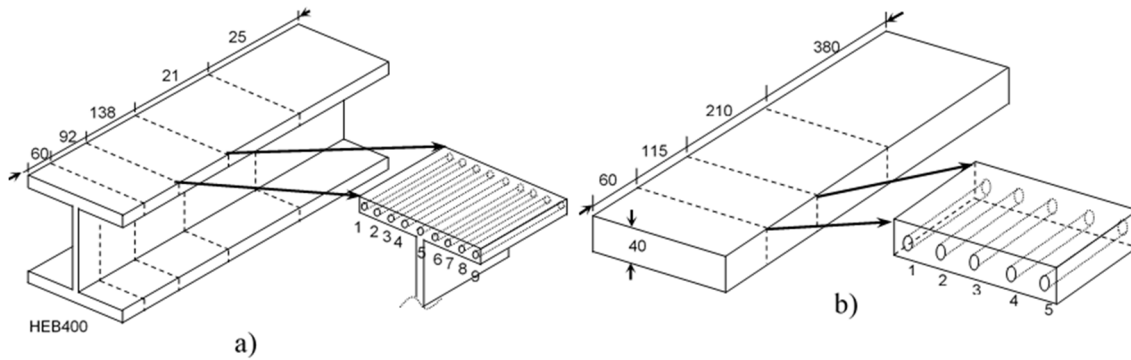
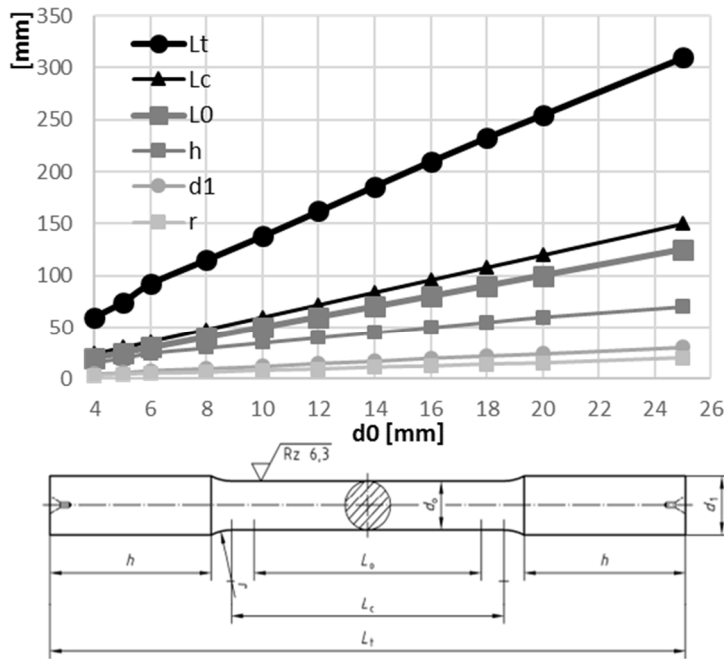
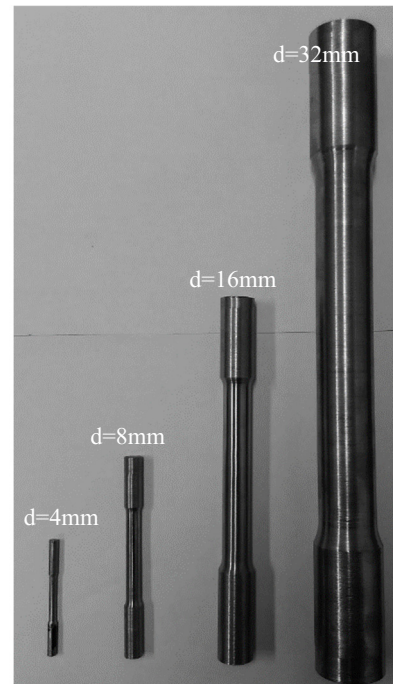


Figure 4.1: Illustration of tensile specimens a) HEB 400; b) 40 mm thick plate

Although the specimen sizes can refer to the corresponding norm, the definition of DIN 50125 limits the specimen size to a diameter 25 mm. Therefore, it is necessary to extend the norm to provide the large size specimens. Figure 4.2 a) shows the linear relationship between the diameter of the specimen and the other sizes. This means that the specimen sizes can be obtained by linear relationship for the larger specimens after determining the specimen diameter. The comparison of the small and big size specimen is shown in Figure 4.2 b).



a)



b)

Figure 4.2: Extended geometry for big specimen a) the relationship between different specimen sizes, b) Specimen from 40 mm plate

Nine specimens were produced from every five-upper flange, which were cut from the same HEB section made of S235. The specimen diameters of each segment were respectively 4, 6, 10, 16 or 20 mm. Moreover, the lengths of the beam segment are adapted as shown in Figure 4.1 a). The mean values and coefficients of variation of strength per tensile testing specimens are summarized in Table 4.1 and shown in Figure 4.3 a).

Table 4.1: Statistical results of tensile test from HEB 400

Spezimens	$\Phi=4$ mm			$\Phi=6$ mm			$\Phi=10$ mm			$\Phi=16$ mm			$\Phi=20$ mm		
	σ_{eH}	σ_{eL}	σ_m	σ_{eH}	σ_{eL}	σ_m	σ_{eH}	σ_{eL}	σ_m	σ_{eH}	σ_{eL}	σ_m	σ_{eH}	σ_{eL}	σ_m
$E(\sigma)$ [MPa]	302.2	296.0	470.0	301.4	289.3	448.2	292.0	279.7	437.2	281.8	276.3	441.8	280.5	275.0	437.8
$Var(\sigma)$ [MPa]	22.4	23.3	26.3	16.3	14.6	6.6	14.4	12.5	4.4	13.7	13.1	4.8	13.3	13.0	5.9
C_v [-]	7.4%	7.9%	5.6%	5.4%	5.0%	1.5%	4.9%	4.5%	1.0%	4.9%	4.8%	1.1%	4.7%	4.7%	1.3%

Φ : Diameter, σ_{eH} : upper yield stress, σ_{eL} : lower yield stress, σ_m : tensile strength.

The results of the strength with HEB 400 have presented only the upper flange, because the lower flange has equivalent results. It is not the same with the results from Urban [106], there is no definite mathematical distribution for the yield strength of the I-shaped profile since the distribution depends on the specimen size. It is clear that the fluctuation of the yield and tensile strength increases with decreasing diameter. Figure 4.3 b) shows that the corresponding coefficient of variation ω decreases with increasing volume. Obviously, this trend is comparable to the theoretical approach.

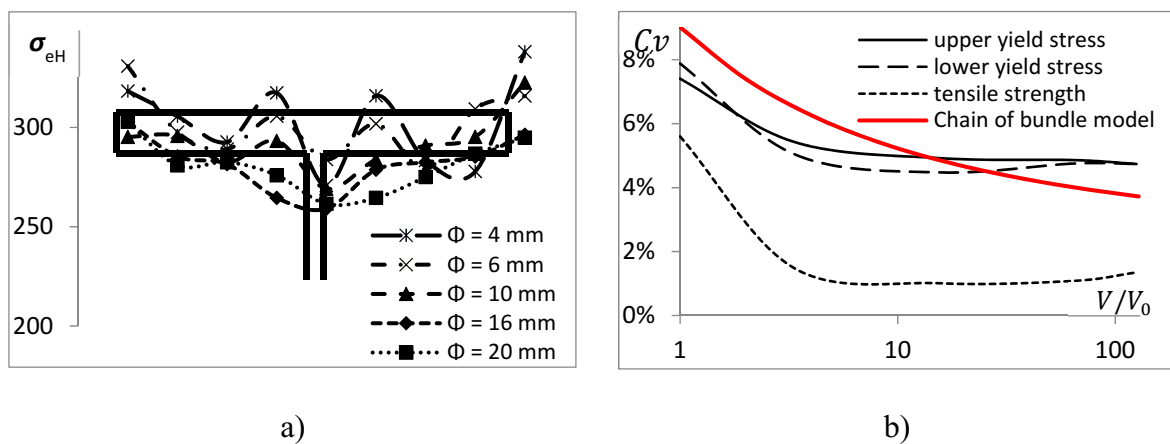


Figure 4.3: a) Distribution of yield strength through flange with different specimen size, b) relationship between the coefficient of variation and specimen volume

It should be noted that the standard deviations and coefficient of variance, which is determined by the test results, may depend on the specimen position in the steel profile. The distribution of yield strength in the flange is generally not detectable, but the distributions are symmetrical according to the experimental results in Figure 4.3 a). Urban has found that the distribution of yield stress is periodically recorded. The variance will be reduced when the periodic portion is removed, i.e., the calculated coefficient of variance is greater than the real value.

According to the proposed approach in section 2.2.5, the material constant ξ is 0.09 for HEB 400 with the help of Figure 2.13, and the ratio between different volumes and the corresponding coefficient of variation are available in Table 4.1. It is evident that the Weibull model deviates from the experimental values about 18% in Figure 4.4. Due to the influence of the rolling process and the periodicity of the coefficient of variation, the real material constant ξ for HEB 400 is theoretically smaller than 0.09. It is generally acceptable that the deviation between the chain of bundles model and the tensile tests is negligible.

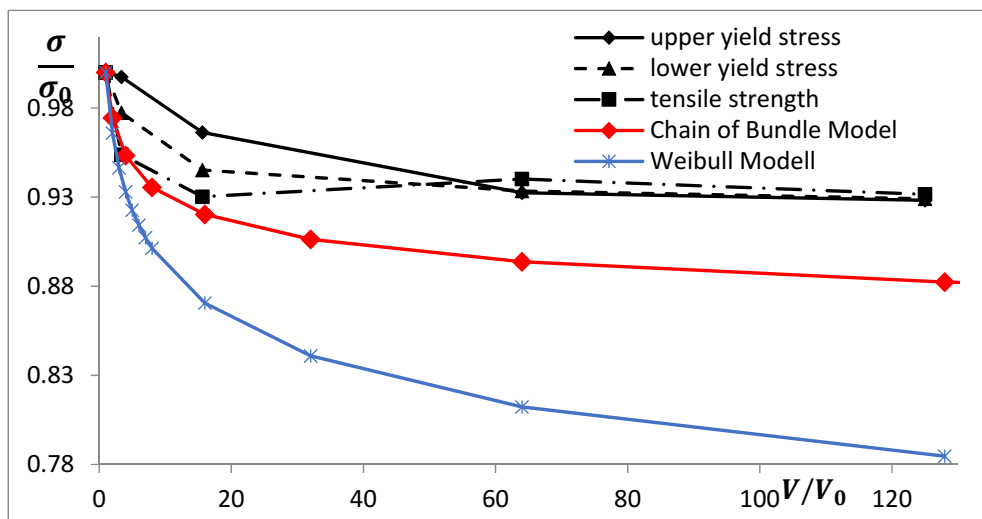


Figure 4.4: Influence of the volume on the strength of specimens from HEB 400

As a supplement to the tensile tests, all five tensile specimens were taken from a 40 mm thick plate made of S355 at 4 different positions Figure 4.1 b). The tensile specimens were taken in an axis along the rolling direction, so that the mechanical properties of steel are symmetric in the thickness direction on the plate.

Table 4.2 shows the results of tensile specimen strength with different diameters. It is easy to find that the average values of the upper and lower yield strength are greater than the theoretical value at relatively large diameter, since the material properties of a thick plate in the thickness direction are different from each other.

Table 4.2: Statistical results of tensile test from 40 mm thick plate

Specimens	$\Phi=4$ mm			$\Phi=8$ mm			$\Phi=16$ mm			$\Phi=32$ mm		
	σ_{eH}	σ_{eL}	σ_m	σ_{eH}	σ_{eL}	σ_m	σ_{eH}	σ_{eL}	σ_m	σ_{eH}	σ_{eL}	σ_m
$E(\sigma)$ [MPa]	410.8	400.5	610.8	388.5	379.1	562.8	394.2	386.5	569.5	401.6	391.1	555.4
$Var(\sigma)$ [MPa]	10.04	10.38	7.32	6.49	5.88	5.39	4.93	4.00	3.07	4.01	3.55	0.40
C_v [%]	2.44	2.59	1.20	1.67	1.55	0.96	1.25	1.03	0.54	0.97	0.91	0.07

Φ : Diameter, σ_{eH} : upper yield stress, σ_{eL} : lower yield stress, σ_m : tensile strength.

Figure 4.5 a) shows that the yield strengths on the surface are about 5 to 10% greater than in the middle, which is opposite to the tensile strength. This phenomenon means that the mechanical properties of the larger tensile specimens in the transverse direction are uneven. The cross-sections of the specimen after fracturing with different sizes of the specimen are presented in Figure 4.5 b). Due to the non-uniformity of the material in the rolling direction, the cross-section is not circular but elliptical.

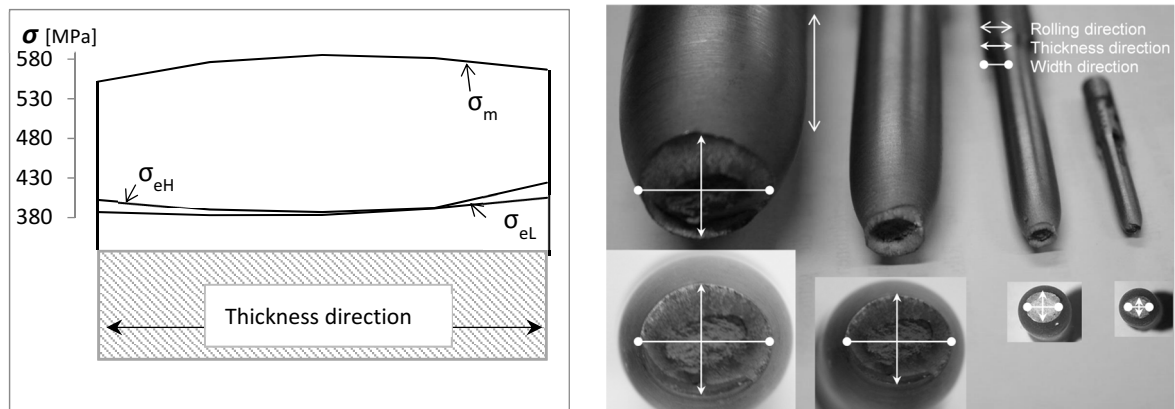


Figure 4.5: a) The distribution of the strengths in the thickness direction, b) shape of the fracture surface

In order to reduce the influence of the yield strength distribution in the thickness direction on the statistical results, the yield strengths of larger specimens are reduced according to the ratio of sectional area and the measured yield strength in the thickness direction. The material constant $\xi = 0,01$ would be determined for the 40 mm plate using Figure 2.13. The coefficient of variance, which is determined by the experiments, corresponds to the theoretically analyze results in Figure 4.6 a). It is obvious in Figure 4.6 b) that the result of tests matches up with the chain of bundle model.

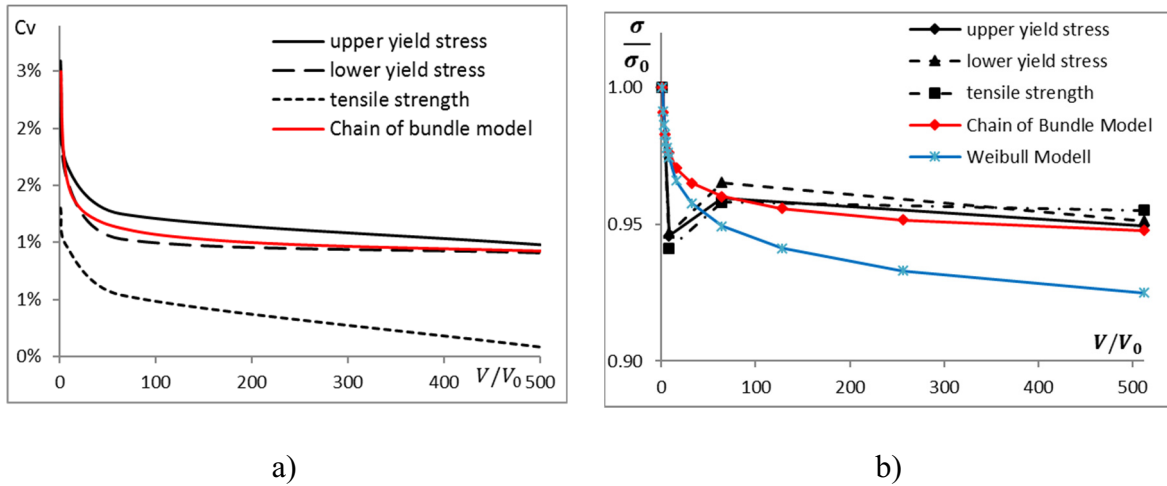


Figure 4.6: Relationship between the statistical results and the volume of the specimen, a) coefficient of variance, b) mean value

4.2.2 Bending tests with stress gradient

Usually, it is considered that the volume under yield stress in the case of four-point (4P) bending test is bigger than the one under three-point (3P). The peak stresses are produced in the 4P bending along an extended region of the specimen. Hence, a larger volume of the specimen is possible with more potential to show the mechanical defects of the specimen. Since the 4P bending test can get more relevant information from the statistical point of view, the difference of statistical strength can be reflected by these two different experiments. Therefore, the 3P bending tests and 4P bending tests are carried out with different specimen size to verify the statistical size effect in the structure with stress gradient.

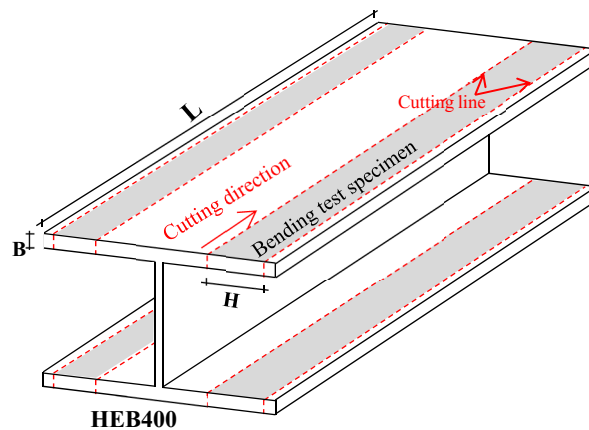
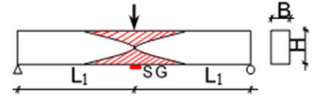
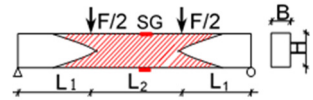


Figure 4.7: Illustration of flexural members for Waterjet cutting

Due to the relatively simple distribution of the strength in rectangular cross-section, the specimens are cut from the flange of the HEB400. In order to reduce the residual stress produced by

thermal cutting, all specimens are made by using Waterjet cutting as shown in Figure 4.7. Theoretically, the slenderness of the specimen should be as small as possible, so that there would be no instabilities. The measurements of the specimen sizes are shown in Table 3.1.

Table 4.3: Sketch and essential sizes for bending tests

Bending Test	Sketch	B [mm]	H [mm]	L [mm]	L ₁ [mm]	L ₂ [mm]
3-point		20	30	280	140	140
		24	75	1000	500	500
4-point		20	30	280	87.5	105
		24	75	1000	350	300

To get the strain from the tests, a strain gauge (SG) was placed in the center of the specimen as in Figure 4.8. The moment of the 3-point bending test is $F * L_1/4$, and in other cases, $M = F * (L_1 - L_2/2)/4$ is assumed. The 4-point bending test leads to an elongated flow zone and larger effective volume under stress.

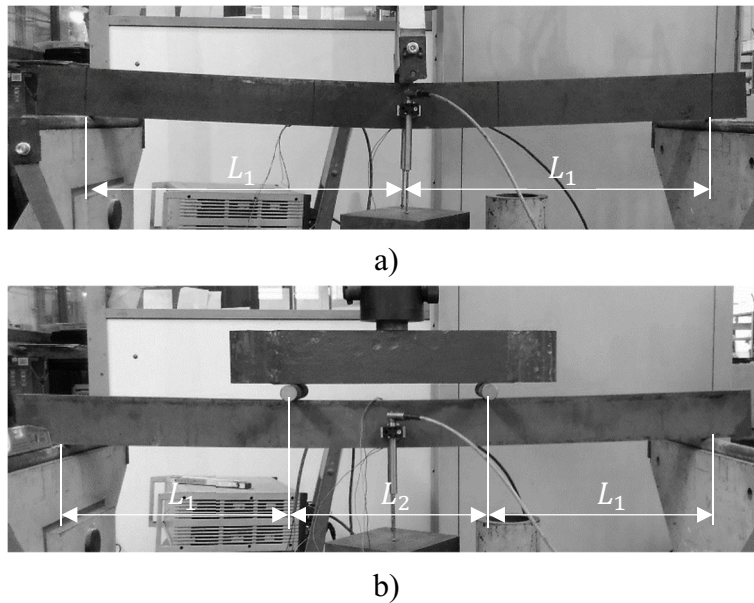


Figure 4.8: a) 3-point bending tests, b) 4-point bending tests

In the classical research project, the maximum elastic bending moment is defined by technical mechanics as $W * f_y$, where W is the section modulus. The theory, which is based on analytical mechanics, is an approximate method and the stress distribution in the actual specimen is not ideal. The experimental measurement and the maximum elastic moment obtained based on the specimen section may be different. In this thesis, it is assumed that the

transition of the linear and nonlinear relationship between moment and maximum strain is the maximum elastic moment M_{el} in experiments.

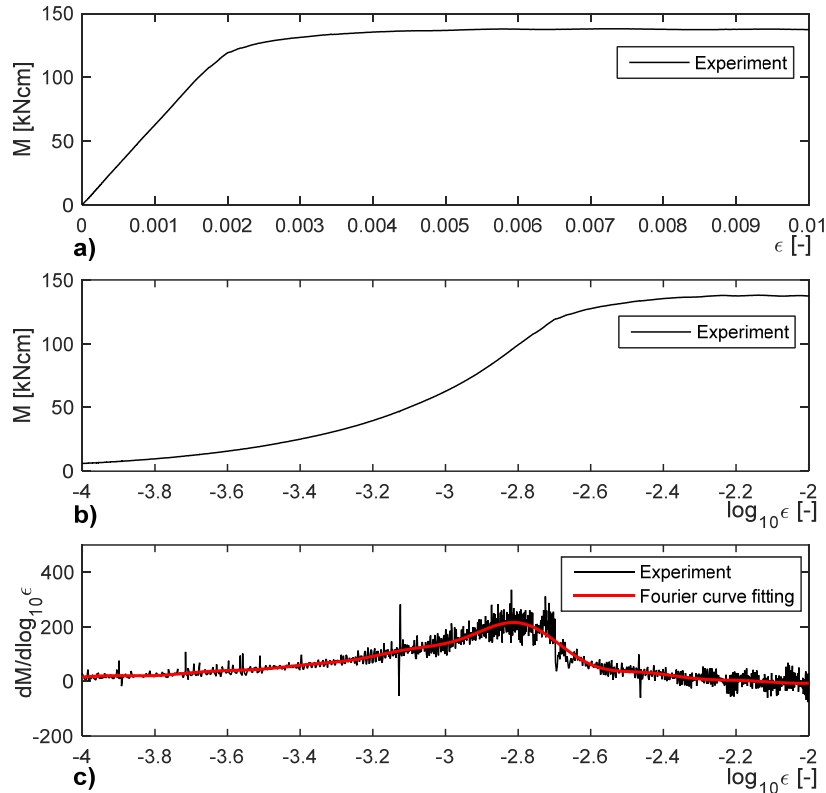


Figure 4.9: Representation of the definition of the maximum elastic moment

The strain axis of the moment-strain curve in Figure 4.9 a) is changed by logarithmic transformation. By this method, the mission of finding linear and non-linear transition points is transformed into the determination of the inflection point in Figure 4.9 b). The slope of the curve in b) must be increased steadily within the linear range. Figure 4.9 c) shows the derivative of the curve in b) which is determined values by experiment. The experimental evaluation is based on the discrete data, which is reflected in the fluctuations of the curve. To adjust the measured data, the derivatives of the moment are replaced by Fourier curve fitting method. The maximum value of the derivatives in Figure 4.9 c) corresponds to the position of the determined M_{el} from the experiments.

4.3 Simulation with stochastic material model

4.3.1 Models building

The geometry, mechanical properties and boundary conditions have to be obtained with great attention by modeling using the finite element method, so that it is possible to get the results, which are identical to those obtained from the tests. In the present work, the FEM using

ABAQUS software is employed with the corresponding user Subroutine. The modeling process and the selected analysis type are as much as possible to save the time required to complete the analysis since the element type and the mesh size has great importance to represent the models accurately. The steel structural components in this work were modeled with use of the 8-node linear hexahedral solid element, namely C3D8. For the simulation of uniaxial tensile tests with the stochastic material model, the size of each element was defined general coarse and as one-tenth of the diameter $L_{elem} = d/10$, because the specimen stress is evenly distributed in each specimen. The grip section of the tensile test specimen was modeled with a rigid body in ABAQUS, and it shown in Figure 4.10. Finally, the gage section of the specimen meshed into 4800 elements. Because the stochastic material model need integrate the stress over the whole volume, the modeling process cannot performed only a half or quarter specimen like the traditional tensile test simulation, but rather simulate the entire specimen. The simulation of the tensile test was carried out by a series of tests, where the specimens with different volumes have the same ratio of geometry.

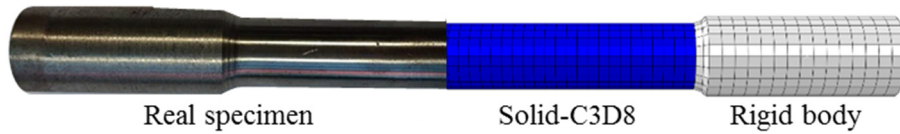


Figure 4.10: Real and simulated tensile test specimen

As the reduction coefficient γ of strength is determined by the stress distribution of the structure and the volume of the structure in the stochastic material model, a new parameter effective volume V_{eff} is introduced for the straightforward description of the statistical size effect in the flexural members. Let the ratio of the equivalent stress of finite element and von Mises stress denoted as a weight function. The weighted sum of all element volume is defined as effective volume,

$$V_{eff} = \int f(\sigma)dV/f_y = \sum_{i=1}^N \frac{\sigma_{mises}}{f_y} V_{ELEM,i} \quad (4.1)$$

where N represents the total number of the element, and $V_{ELEM,i}$ is the volume of i th element. It is clear that the yield stress of the material decreases with increasing V_{eff} in the bending simulation.

4.3.2 Material description of stochastic material model

The experiments are limited to the material steel S235 from HEB400 and S355 from plate with 40 mm thickness. Defining the material properties of the steel members in the models was done

by the use of the true stress-strain curves in Figure 4.11. Theoretically, the determination of the mechanical properties can be done by the tensile test with arbitrary volume. In this research, the stress-strain curve obtained by the smallest volume of the specimen, namely diameter is 4 mm, is defined as the reference strength.

Five samples were tested for the diameter 4 mm of tensile specimens. The reference engineering stress of the material was obtained by averaging the five stress-strain curves, and then the engineering stress-strain curve was fitted and simplified, so that a smooth and simple curve could be obtained to describe the plastic properties of the material. Finally, the real yield stress f_y of S235 and S355 steel were respectively defined as 300 MPa and 400 MPa for the tensile specimen according to the test results. The plastic properties of the steel were referred to the table in Figure 4.11. By comparing the experiment, Young's modulus and Poisson's ratio of the materials are more stable, as well as these are respectively 210 GPa and 0.3.

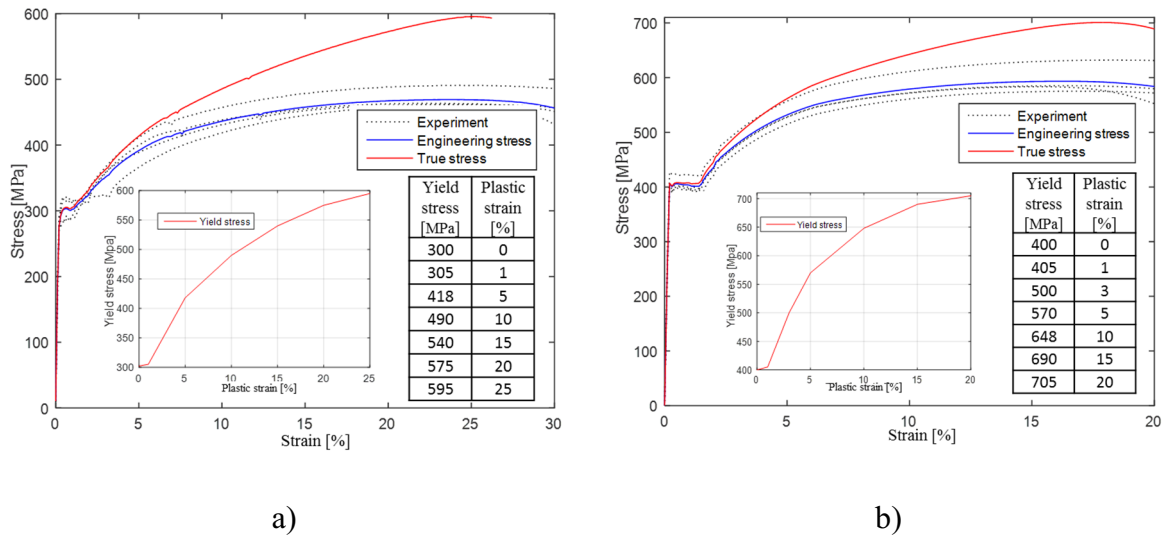


Figure 4.11: Stress-strain curve, a) S235 from HEB400, b) S355 from 40 mm plate

The material constant of the stochastic material model was measured by experiment as approximately 0.09 for HEB400 and 0.01 for steel plate with 40 mm thickness. However, it is very difficult or very expensive to measure this material constant accurately by experiments, because the material constant is obtained by the statistical theory, which is based on a plenty test results. On the other hand, this material constant is also very sensitive to the measurement conditions. Especially, it is not easy to exclude the correlation of the strength for each specimen. It is possible to increase the accuracy of the material constant of the stochastic material model by more tests; however, this is a very uneconomical method. The more efficient method is proposed. The approximate value of the material constant is obtained with a few numbers of experiments and the simulation with the stochastic material model would be implemented with different

material constant. Finally, the exact material constants are deduced by comparing the simulation results with the experimental results.

4.3.3 Investigation of material parameters

It is known from the Eq. (2.19) in section 2.3.1 that, solving the statistical size effect coefficient γ is necessary to determine the two unknown quantities, the material constant ξ and the volume of RVE V_{RVE} . As mentioned above, the approximate range of material constants is obtained by experiment, but the V_{RVE} -value is difficult to measure directly. According to the definition of the SSE coefficient, the γ is the ratio of true yield stress at two different volumes. Therefore, the parameters of the stochastic material model can be obtained based on the relationship between the strength and specimen size.

Figure 4.12 shows the influence of these two parameters on the yield strength, which is obtained by the FEM simulation using the stochastic material model with different specimen volumes. The most significant results is that the yield strength decreases as the specimen volume increases. With the increase of the material constant ξ , the reduction rate of yield strength on specimen size is accelerating. However, the increase of other parameters $1/V_{RVE}$ -value results in a decrease of the reduction rate of the yield strength with the relatively big specimen.

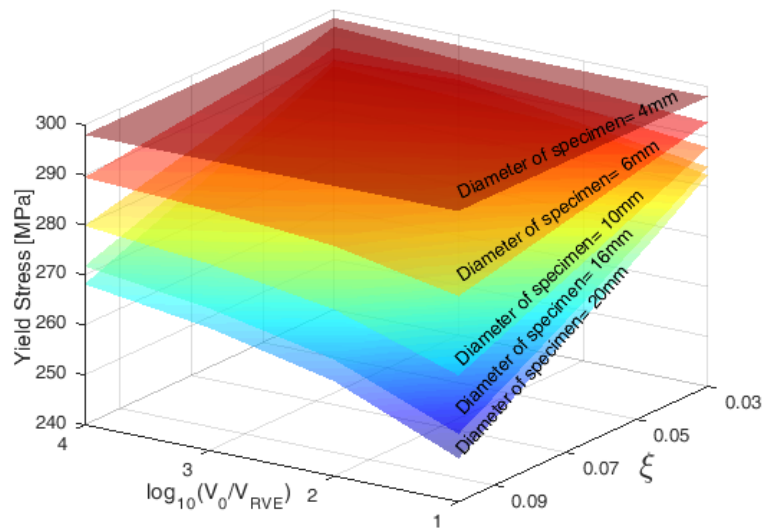


Figure 4.12: Influence of two parameters on the yield strength

It is worth noting that the yield stress is monotonically decreasing as the both parameters ξ and V_{RVE} -value increase. In this thesis, the determination of material parameters is based on the same ratio of yield strength reduction with different specimen volumes between the tests and the numerical calculations. If the relationship between the yield strength and volume is known, only one parameter can be obtained, and another parameter requires a pre-assumed value, due to the monotonicity between yield strength and parameters.

As the physical meaning of the ξ -value in the stochastic material model is a constant that describes the randomness of material properties, at the same time, the volume of RVE does not have physical meaning, the V_{RVE} -value is assumed as 1 mm^3 . Figure 4.13 shows the relationship of the yield strength of specimen with diameter 20 mm and the V_{RVE} -value. It is obvious that the yield stress increases with the decreased V_{RVE} -value. However, the rate of change is reduced when the volume of RVE decreases, because the abscissa is represented by a logarithmically form. Although the V_{RVE} -value has an effect on yield stress, this difference can be corrected by the parameter ξ -value.

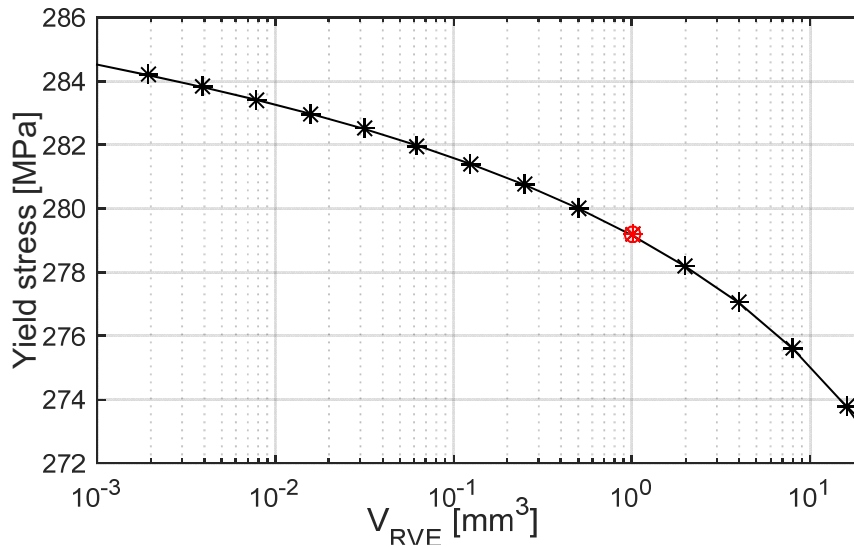


Figure 4.13: Monotonous relationship between yield stress and V_{RVE} -value

The strength change of the experiment results and simulations regarding the specimen volume are presented in Figure 4.14 a) for the steel from HEB400 and in Figure 4.14 b) for the specimen from steel plate with 40 mm thickness. It is clear that the overall trend of result curves from the tests and simulations are consistent. Meanwhile, adjusting the material constant ξ can make the experiment and simulation results with more consensus. It was found that the simulation can completely describe the experimental results for the material from HEB400 as the material constant is equal to 0.06. The same conclusion can be drawn to the material from 40 mm plate as $\xi=0.035$. In consequence, the material constant of the stochastic material model for steel S235 and S355 can be considered to be between 0.03 and 0.06.

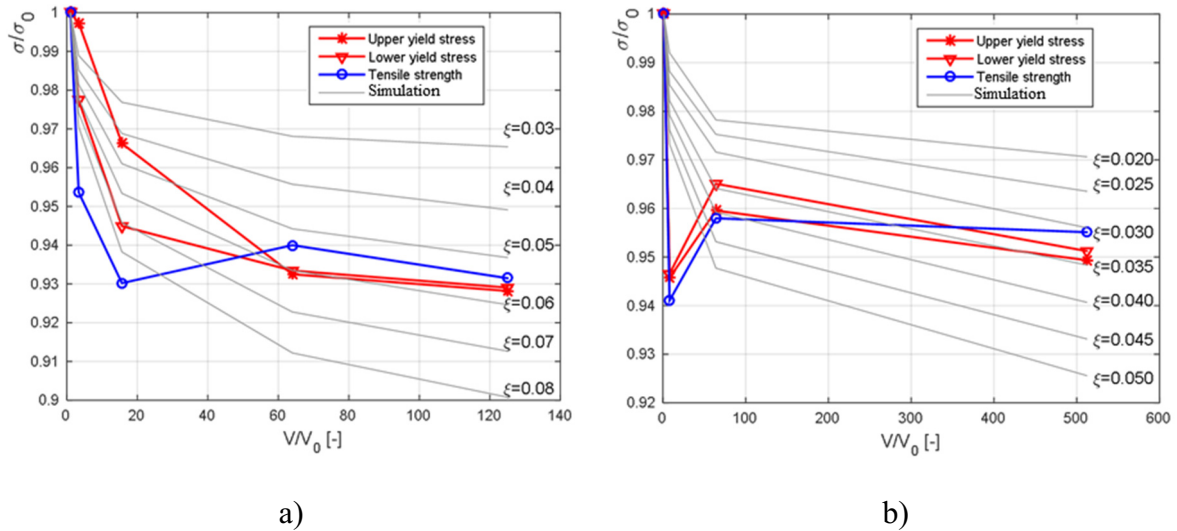


Figure 4.14: Experimental and numerical results of yield strength with various specimen volume, a) S235, b) S355

4.3.4 Simulation of flexural members

To study the stochastic material model used in the simulation of structural component with the stress gradient, a three and four points bending simulation were performed with two different specimen volume, which is carried out in the bending tests. The geometry of all specimens is consistent with the experiments. To avoid a huge stress concentration at the support and loading point, the semicircular rigid body in Figure 4.15 was modeled at these positions as well as the connection between the rigid body and the specimen is simplified as the frictionless contact surface.

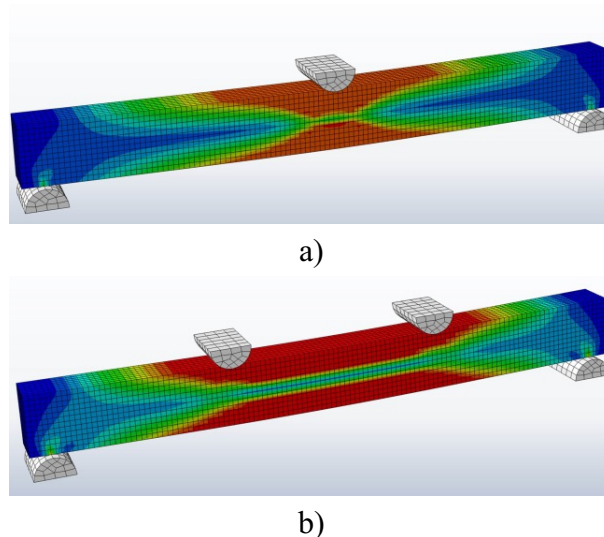


Figure 4.15: Illustration of the simulated 3-point a) and 4-point bending test b)

Due to the presence of the stress gradient in the bending direction of the flexural member, the size of the simulation with the stochastic material model is limited. The average stress on each

finite element has a relatively larger error when the element mesh is not fine enough. Figure 4.16 shows the load capacities of FEM simulation for 3- and 4-point bending flexural experiments with different FE mesh. Evidently, the relatively exact load is achieved at the ratio $H/l_0 = 10$ between the height of beam H and the mesh length l_0 of the entire structural component. The ultimate load capacities are reduced with increasing FE mesh and is almost constant if the FE mesh would be greater than $H/10$.

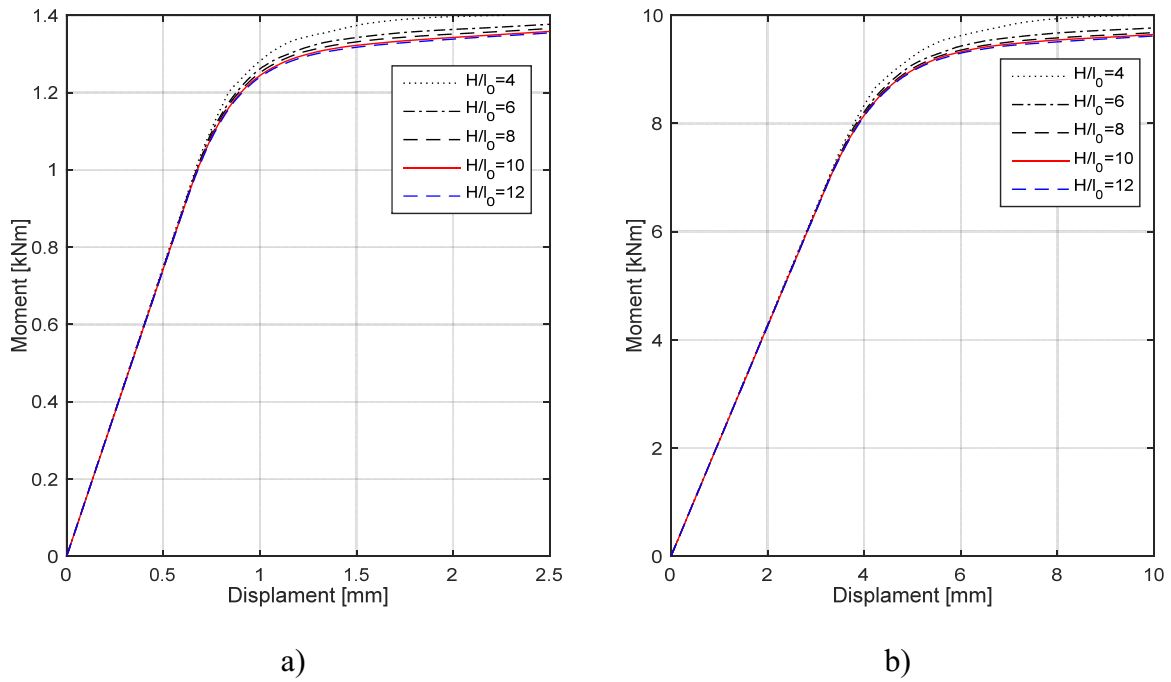


Figure 4.16: Influence of FE mesh on loads, a) 3-points bending simulation, b) 4-points bending simulation

The relationship of the stress-strain for the element, which is located at the center of the bottom surface of the 3P and 4P bending beam, is shown in the Figure 4.17. The full red line represents the predefined material constitutive relation. The yield strength in the simulation is small than the pre-defined value when this element reaches the plastic stage and the reduction of yield stress in 3P bending is lesser than in 4P bending. The reason can be explained by the change of effective volume V_{eff} with the different bending types and strain states. The black dotted lines are the effective volumes. Obviously, the V_{eff} in 4P bending specimen is greater than the 3P specimen, as well as the effective volume is significantly increased regardless of the type of bending in the plastic phase. It was noticed that the yield stress decreases with increasing effective volume V_{eff} . This phenomenon is consistent with the statistical size effect. The ultimate bending bearing capacity of the 3- and 4-point bending simulation will be described in detail in section 4.5.

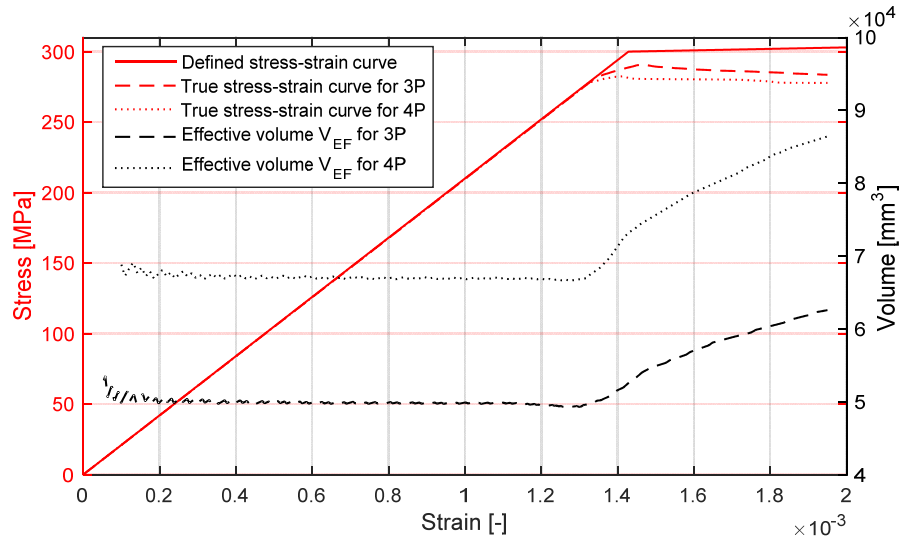


Figure 4.17: Defined and true stress-strain curve in simulation and corresponding effective volume

4.4 Simulation by stochastic FEM

4.4.1 Random field of elasto-plastic material

The randomness of material properties at the macroscale is determined by the mechanical uncertainty of the material at the microscale. Due to the huge change of scale from microscopic to macroscopic structure, the macroscopic material properties are difficult to be determined by the simulation of the microstructure of the steel structures. To simplify the randomness at the macroscale, it is assumed that the uncertainty of material properties is homogeneous and can be quantified by using random variables or fields with a specific probability distribution and correlation structure in this research. This assumption allows modeling of the uncertainty based on the macroscopic material properties. These statistical parameters should be arbitrarily assumed in the most situations. The parametric studies can be performed by determining the influence of each hypothesis on the stochastic response. The randomness of the elasto-plastic material strength is achieved by simplifying and assuming that the stress-strain curve of the material is random and can be described with the combination of some random field.

Figure 4.18 shows the schematic sketch for the stochastic elasto-plastic material. The randomness of the elasto-plastic property of homogeneous material is defined using different probabilities distributions of Young's modulus $P(E)$, yield strength $P(f_y)$ and ultimate tensile strength $P(f_u)$ in Figure 4.18. The Poisson's ratio is also a stochastic variable, but it is not considered in this work, because the change in Poisson's ratio has hardly influence on the material strength. The uncertainties of material properties are often assumed to be Gaussian (Young's modulus)

due to its simplicity, but the most material uncertainties in engineering systems are non-Gaussian (yield strength and ultimate tensile strength) in nature.

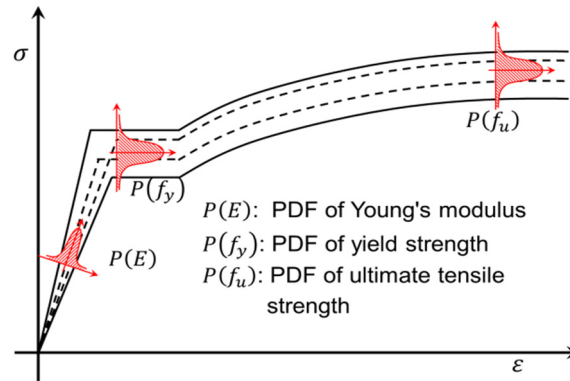


Figure 4.18: Estimated assumptions of stochastic fluctuations of elasto-plastic material properties on stress-strain curve of steel

It is generally accepted that the yield strength and tensile stress of a material vary proportionately, but the correlation between f_y and f_u , $corr(f_y, f_u)$, is equal to 0.75 from the experimental research in [107]. Accurate consideration of this correlation requires higher dimensional random fields for describing the material properties. Thus, this will increase the difficulty of establishing the random field and discrete calculations. In this study, it is assumed that $corr(f_y, f_u) = 1$ because the value of the maximum plastic stress in the steel structure is slightly larger than f_y and much smaller than f_u . Moreover, the maximum bearing capacity of the specimen is dependent on the randomness of the yield strength. Therefore, herein, the calculations of the maximum bearing capacity or plastic moment capacity are focused on the random field of the yield strength.

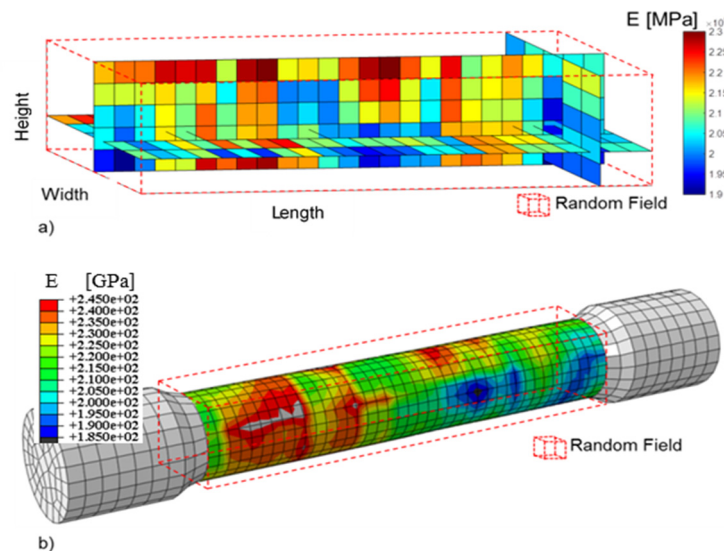


Figure 4.19: Random distributed Young's modulus, a) slices of RF, b) tensile specimen in RF

In this thesis, the random field is modeled with a 3D rectangular space for the specimen with any shape. Because we are interested only the stretched portion of the tensile specimen, the length of random fields of Young's modulus in Figure 4.19 and yield strength Figure 4.20 for the tensile test is confined in the length of stretchable part considering the computational efficiency.

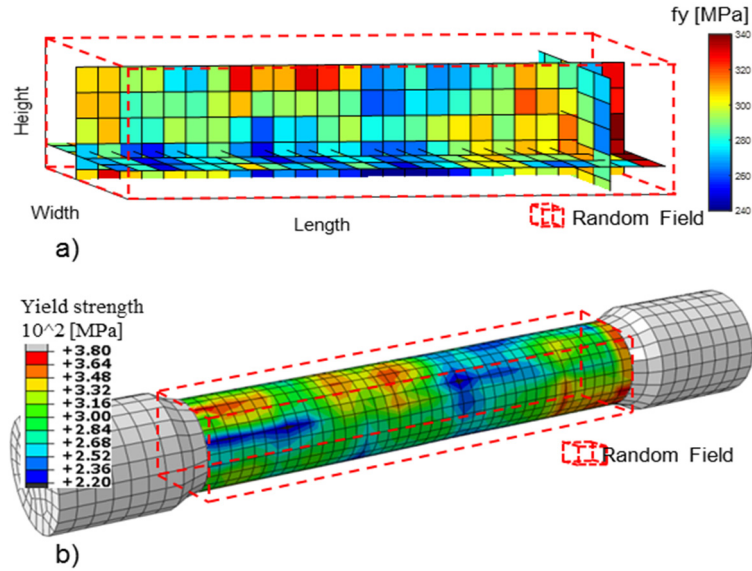


Figure 4.20: Random distributed yield strength, a) slices of RF, b) tensile specimen in RF

Usually, Young's modulus is used to characterize the elasticity of the material. The bearing capacity of the structure is determined by the yield strength of the material. If the problem involves only an isotropic linear elastic regime, obtaining a random response of the structure degenerates into a stochastic linear problem [58]. For the randomness of material, two groups of simulation with different random fields are performed to compare with each other.

- a) A random field containing only the yield strength of steel: It is assumed that the yield strength of the random field follows the lognormal distribution with constant mean value $\mu_L = 300$ MPa and standard deviation $\sigma_L = 30$ MPa.
- b) A random field containing two independent variables (Young's modulus and yield strength of steel): Mean value ($\mu_N = 210$ GPa) and standard deviation ($\sigma_L = 10.5$ GPa) of Young's modulus that follows the Gaussian distribution is assumed for the first variable. The distribution and parameters from the first group are directly applied for the spatially varying yield strength of this random field.

Figure 4.21 shows results of the relationship between displacement and force for simulation of tensile test with spatially varying variables. The Young's modulus which is inputted with a random field only changes the force of specimen in the elastic region. The maximum bearing

capacity of the specimen is dependent on the randomness of the yield strength. Therefore, the calculations of the maximum bearing capacity or the plastic moment capacity only need to focus on the random field of yield strength. On the other hand, the random field of Young's modulus should be considered calculating with the elastic material.

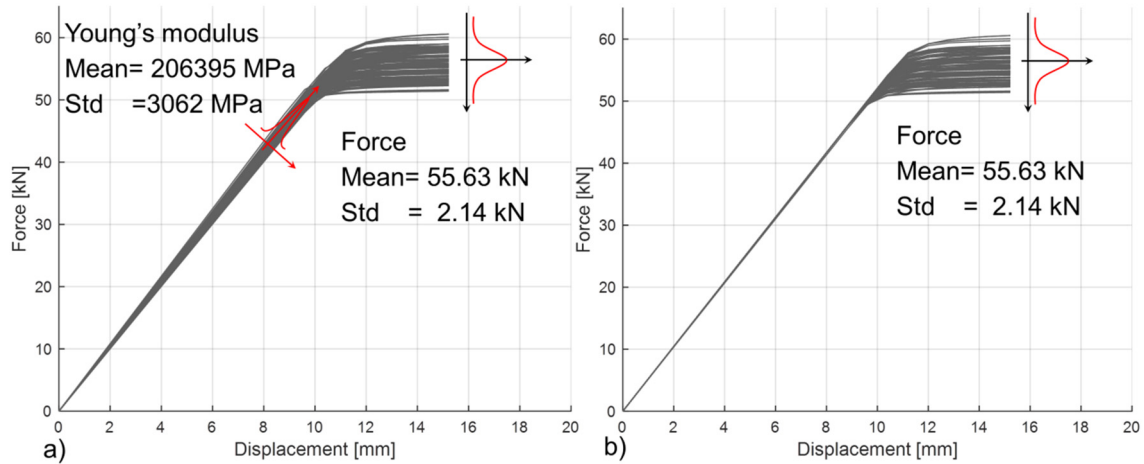


Figure 4.21: Response of stress-strain curve, a) with RF of Young's modulus and yield strength, b) with RF of yield strength

4.4.2 Numerical simulation of tensile members

The simulation of uniaxial tensile test for the steel S235 is carried out with SFEM, and the solid element C3D8 is employed for the tensile specimen. The average stress-strain curve in Figure 4.11 from tensile tests is used as the basic material properties. The basic parameters of the random field, namely coefficient of variation and correlation length, are treated as unknown quantities of study in this section. For the simulation, the correlation length L_c is assumed to be proportional to the length L_{RF} of RF mesh. 1% is defined as the target accuracy $\bar{\epsilon}_{tar}(\mathbf{X})$.

In order to demonstrate the capability of SFEM for simulating the stochastic material response, direct MCS is performed. 200 samples of RF are generated by using LHS and assuming lognormal distribution. The simulations with different specimen sizes are carried out to show the effect of the randomness of material properties on the yield strength.

Figure 4.22 a) and c) present the PDF and CDF of yield strength on all nodes at random field. The PDF and CDF of statistically simulated responses based on the tensile specimen with diameter 10mm are presented in Figure 4.22 b) and d). It is clear that distribution of the yield stress at the integration point mapped from the random field is consistent with the target distribution function. However, the distribution of the stress response of the entire specimen will not be conformed to the lognormal distribution.

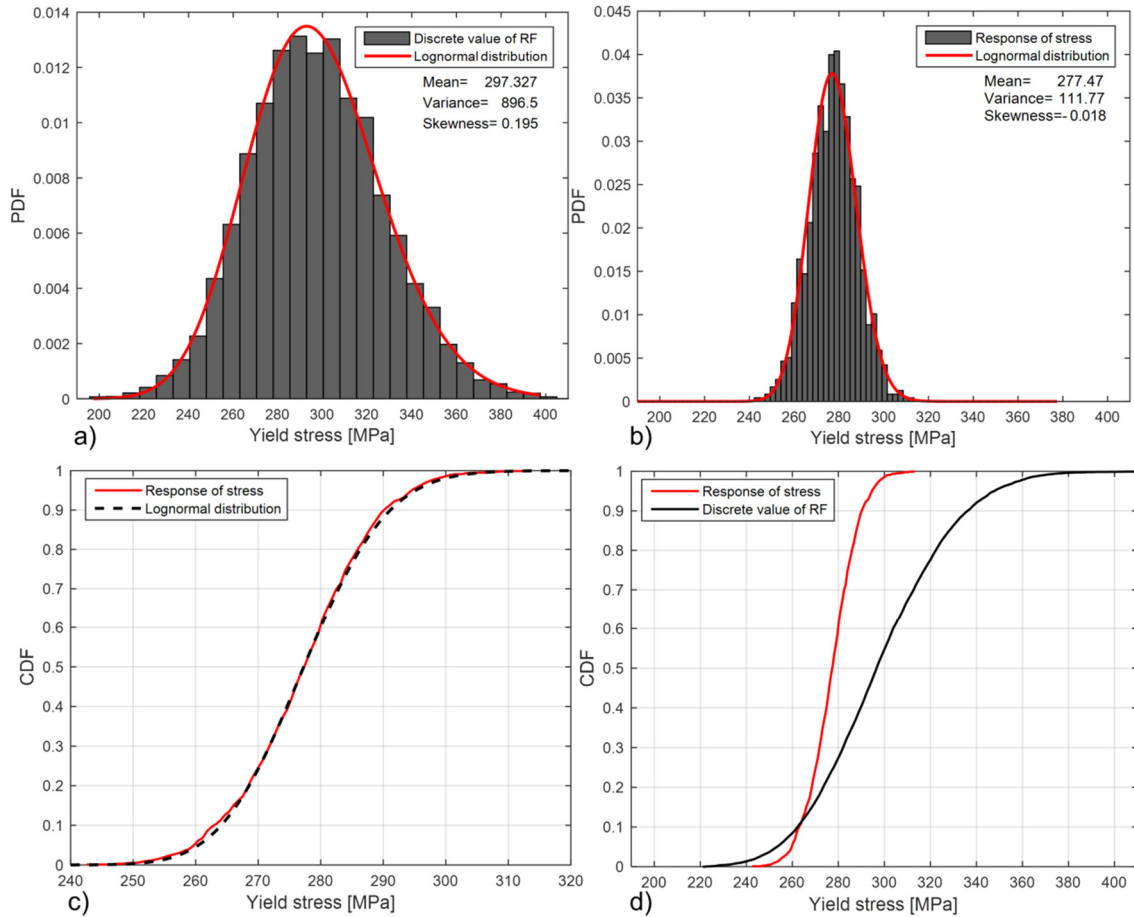


Figure 4.22: PDF and CDF of the pre-defined random field and stochastic response of the yield stress

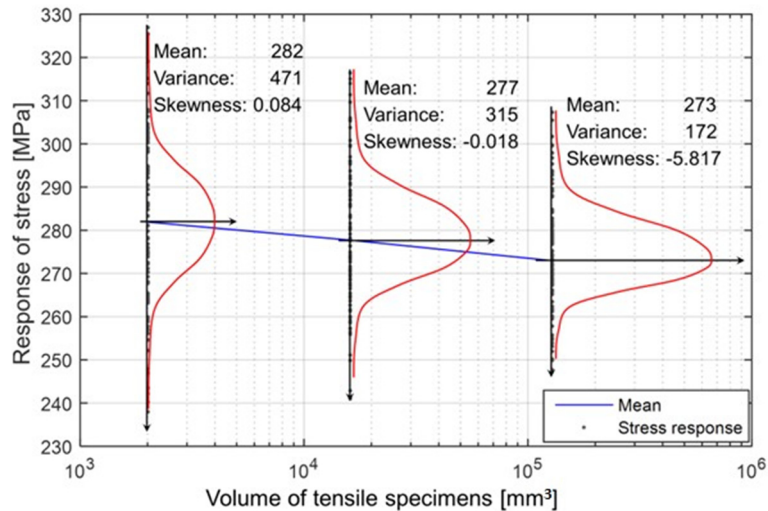


Figure 4.23: Relationships between the response of stress and volume of specimens

Figure 4.23 shows that the distribution of stress response of entire specimen is gradually changed with increasing volume of specimens. i.e., the mean value of the yield stress response decreases from 297.3 MPa, which is the mean value of yield strength in the random field, to 277.5 MPa. The statistic variance of yield strength with larger volume is relatively small in the

uniaxial tensile test, and the left tail of this distribution is longer. Because the abscissa is expressed in a logarithmic form, the rate of the mean variation of the stress response decreases with the enlarged volume. This phenomenon is consistent with the statistical size effect in the literature [10].

The establishment of yield strength random field is based on the reasonable approximation of the strength statistical characteristics and the corresponding spatial correlation. For steel structure, a lognormal distribution is recommended for the yield and tensile strength in [3,107]. The mean value of yield strength in the random field can be obtained by the uniaxial tensile tests. The coefficient of variance (C_v) of the RF variables is not exactly the same as the strength C_v of the entire structural component due to the existence of the correlation in RF and the influence of the correlation length. The C_v relationship between the target RF and simulated tensile specimens with different specimen sizes and correlation length is shown in Figure 4.24. Overall, the strength C_v with different specimen sizes monotonically increase with the increasing C_v of RF, and the specimen strength C_v is always less than the C_v in target RF. The difference of two C_v increases with the increasing specimen size and (or) the decreasing RF correlation length. The yield strength C_v for structural steel is usually defined as 0.07 in [107], as well as this value for steel S235 is between 0.05 and 0.08, according to the tensile tests with different specimen sizes in Table 4.1. To summarize, the yield strength C_v of RF in steel structures is assumed as 10%.

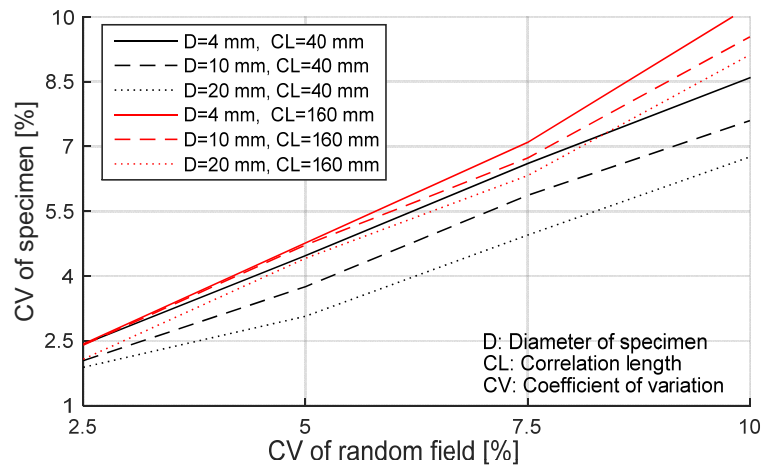


Figure 4.24: Coefficient of variation of random field and yield strength of specimen

The other epistemic uncertainty is in determining the correlation length. The correlation length of yield strength is actually a parameter used to describe the material randomness, and correlation and it can be theoretically measured through the experiments. However, the directly and accurately measurement of the correlation length of yield strength is difficult and very resource-

intensive, according to current measurement techniques. To display the influence of the correlation length on the specimen yield strength, the ultimate bearing capacity of different specimens was simulated with a series of RF correlation length. Figure 4.25 presents the relationship between the correlation length and the yield stress reduction with varying sizes of the specimen. The vertical axis in Figure 4.25 represents the ratio of the average yield stress from 200 simulations to the target yield strength of RF. When the correlation length is greater than 0 mm, the yield stress is reduced with the increased specimen size, which is consistent with the so-called SSE phenomenon. The reduction ratio of the yield stress for all specimens decreases continuously as the correlation length increases. If the correlation length approaches infinity, the SSE phenomenon will completely disappear. Due to the monotonic relationship between the correlation length and specimen yield stress, the more efficient approach to get the correlation length is that the L_c of yield strength could be obtained with plenty of numerical simulations based on the structural response inverse analysis.

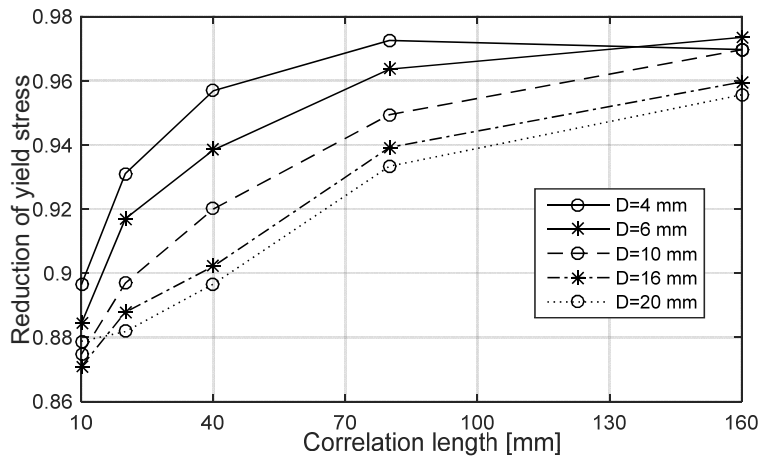


Figure 4.25: Relationship between correlation length and reduction of yield stress with different specimen sizes

To clearly describe the SSE in steel with SFEM, the simulation results of each different size specimen with various correlation length $L_c \in \{5, 10, 20, 40, 80, 160\} \text{ mm}$ is presented in Figure 4.26. The vertical axis represents the ratio of yield stress σ for each specimen size to the specimen yield stress σ_0 with minimum volume (4 mm diameter). Furthermore, the experiment results are incorporated into Figure 4.26 as contrast values. In general, the simulated yield stress always decreases as the specimen volume increases regardless of the correlation length. According to the simulation results, it is clear that the SSE is becoming more obvious as the correlation length increases until it equals 40 mm. When the L_c is equal to 40 mm, the numerical results with SFEM are consistent with the experimental results. The reduction of yield stress in

the relatively larger specimen will gradually decrease if the correlation length continues to increase. Consequently, the correlation length of steel S235 is assumed as 40 mm.

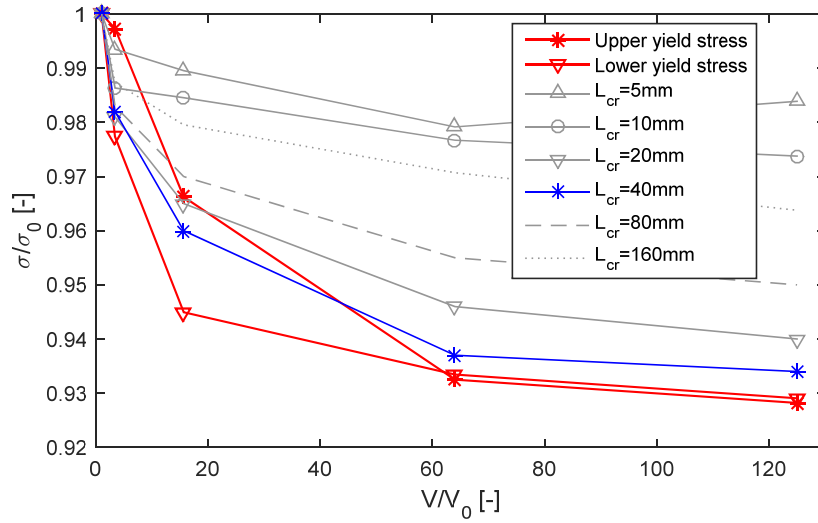


Figure 4.26: Comparison of experimental and simulated results with different correlation length

4.4.3 Numerical simulation of flexural members

In order to analyze the statistical size effect with SFEM in flexural members, 3 and 4-point bending simulations of rectangular cross-section beam with different beam size were implemented by using the random field of yield strength. The average stress-strain curve of the material properties is also determined by tensile tests with 4 mm specimen. The corresponding results are compared with the bending tests and other simulations. It is assumed that the yield strength is distributed follows a lognormal distribution in the RF and the corresponding mean value is 300 MPa. The isotropic exponential function is defined as autocorrelation function of random field, and the value 1% will be defined as the target accuracy $\bar{\epsilon}_{tar}(\mathbf{X})$. According to the results of the above section, the correlation length L_c is defined as 40 mm, as well as 0.1 is employed as the coefficient of variation of the random field for this simulation.

The geometries of different specimens are defined according to the Table 4.3. To save computing resources, the sizes of two RFs are determined with reference to the sizes of the different specimen, and it is shown in Figure 2.1. Although the size of the random field is different, the parameters of the RF are exactly same. Because the RF sizes are theoretically not affecting the properties, the results of the different specimen can be compared with each other. By 200 repetitions of SFEM, the moments of the structural component are obtained for the different specimen with various load types.

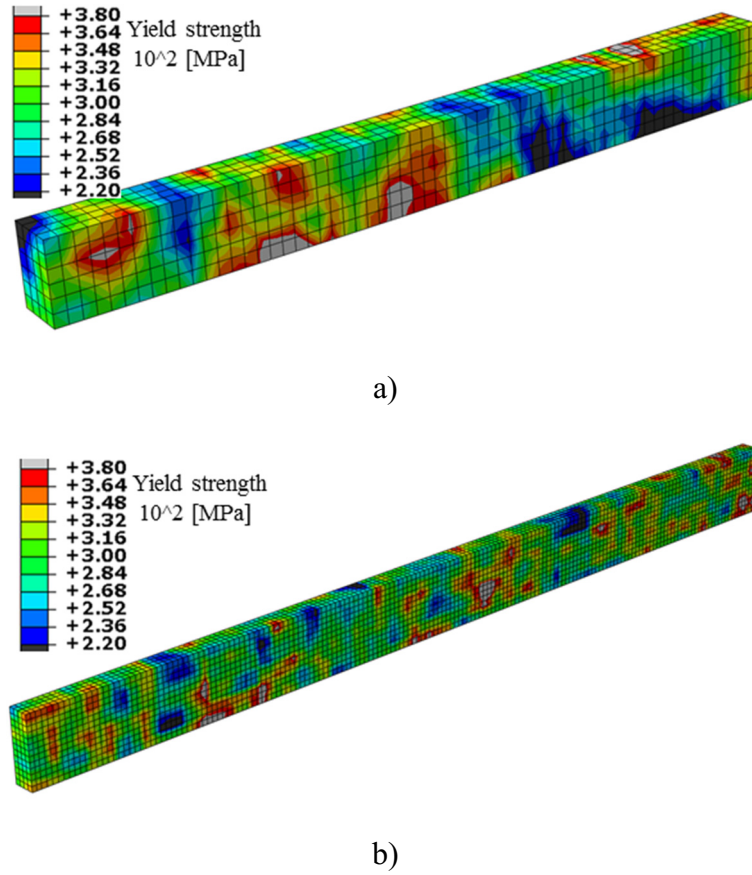


Figure 4.27: Random distributed yield strength in different specimens

Table 4.4 shows the statistical results for the plastic moment when the maximum strain of the specimen is equal to 1%. One important observation in both specimens is the effect of the load type on the mean value, variance, skewness and kurtosis of the plastic moment. The variation of the first four order statistical moments of the structural response is in accordance with the description of statistical size effect. Since the 4P bending specimens have a greater effective volume, the 3P bending members have relatively big bearing capacity. However, the variance of the bearing capacity in 4P bending members is smaller than 3P bending tests. This means that the SFEM with the random field can be used to study the SSE in flexural members in steel structures.

Table 4.4: First four order statistical moments of structural response

Statistical moment		mean value $\mu(R)$ [kNmm]	variance $\sigma^2(R)$ [kNmm ²]	skewness $\gamma(R)$ [kNmm ³]	kurtosis $k(R)$ [kNmm ⁴]
Small specimen	3P	1411.7	20358	291.1	31609
	4P	1308.9	7692	-358.5	30976
Big specimen	3P	10003.0	263704	-235.9	27764
	4P	9649.1	118118	-352.5	32655

The descriptions of the results will be presented in detail and the comparison with tests and another approach will also be implemented in section 4.5. Since the change in the first four moments means that the distribution function of the bearing capacity is constantly changing, the statistical size effect has a great impact on the reliability of the structure. Therefore, the evaluation and evolution of the PDF of the plastic moment and the influence of the SSE on the reliability will be analyzed in chapter 5.

4.5 Comparison of experiments and simulations results

In this thesis, the linear relationship of the moment and strain is defined as the maximum elastic moment M_{el} . According to the approach in the section 4.2.2, the maximum moment in the elastic stage of the tests and the numerical simulation with the stochastic material model is determined and shown in Table 4.5. It is obvious that the M_{el} of the 4P bending test is relatively smaller than the elastic moment in the 3P bending tests despite the same geometry. The same results also appear in the simulations, but the difference of the moment M_{el} between 3P and 4P bending simulations with the stochastic material model is more evident with the classical material model. Because the elastic moment is obtained by the formula in statics based on the assumptions, the mechanical method is not able to distinguish the difference between various bending types.

Table 4.5: Comparison of maximum elastic moments from experiment and simulation

Bending flexural test		Test 1 [kNmm]	Test 2 [kNmm]	FEM with size effect [kNmm]	FEM without size effect [kNmm]	Technical me- chanics [kNmm]
H: 30 mm L: 280 mm small specimen	3-point	962.1	964.2	956.1	956.1	915.0
	4-point	914.3	918.2	914.1	936.7	915.0
H: 75 mm L: 1000 mm big specimen	3-point	6848.7	6943.5	6828.4	7188.9	6862.5
	4-point	6611.9	6560.2	6580.3	7073.3	6862.5

To compare the influences of the specimens with different sizes on yield stress with each other, the equivalent yield stress is defined by engineering mechanics, i.e., $f_{y,eq} = M_{el}/W$. The equivalent yield stresses of the 3- and 4-point bending tests with different specimen geometry are shown in Figure 4.28. It is clear that the equivalent yield stresses for the elastic ultimate bearing capacity have a more significant difference with stress distribution and the structural

component volume. The equivalent yield stress of the structure decreases with the increase of the effective volume under stress. The statistical size effect in steel structures is present in the bending member and affects the maximum elastic bearing capacity of the structure, where these results cannot be received by the conventional analysis and numerical simulations.

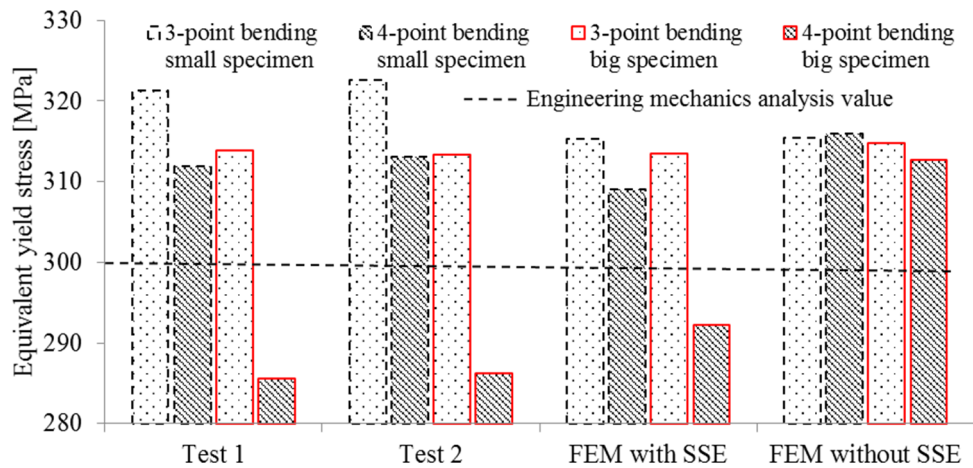


Figure 4.28: Graphical representation of the equivalent yield stress

Figure 4.29 shows moment-strain diagrams based on experiments and simulations using different plastic theories for 3P and 4P bending tests with different specimen sizes. The results of FEM simulation with the stochastic material model, in which the statistical size effect is considered, are compared with the results using the conventional method. Furthermore, to compare the results with tests and other simulation method, the mean values of the moment, which is obtained by 200 simulations with SFEM for the 3P and 4P bending beam, are calculated and shown in Figure 4.29. In addition, the plastic moment M_{pl} by plastic hinge theory (PHT) is also added to Figure 4.29 as a reference value.

It is found that the plastic moment according to plastic hinge theory is smaller than the moment based on yield zone theory in Figure 4.29 a) and c), because plastic hinge theory considers only a uniaxial stress state and neglects the interaction of shear and normal stresses. This phenomenon is already described by Petersen and Scheer in [108,109]. Therefore, the plastic hinge theory, which is used in the design norm, may be no more suitable to analyze accurately the plasticity in steel structures. Although the classical yield zone theory can consider the interaction of shear and normal stresses, its application is limited to the ideal material, as well as it can not deal with the influence of material randomness.

It is obvious that the plastic moments of the classical yield zone theory in FEM simulation are greater than the moments determined by the experiment in the plastic stage in Figure 4.29. The deviations of the plastic moments increase with the rise of strain. The computational results of

the FEM simulation with consideration of the statistical size effect show that the plastic moments in the partially plastic area are relatively small when compared with the moments of the experiment. However, the deviation of the full-plastic moments according to both methods is negligible. Additionally, the differences of the full-plastic moment with the statistical size effect in simulation increase due to the larger volume.

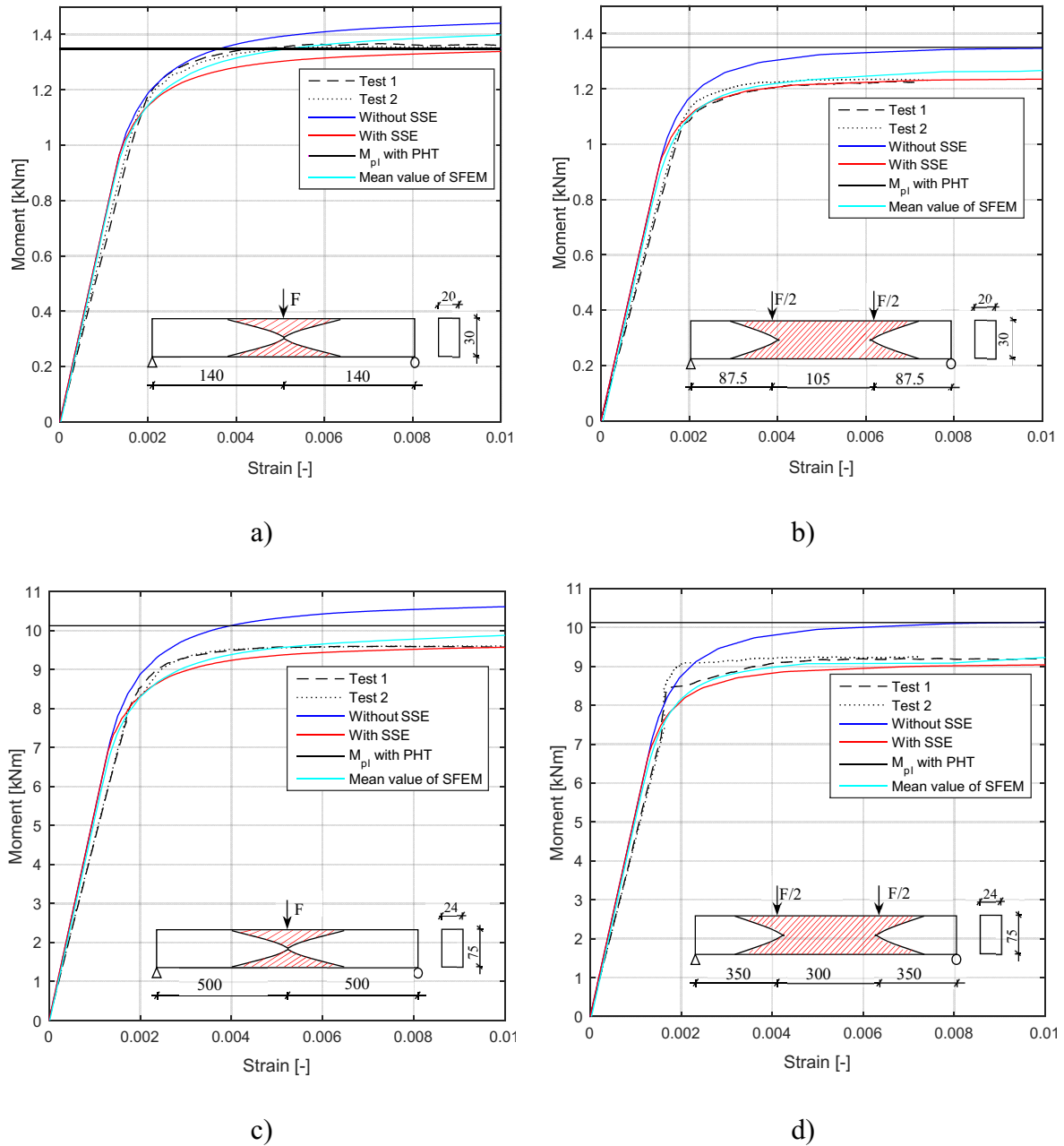


Figure 4.29: Moment-strain curves, a) 3-point test with small specimen, b) 4-point test with small specimen, c) 3-point tests with big specimen d) 4-point test with big specimen

Because of the variation of stress gradient in different specimens, the M_{pl} of 4P bending tests in Figure 4.29 b) and d) are smaller than the plastic moments of the 3P bending tests in a) and c). Moreover, the average plastic moment of the SFEM simulation with the random field of

yield strength is consistent with the tests and the simulation results with the stochastic material model in Figure 4.29. This means that the SFEM can consider the statistical size effect in steel structure with different stress gradients.

To analyze the influence of randomness of material properties on the structure strength, the two different numerical simulation methods, which are based on the classical FEM with the stochastic material model and SFEM with the random field, can be employed as a complement and extension of traditional simulation. Despite the difference of basic theory of these two simulation methods, the similar results of the flexural member can be obtained. The stochastic material model based on the distribution of RVE material and statistical theory provide a significant efficient method to calculate the SSE, because it does not require a lot of repetitive calculations. The SFEM with direct MCS is the approach at the expense of a prohibitive computational cost. However, this method is easy to understand, and its physical meaning is also very clear. In addition, the SFEM can not only deal with the influence of the randomness of the material properties on structure, but also can be used to analyze the randomness of other parameters in the structure, such as the randomness of the boundary conditions and geometry model of the structure. Moreover, the SFEM can directly combine the reliability theory for analyzing the structural safety.

4.6 Conclusions

In this chapter, the uniaxial tensile tests with different specimen sizes and different material, namely S235 from HEB400 and S355 from 40 mm thick plate, were carried out to demonstrate the statistical size effect in steel structures. Besides, the 3- and 4-point bending tests with two different specimens from HEB400 were performed with a rectangular cross-section. The results of tensile tests show that the variations of the yield and tensile strength increase with the declined specimen sizes, despite the material types are different. According to the bending tests, it was found that the structural component strength did not only depend on the specimen sizes, but also related to the stress distribution of the entire specimen volume.

The material constant ξ of the stochastic material model for steel was determined based on the comparison of the tensile tests and corresponding numerical simulations. The results show that the material constant for steel S235 and S355 is between 0.03 and 0.06. According to the simulations with stochastic FEM using different random fields, the plastic bearing capacity of the specimens is only affected by the random field of yield strength. By comparing the tensile tests, the correlation length L_c and coefficient of variation C_v of the corresponding random field were obtained using the with numerical calculations. The random field with lognormal distribution

and the isotropic exponential correlation function were employed to describe the randomness of steel yield strength. The results of 3- and 4-point bending simulations, where the corresponding correlation length and coefficient of variation of the random field are respectively $L_c=40$ mm and $C_v = 10\%$, were consistent with the experimental results and the simulations by using the stochastic material model. Besides, the following conclusions can be summarized:

- In steel structures, it appears the statistical size effect, which is similar in brittle or quasi-brittle material. The smaller the specimen size is, the greater the material strength is. The statistical size effect exists not only in the structural components under uniaxial loads, but also in the flexural members with stress gradients. The equivalent yield stress is closely related to the stress distribution and volume of the structural component.
- The two proposed simulation methods, which are an extension and supplement to traditional simulation methods, can effectively simulate the statistical size effect for the tensile and flexural members in steel structures. Simultaneously, since these two methods can provide the randomness of the structural response, they also have the potential to analyze the influence of statistical on structural safety with the help of reliability theory.
- From the results, it can be seen that the material strengths obtained by relative small specimen by statistical analysis in the laboratory are no longer valid or not optimal for large structures in practice. Especially, the maximum elastic moment and plastic moment of the steel profile need to be corrected with consideration of the statistical size effect.

5 Reliability assessment under considering material uncertainty

5.1 Introduction

In recent decades, the design of structures has focused on the probabilistic limit state design in civil engineering. The key problem in the structural design is to properly account for the uncertainties on the boundary conditions and the material properties. The finite element approaches in connection with stochastic and probabilistic methods, which can analyze the structure with the inputted uncertainty, has developed very fast in the last decades. The stochastic FEM can estimate the statistical description of response quantities. A more accurate and efficient calculation approach of the structural reliability based on the structural response from stochastic FEM has always been the focus in this research area.

Usually, the statistical response characterization method uses an explicit limit state function in which the response of the structure is obtained by the SFEM. Then, the reliability analysis is performed using the FORM or SORM. Ghanem and Spanos [56] attempt to extend this approach to SSFEM for probabilistic representation of response quantities and reliability assessment. However, this approach can be applied to analyze reliability problems involving linear problems. Because the SFEM with direct MCS for the elasto-plastic material requires many iterative calculations, the sample size of the structural response is limited, and the accuracy of the reliability evaluation is often difficult to be satisfied.

As an alternative, the probability density function of the structural response can be obtained using traditional fitting techniques, and the corresponding parameters of the theoretical probability distribution can be estimated. However, the accuracy of the results depends on the selected probability model and the sufficiency of the sample. It is worth noting that the guarantee of accuracy is a prerequisite for FORM or more accurate SORM: the distribution of random variables is correct, as well as the corresponding statistical parameters are accurate. In the case of a small number of samples, some different distributions may be accepted at the same time, and the statistical parameters of the random variable may differ from the true values. Especially, the resistance distribution of structural response obeys the combination of two distributions considering the statistical size effect. The maximum Entropy fitting method provides a possibility to obtain relatively accurate probability distribution with small available data. Therefore, the ME fitting function was used to construct the optimal probability distribution for the distribution of M_{re} under the known information in this thesis.

In this context, a framework for the reliability assessment with statistical size effect is proposed that combines the use of the maximum entropy fitting method for probabilistic modelling of the response with the MSC for reliability calculation. This method will be programmed in the general mathematical software MATLAB with FEM software ABAQUS to analyze the reliability of 3P and 4P flexural members with the various profile under considering statistical size effect.

5.2 Maximum Entropy fitting method

5.2.1 Information and Entropy

The information is an extremely wide used concept that has different interpretations from different perspectives. In general, the information is a signal that is given by the source and is received or understood by the user. The information is not the event itself, but it is used to characterize the properties of the event and contains all the information. In the past research and exploration, it was found that the uncertainty or randomness of the event is closely related to the information. For example, a recurring event occurs once, will not bring more information, because the similar information is no longer important for an event. On the contrary, an event which rarely happens occur once, but can give us more information. The occurrence of rare events is very useful for understanding the properties and characteristics of events, as well as it contains more information.

In order to measure information, the measures of uncertainty were proposed by C.E. Shannon [110] in the year 1948, and a measuring method of the information is presented. It is assumed that an event has $\langle A_1, A_2, \dots, A_n \rangle$ a total of n possible outcomes and the probability of each result is respectively $\langle p_1, p_2, \dots, p_n \rangle$. The quantities of uncertainty H of the event is given by the following formula,

$$H = -C \sum_{i=1}^n p_i \ln(p_i) \quad (5.1)$$

where C is a constant. The above formula is applied to the discrete random event. If the probability density function $f(x)$ for an event is a continuous distribution function, the H of the event is as follows,

$$H = -C \int_{-\infty}^{+\infty} f(x) \ln f(x) dx \quad (5.2)$$

In the information theory, H is called entropy. In fact, if the occurrence probability of an event is equal to one $p_i = 1$, the remaining $\langle p_1, \dots, p_{i-1}, p_{i+1}, \dots, p_n \rangle$ are equal to zero. This means the entropy $H = 0$, because the results of the test don't have any uncertainty. On the

contrary, if nothing is known about the results in advance, then all p_i are same ($p_i = 1/n$). In this case, the Entropy reaches the maximum value $H_{max} = C \ln(n)$, and the results of the event have the greatest uncertainty.

5.2.2 Maximum Entropy principle and maximum Entropy fitting method

The maximum Entropy principle was proposed by Jaynes in 1957 [73], and he indicated that the distribution with the least biased has the greatest Entropy based on additional constraints under known information. The distribution with the greatest uncertainty can be used as the distribution function of the random variable under the given constraint condition when the entropy is considered to be the appropriate quantity of measurement uncertainty. To select the probability distribution with the maximum entropy means that the distribution contains the greatest amount of information. The maximum Entropy principle provides an approach to construct an optimal probability distribution under known information. According to the given constraints, the maximum Entropy principle can be derived from many well-known probability models. For example, if the interval of the random variable is known, the distribution with maximum entropy is uniformly distributed; if the mean and variance of the random variables are known, the maximum entropy distribution is the Gaussian distribution.

The maximum Entropy fitting method is based on the maximum Entropy principle under the constraints supplied by the available information. In this thesis, the MEFM was used to construct the optimal probability distribution for the structural response, which was obtained by the stochastic FEM with the randomness of material properties. The purpose of the MEFM is to find a probability density function $p(x)$ with the ME H under the constraints [111]. This is formulated as a constrained optimization problem,

$$\begin{cases} \text{Maximize} & H = -C \int f(x) \ln f(x) dx \\ \text{subject to} & E\{\phi_i(x)\} = \int \phi_i(x) f(x) dx \end{cases} \quad (5.3)$$

where $\phi_0(x) = 1$ and $\phi_i(x) = x^n$. By the MEFM, the optimal distribution function of the structural response can be determined by the moments of the basic random variables. The $E\{\phi_i(x)\}$ is the i th moment of the random variable. Due the constant C has no influence on the maximum value of entropy H , let $C = 1$ for ease of calculation. The conventional method to solve the optimization problem is to introduce the Lagrange multiplier λ_i in Eq. (5.3).

$$H_\lambda = - \int_{-\infty}^{+\infty} f(x) \ln[f(x)] dx - \sum_{i=0}^n \lambda_i \left[\int_{-\infty}^{+\infty} x^i f(x) dx - E\{\phi_i(x)\} \right] \quad (5.4)$$

H_λ is a function of $f(x)$, The condition for the existence of stationary point is:

$$\frac{\partial H_\lambda}{\partial f(x)} = 0 \quad (5.5)$$

Thus,

$$\int_{-\infty}^{+\infty} \left[-\ln[f(x)] - \sum_{i=0}^n \lambda_i x^i \right] dx = 0 \quad (5.6)$$

so, $f(x)$ is wittier with the Lagrange multiplier λ as following,

$$f(x) = \exp \left[- \sum_{n=0}^N \lambda_n x^n \right] \quad (5.7)$$

The $\lambda = [\lambda_0 \cdots \lambda_n]$ is obtained by solving the set of $n + 1$ nonlinear equations.

$$F(\lambda) = \int x^i \exp \left[- \sum_{n=0}^N \lambda_n x^n \right] dx = E\{x^n\} \quad (5.8)$$

Theoretically, Eq. (5.8) can be solved by any method for nonlinear equations. However, the actual calculation shows that the iterative calculation of this kind of equations is very strict to the initial value. In the vast majority case, the iteration cannot converge because the appropriate iteration initial value cannot be found. However, some optimization methods were developed to solve these problems in last decades, such as generalized or improved iterative, classic or improved Newton method [112,113].

Usually, these equations are efficiently solved by the Newton method, which consists of expanding $F(\lambda)$ in Taylor's series around trial values of the λ , drop the quadratic and higher order terms, and solve the resulting linear system iteratively as in Eq. (5.9).

$$F(\lambda) \cong F(\lambda^0) + F'(\lambda) * (\lambda - \lambda^0) \quad (5.9)$$

Noting the vectors δ and μ by

$$\delta = \lambda - \lambda^0 \quad (5.10)$$

$$\mu = [E\{x^0\} - F_0(\lambda^0), E\{x^1\} - F_1(\lambda^0), \dots, E\{x^n\} - F_n(\lambda^0)] \quad (5.11)$$

This method is solved for δ from which we drive $\lambda = \lambda^0 + \delta$, which becomes our new initial vector λ^0 and the iterations continue until δ becomes appropriately small. The flowchart of this method is shown in the following figure.

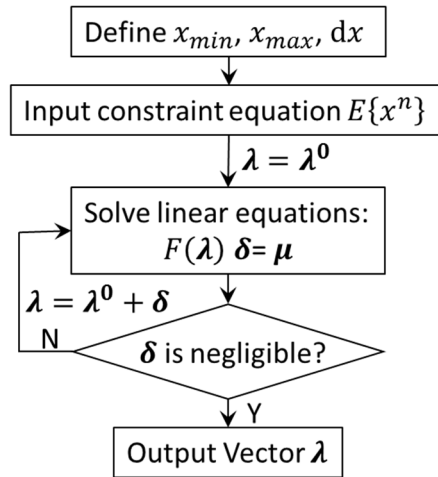


Figure 5.1: Algorithm flowchart with Newton method for nonlinear equations

To verify the MEFM, the four most frequently used distribution of random variables for the structural reliability analysis were simulated, i.e., Gaussian distribution in Figure 5.2 a), logarithmic normal distribution in b), Weibull distribution in c) and Extreme value distribution type I (Gumbel distribution) in d).

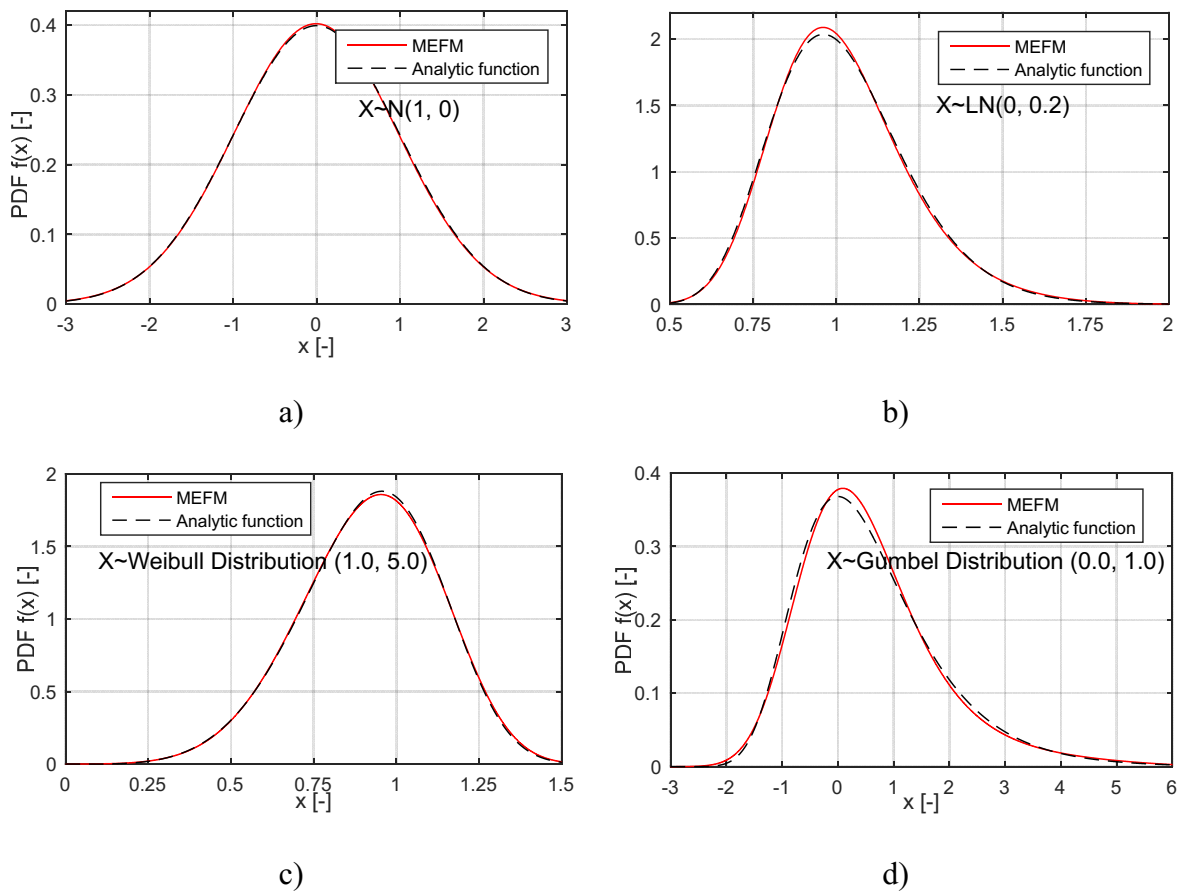


Figure 5.2: Theoretic distribution of the random variables and the maximum Entropy distribution under the first four moments constraints

Moreover, the comparison of the probability density distribution function (PDF) of the maximum Entropy distribution under the first four moments constraint and the original theoretical distribution is shown in Figure 5.2. All the maximum entropy distributions are based on 1000 samples of simulation. The comparison between MEFM and the analytic function was indicates that the MEFM could be used efficiently to fit accurate PDF based on small samples. Therefore, it is feasible and important to use the maximum entropy principle for structural reliability analysis.

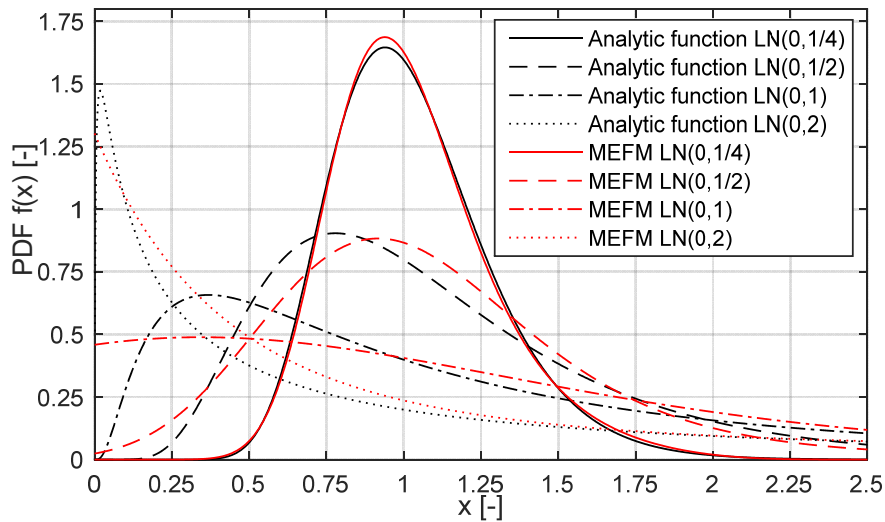


Figure 5.3: Fitting lognormal distribution by MEFM with different statistical parameters

Figure 5.3 shows the comparison between the MEFM and the analytic function with different parameters of Lognormal distribution $LN(\mu, \sigma)$. In the Lognormal distribution, the skewness γ is increasing with the increased parameter σ by the Eq. (5.12).

$$\gamma = (e^{\sigma^2} + 2)\sqrt{e^{\sigma^2} - 1} \quad (5.12)$$

With the increase of the skewness, the error of the PDF obtained by MEFM and analytic functions is increasing. This means that the MEFM with the constraint of first four moments is able to obtain a relatively accurate probability density function with small skewness. In the case of big skewness, to get a reasonable PDF may need to increase the number of constraint equations and higher order statistical moments. Therefore, the obtained PDF need to be tested whether the distribution function is accepted.

For the proposed MEFM, the K-S test is employed to decide if a sample derives from a population with a specific distribution [84]. The basic idea of this test is:

- Generate a sample from PDF, which is obtained using MEFM from the sample of SFEM.

- Compare the two samples using K-S test and decide, if there were significant differences and determine whether the two samples from the same distribution.

If the result of the K-S test is not rejected, it means that the obtained PDF can be used as a distribution function of the structural response sample. An attractive feature of this test is that the distribution of the K–S test statistic itself does not depend on the underlying cumulative distribution function being tested. Moreover, the K-S test is a completely nonparametric test for comparing two samples rather than relying on the approximate distribution. This test can work for any types of the samples, even if the distribution is unknown.

5.3 Structural reliability analysis

In structural engineering, to ensure the safety or reliability of the structure, it is necessary to study the various stochastic uncertainties, which may exist from the materials of the structure, the conditions of use and environment, construction and other aspects. Afterward, the uncertainties need to be considered by appropriate mathematical methods to analyze the safety or reliability of the structure. The system is subdivided into components and the system failure, which is the source of the joint failure of components. Because the failure of components is the basic element of the system failure, the determination of the probability of failure of each component is of paramount importance. This chapter will focus on the procedures for evaluating this component reliability.

The design of the structure need to consider the relevant reliability parameters, and these parameters are mainly divided into two categories: The first type is the direct effect imposed on the structure or the indirect effect causing structural deformation. The internal stress and deformations of structures or structures caused by these effects are called action effect S . The other is the ability of the material of the structures or components to bear the effect, known as resistance R . The resistance depends on the strength of the material, cross-section, component size, connection conditions, etc.

5.3.1 Limit state of structure

In order to correctly describe the working state of the structure for the structural reliability analysis and design, it is necessary to specify the safety and failure limit states of the structure. The limit state of the structure is essentially a threshold for the working state of the structure. If the threshold is exceeded, the structure is in an unsafe, unsustainable and unsuitable state; if it does not exceed this threshold, the structure is in a safe, durable and applicable state. For example, for a steel structure, the component will fail when the bending moment of the load

exceeds the resistance moment of the structural component. If the applied moment is equal to the resistance moment, the component reaches the limit state of the carrying capacity.

Let $\mathbf{X} = (X_1, X_2, \dots, X_n)$ denote the set of all basic random variables pertaining to the structure under consideration. If random fields are involved, the discretization schemes mentioned in chapter 3 can be used to represent them in terms of a finite set of random variables \mathbf{X}_n , i.e., $\mathbf{X} = (\mathbf{X}_1, \mathbf{X}_2, \dots, \mathbf{X}_n)$. The $g(*)$ represent a function that describes the working state of a structure, called a structural limit state function. The state of the structure can be expressed as follows.

$$\mathbf{Z} = g(\mathbf{X}) \begin{cases} < 0 & \text{failure state} \\ = 0 & \text{limit state} \\ > 0 & \text{safe state} \end{cases} \quad (5.13)$$

5.3.2 Structural reliability and reliability index

In structural design, the traditional principle of structural reliability is to compare the mean value of resistance $\bar{\mathbf{R}}$ with the mean value of action effect $\bar{\mathbf{S}}$. When $\bar{\mathbf{R}}$ is greater than $\bar{\mathbf{S}}$, the safety factor is greater than one, which means that the structure is reliable. However, since the resistance and the action effect have random properties and can use some random variables of the random field, it is a possibility that the resistance \mathbf{R} is less than the action effect \mathbf{S} , although they satisfy the conditions from the mean value. Therefore, this possibility can be expressed as the probability of structural safety.

The structural safety is measured by reliability. The reliability is defined as the probability that the structure will perform a predetermined function within the specified time and within the specified conditions, which expressed as P_s [29]. On the contrary, if the structure cannot complete the designed function, then the probability of the corresponding structure is called the probability of failure and expressed as P_f . The safety and failure of the structure are two mutually incompatible events, so the structural reliability probability of P_s is complementary to the failure probability P_f and can be expressed as follows.

$$P_s + P_f = 1 \quad (5.14)$$

The failure probability P_f is commonly used to measure the failure of the structure in the reliability analysis. The primary task of structural stochastic reliability analysis is processing stochastic information and failure probability calculation.

According to the definition of structural reliability and the basic principle of probability theory [84], the failure probability of the structure is given by:

$$P_f = p(Z < 0) = \int_{g(\mathbf{X}) \leq 0} f(\mathbf{x}) d\mathbf{x} \quad (5.15)$$

If the structure has two independent random quantities \mathbf{R} and \mathbf{S} and the corresponding PDF are $f_R(r)$ and $f_S(s)$, the failure function of the structure is as follows:

$$P_f = \int_{-\infty}^{+\infty} f_S(s) \left[\int_{-s}^{+\infty} f_R(r) dr \right] ds = \int_{-\infty}^{+\infty} f_R(r) \left[\int_{-\infty}^r f_S(s) ds \right] dr \quad (5.16)$$

The Eq. (5.16) contains two major difficulties. The joint PDF $f(\mathbf{x})$ of the resistance and action effect is usually unknown even if the basic random variables or random fields \mathbf{X} are known information. Another problem is that the multi-fold integral over the failure domain is not easy to compute. Thus approximate methods have been developed in the last years and can be found in the reference [43,114].

The reliability index β is a quantitative indicator used to measure structural reliability by Cornell [115]. It is a value of the inverse function of the standard normal distribution at a reliable probability and has a precise correspondence with the probability of failure. In the standard normal space, the limit state surface is replaced by the tangent plane at the point with minimum distance from the origin. The probability of failure can be written as follows:

$$P_f = \Phi(-\beta) \quad (5.17)$$

where $\Phi(*)$ denote the standard normal cumulative distribution. The reliability index β can also be written as a ration between mean value μ_Z and standard deviation σ_Z , i.e., $\beta = \mu_Z/\sigma_Z$, when the limit state function is subject to normal distribution. In the practical engineering problem, the structure of the \mathbf{Z} function generally does not obey the normal distribution function. Thence, the reliability index β is only a form of conversion of failure probability in this thesis.

5.3.3 Calculation of structural reliability

In structural reliability, there are two main methods: the analytical method based on probability and mathematical analysis and the Monte Carlo method based on statistical principle. The failure probability P_f in Eq. (5.16) can be solved by numerical integration, but the computation is too large for most practical problems. The basic idea of the analytical method for structural reliability is that the limit state function \mathbf{Z} is expanded by Taylor series to linearize. Then the mean value μ_Z and standard deviation σ_Z of \mathbf{Z} are obtained by using the first and second moments of the random variables or random field \mathbf{X} to determine the reliability index of the structure. This linear expansion method is often referred to as a First Order Reliability Method

(FORM). However, since the limit state function uses a first-order Taylor expansion, the accuracy of the calculation result is difficult to guarantee when the limit state function is strongly nonlinear. Some research [116,117] have used the Laplace method in mathematical approximation to study the reliability of structure and have achieved good results. Because the method uses the second order partial derivative term of the nonlinear limit state function, it should belong to the Second Order Reliability Method (SORM). It is clear that the result of SORM is based on the result of the FORM with a correction factor, which can consider the limit state function quadratic nonlinearity. Therefore, the SORM can be seen as a correction of the results of the FORM.

Whether for FORM or more accurate SORM, the reliability of the structure is essentially estimated by the first two moments of the limit state function. The information contained in higher-order statistical moments can not be efficiently used. In the traditional analytical method, the distribution function of the random variables is mostly the ideal mathematical model. There may be some unknown distribution in real situation issues that are not considered by FORM and SORM. In particular, in dealing with the reliability of the structure considering the statistical size effect, the application of these analytical methods may result in relatively greater errors, because the higher order moments of the structural response in the statistical size effect are significant and can be summarized. The Monte Carlo approach provides an alternative approach for solving such problems.

The Monte Carlo method avoids the mathematical difficulties in structural reliability analysis. It does not need to consider the complexity and the nonlinear of limit state function. Its shortcomings are computationally intensive and inefficient. However, with the improvement of sampling technology and the improvement of computer technology, the application of this method will be more and more extensive, because the MC method is intuitive, precise and has a strong versatility.

It is given that $\mathbf{X} = (X_1, X_2, \dots, X_n)$ are the random variables or random field of the structure. If the PDF of every random variable X_n is known, the random vector \mathbf{X} is randomly sampled using the mathematical method and the extracted random sample vector \mathbf{x} are substituted into the limit state function $\mathbf{Z} = g(\mathbf{X})$. When $\mathbf{Z} < 0$, the structure will fail once in the simulation. Let N denote the total number of the simulation, and the n_f means the number of $\mathbf{Z} < 0$, the estimated value of structural failure probability \hat{P}_f is as follows:

$$\hat{P}_f = \frac{n_f}{N} \tag{5.18}$$

Eq. (5.18) is derived from the relationship between the frequency and probability in probability theory and statistics. The failure probability P_f of the structure has another form if the integral is extended to the real space.

$$P_f \approx \hat{P}_f = \int_{-\infty}^{+\infty} I[g(\mathbf{X})]f(x)dx = \frac{1}{N} \sum_{i=1}^N I[g(\mathbf{X}_i)] \quad (5.19)$$

$$\text{where } I[g(\mathbf{X})] = \begin{cases} 1 & g(\mathbf{X}) < 0 \\ 0 & g(\mathbf{X}) \geq 0 \end{cases}$$

$$\lim_{N \rightarrow \infty} P \left(\left| \frac{n_f}{N} - P_f \right| < \varepsilon \right) = 1 \quad (5.20)$$

According to the law of large numbers theory in Eq. (5.20), it is clear that the \hat{P}_f converges to P_f with a probability of one. This also means that the convergence of MC simulation is independent of the dimension of the basic random vector and the complexity of the limit state function. However, for the structural failure of small probability events, it is not easy to realize $\mathbf{Z} < 0$ for direct MC simulation and it is more difficult to obtain the failure probability \hat{P}_f .

For structural reliability calculations, the way to improve the efficiency of the MC method is to increase the chances of $\mathbf{Z} < 0$, i.e., let sample points have more opportunities to fall into the failure field. The basic principle of the importance sampling method is changing the sampling center of the random variable, in the case of keeping the original sample expectations unchanged. By changing the probability distribution of the existing sample space, the variance is reduced. By this approach, the probability of structural failure sampling increases and the extracted sample points have more opportunities to fall in the interest area, so that the sampling point is more efficient to achieve the purpose of reducing the computing time.

Let $f^*(\mathbf{X})$ denote an arbitrary distribution of the probability density function as follows:

$$\hat{P}_f = \frac{1}{N} \sum_{i=1}^N \left[I[g(\mathbf{X}_i^*)] \frac{f(\mathbf{X}_i^*)}{f^*(\mathbf{X}_i)} \right] \quad (5.21)$$

where the observed random vector \mathbf{X}_i^* is obtained from the new PDF $f^*(\mathbf{X}_i)$. For simplicity, $f^*(\mathbf{X}_i)$ is the PDF of a uniform distribution in a multidimensional rectangular domain, i.e.,

$$f^*(\mathbf{X}_i) = \begin{cases} 1/A & \mathbf{X}_i \in A \\ 0 & \text{other} \end{cases} \quad (A \text{ is space of domain}) \quad (5.22)$$

The failure probability P_f of a structure is obtained by introducing Eq. (5.22) into Eq. (5.21) and is shown in Eq. (5.23).

$$P_f \approx \hat{P}_f = \frac{A}{N} \sum_{i=1}^N [I[g(\mathbf{X}_i^*)]f(\mathbf{X}_i^*)] \quad (5.23)$$

The number of simulations with importance sampling (IP) methods is not affected by the probability of failure, so the probability can be calculated for cases where the probability of failure is small. The importance sampling method does not need to consider the shape of the limit state surface when constructing the sampling function. In addition, the calculation is simple and don't require much preparation. The MCS with IP technique will be employed to analyze the failure probability of structure consider the statistical size effect.

5.4 Structural reliability with statistical size effect

In this thesis, the flexural members with stress gradient will be analyzed by SFEM considering the uncertainty of elasto-plastic material, which is the reason for the statistical size effect in macroscopic areas. The statistic samples of the ultimate capacity of the flexural member were obtained by the repeated calculation with SFEM, as well as its distribution was determined using the MEFM. Finally, the structural response of the whole structure is applied to the structural reliability analysis with MC simulation with importance sampling.

The reliability approach is intended to evaluate the probability of failure of a structure considering randomness. The failure criteria in mechanics are usually defined by load effect (stress, strain, load or deformation). The limit state function of the structure is defined regarding maximum plastic bending moment for the flexural members.

$$g_{ben}(\mathbf{S}) = M_{re} - M_l \quad (5.24)$$

where $g_{ben}(\mathbf{S})$ represents the limit state function for bending members. The M_{re} and M_l mean the maximum plastic moment of resistance and applied moment, which are random variables due to the randomness of material properties.

The probability density distribution of M_{re} is obtained by MEFM based on the response of structure. Figure 5.4 shows the flow chart of the proposed method for reliability assessment of the structure with random field considering elasto-plastic material properties, and it consists of the following steps:

- (1) Firstly, get the sample of the structural response, which is obtained by the SFEM with the random field of yield strength. The first four moments of the sample are calculated by statistical theory, and the corresponding PDF of the sample is obtained using MEFM.

- (2) Use Kolmogorov–Smirnov (K–S) test to check if the sample size is sufficient. If it is not enough, return to the initial step and generate more sample points from the SFEM.
- (3) Input of the statistical distribution and parameters of the predefined load. The PDF obtained by MEFM from SFEM is used as the distribution function of the resistance of the structure. Then, the limit state function of the structure $\mathbf{Z} = g(\mathbf{X})$ is defined.
- (4) Get the failure probability of the structure using N times MC simulation with the importance sampling. The difference of the failure probability between N and $N - 1$ times MC simulation $|\hat{P}_{f,N} - \hat{P}_{f,N-1}|$ is calculated. If the difference is greater than the tolerance ε , let $N = N + 1$ and recalculate the probability of failure $\hat{P}_{f,N}$.
- (5) If the difference is acceptable, the reliability index β is calculated.

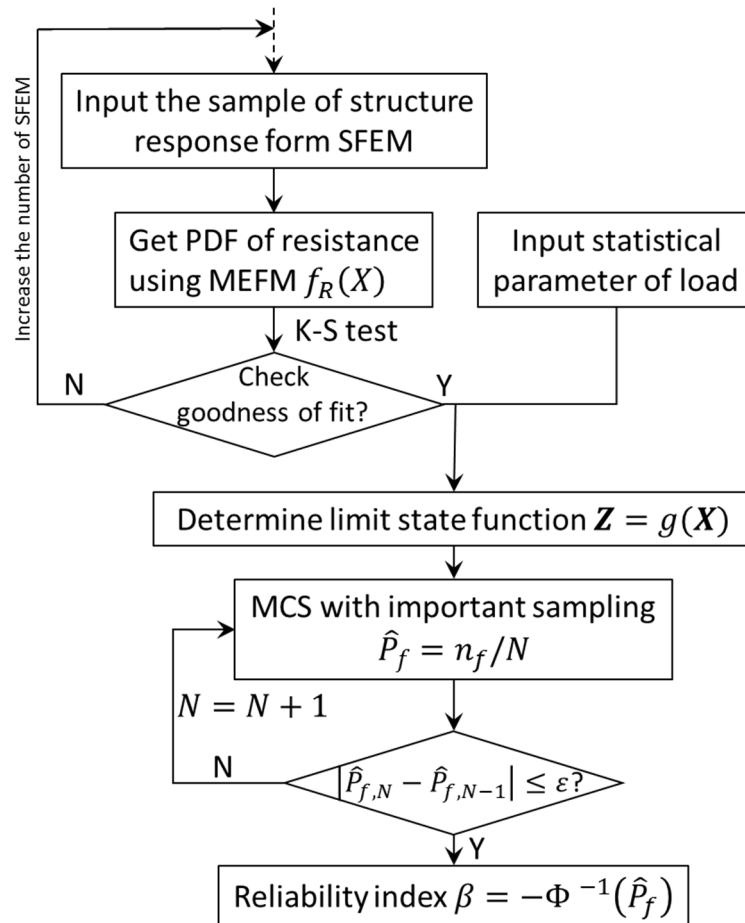


Figure 5.4: Flowchart of the proposed method for reliability assessment with structural response from SFEM

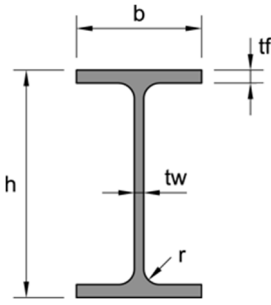
The approach based on MEFM and Monte Carlo simulation with important sampling introduced in this work can be applied in the structural reliability analysis using SFEM with random material properties whenever the PDF of the response obtained is accurate enough. One additional benefit of this method is that it can consider the influence of higher-order moments on

structural reliability and the statistical size effect. Moreover, it provides in all steps of the analysis process measures of accuracy of the approximations that can be improved if it is necessary.

5.5 Probabilistic modeling of the ultimate bearing capacity of flexural members

In order to analyze the reliability and the ultimate bearing capacity of the bending members under considering the statistical size effect, the bending simulations of IPE beam with random fields of yield strength were implemented by SFEM. The simulations are performed with different sizes of IPE profile in Table 5.1 to study the effect of the component volume on structure safety. The length and height of all specimens are proportional, i.e., $L/h = 10$. To demonstrate the relationship of the stress distribution and the structural reliability, the 3P and 4P bending simulations are compared with each other for all specimens. Because the solid element type C3D8 has relatively more integral points and outstanding computational efficiency, it is used to analyze the structural response for each simulation. It is assumed that the load applied on the structure is distributed by the Gaussian distribution, and the corresponding coefficient of variation is 10% as numerical example.

Table 5.1: Geometric parameters of the beams

IPE	h [mm]	b [mm]	t_w [mm]	t_f [mm]	r [mm]	L [m]
	100	55	4.1	5.7	7	1
	200	100	5.6	8.5	12	2
	300	150	7.1	10.7	15	3
	400	180	8.6	13.5	21	4
	500	200	10.2	16	21	5
	600	220	12	19	24	6

The random field with lognormal distribution is employed for the yield strength, as well as the isotropic exponential function is defined as autocorrelation function of RF. According to the study in section 4.4, the correlation length and coefficient of variance of the random field are assumed respectively as 40 mm and 10%. The length of the discrete random field is defined as half the correlation length.

The discretization of the random field needs to consume a lot of computing resource and the eigenfunction generated by the discrete process requires huge storage space. For example, the discrete eigenfunction for IPE600 with 6m length has 99000×99000 points with the proposed

parameters of RF. Therefore, an approximate method is employed, where the random field of IPE profile is divided into three parts, namely RF of upper flange, web (inclusive radius) and lower flange in Figure 5.5. By this approach, the discretization of the random field is to be more efficient. However, this method will cause the correlation of the junction between the flange and web to disappear as in Figure 5.5 a).

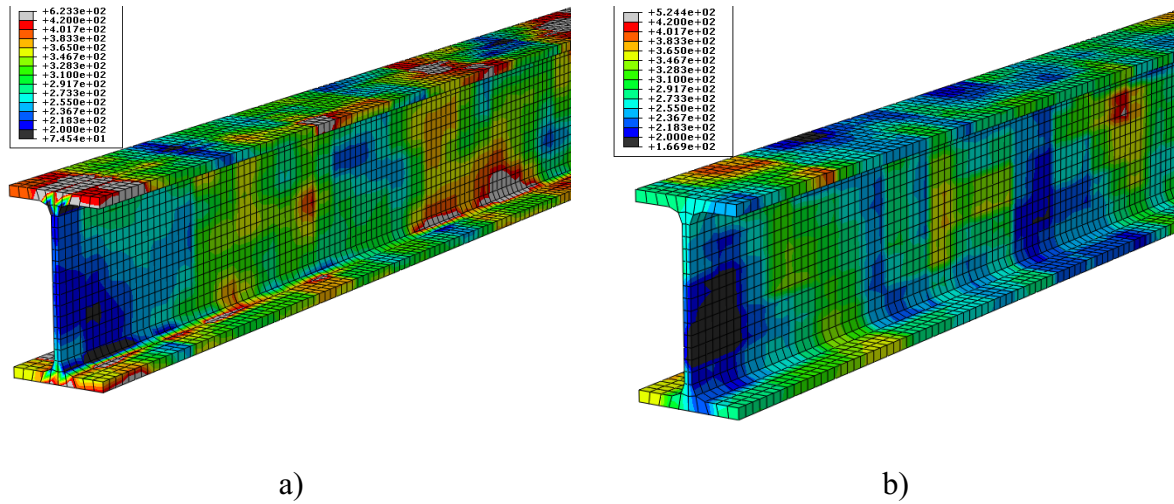


Figure 5.5: Distribution of yield stress in IPE-section beam, a) with 1 RF, b) with 3 divided RFs

Table 5.2 shows the total time of the different discretization approaches and the corresponding errors for various profile types. It is obvious that the times of RF calculation increase as the volume of the structure increases. The required times of a single RF for the 3D lager structure is unacceptable.

Table 5.2: Computing time for discretization of different RFs and corresponding global error

Profile type	IPE100	IPE200	IPE300	IPE400	IPE500	IPE600
Time for 1 RF [s]	$6.8 \cdot 10^2$	$1.8 \cdot 10^3$	$3.7 \cdot 10^4$	∞	∞	∞
Time for divided RFs [s]	$7.2 \cdot 10^1$	$8.3 \cdot 10^2$	$1.2 \cdot 10^3$	$3.8 \cdot 10^3$	$1.0 \cdot 10^4$	$2.8 \cdot 10^4$
Error [-]	2.14%	2.52%	2.98%	-	-	-

To combine three RFs into the target random field is the efficient and achievable method for treating such large-scale structure problems at the expense of acceptable computational accuracy. Because the spatial correlation of the yield stress is partially distorted, the maximum plastic moments of each specimen with the divided RFs are always greater than the actual value. According to the results of 200 repetitions of the simulation, the discretization error is smaller than 5% for the specimens.

To demonstrate the effect of the sample size of structural response on the PDF, Figure 5.6 a) shows the PDFs obtained by the MEFM with increasing sample sizes. It can be seen that the ME PDF provides an acceptable approximation for the PDF of resistance moment when the sample size is larger enough. The verified results of K-S test are presented in Figure 5.6 b). The results show that the ratio between the test statistic of different sample sizes and the approximate critical value calculated for a significance level as of 0.05 is always smaller than 1.0. This means that small size samples can be used to derive an ME PDF to represent the uncertainty on the maximum plastic moment of flexural members, which is a very attractive feature for reliability assessment involving the statistical size effect in steel structures.

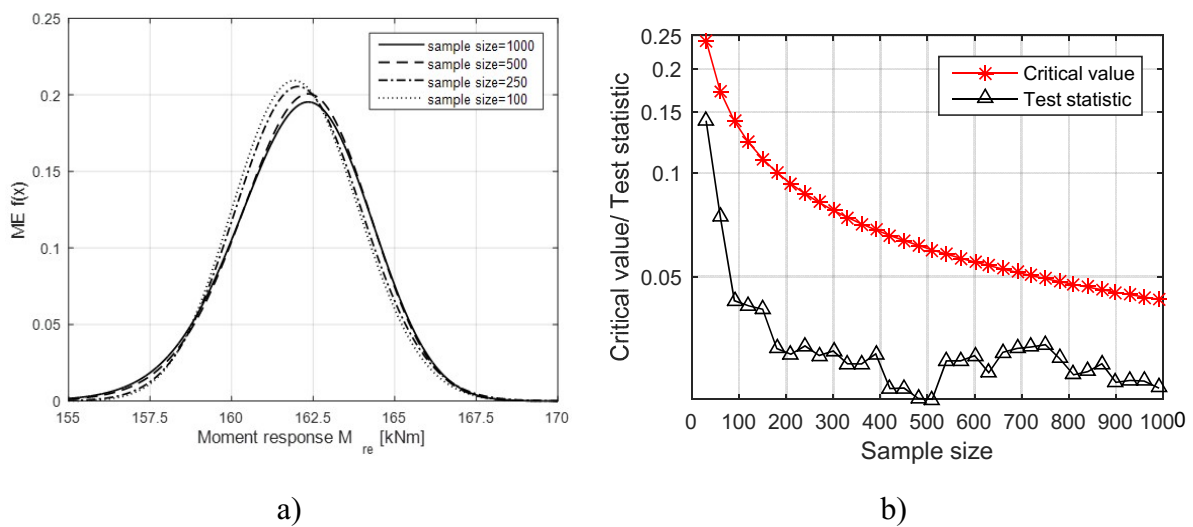


Figure 5.6: a) ME PDFs with different sample sizes, b) K-S test results for different sample sizes

5.5.1 Evolution of strength probability density function

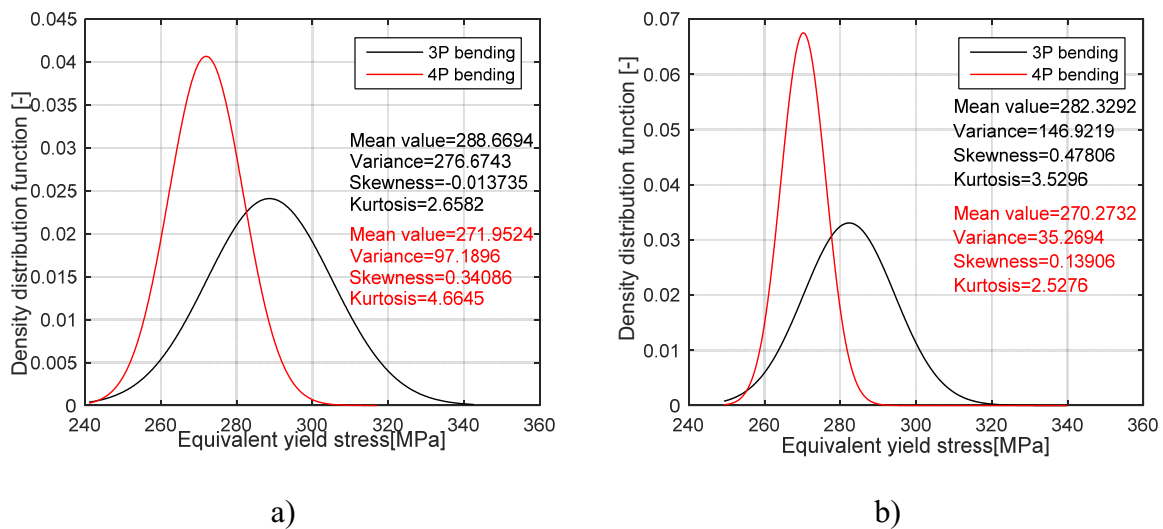
Due to the presence of statistical size effects in steel, the material strength is not the same in structures with different volume mainly dependent on the stress distribution and the size of the structural component. According to the PDF of material strength in Eq. (2.11) for the stochastic material model, it is easy to calculate the mean, variance and skewness of the material strength. Figure 2.8 more intuitively shows the relationship between the material strength and the volume of the structure. It is clear that the mean value and the variance of strength are decreasing as the volume increases and the corresponding reduction rate is slowly decreasing. In addition, the skewness of material strength is changing from positive to negative. These change of the statistical moments for stochastic material strength means that the PDF of the strength is not constant.

In this thesis, the relationship between the effective volume of a structural component and the statistical moments of the strength distribution is called the evolution of strength probability

density function for statistical size effect. Although the evolution of the PDF is based on the stochastic material model, every material must be defective and this evolution is the essential characteristic of the material.

To demonstrate the evolution of the PDF, the probability density functions of the 3P and 4P bending simulation with different I-profile obtained by MEFM are shown in Figure 5.7. For comparing the PDF of the structural response for different specimen, the maximum bearing moment is converted to the equivalent yield stress $f_{y_{eq}} = M_{pl}/W_{pl}$. The 3P bending simulation can obtain greater equivalent yield stress in each specimen with the different volume since the effective volume in 3P bending simulation is always larger than in 4P simulation.

The mean and variance of the equivalent yield stress in the 3P simulation or the 4P simulation are both reduced when the volume of the specimen becomes larger. For example, the mean value and variance of equivalent yield stresses in 3P bending IPE100 are 289 MPa and 277 MPa, but corresponding values are reduced to 263 MPa and 31 MPa in the 3P bending IPE600. However, the fluctuations of skewness of the equivalent yield stress are not particularly noticeable and the values vary almost around zero. This phenomenon should be due to the sample size for the MEFM being too small. For the reliability assessment, the impact of high-order statistics will be greatly reduced. The PDF obtained by MEFM based on the structural responses, which are calculated by the SFEM with the material uncertainty, can characterize the evolution of distribution function.



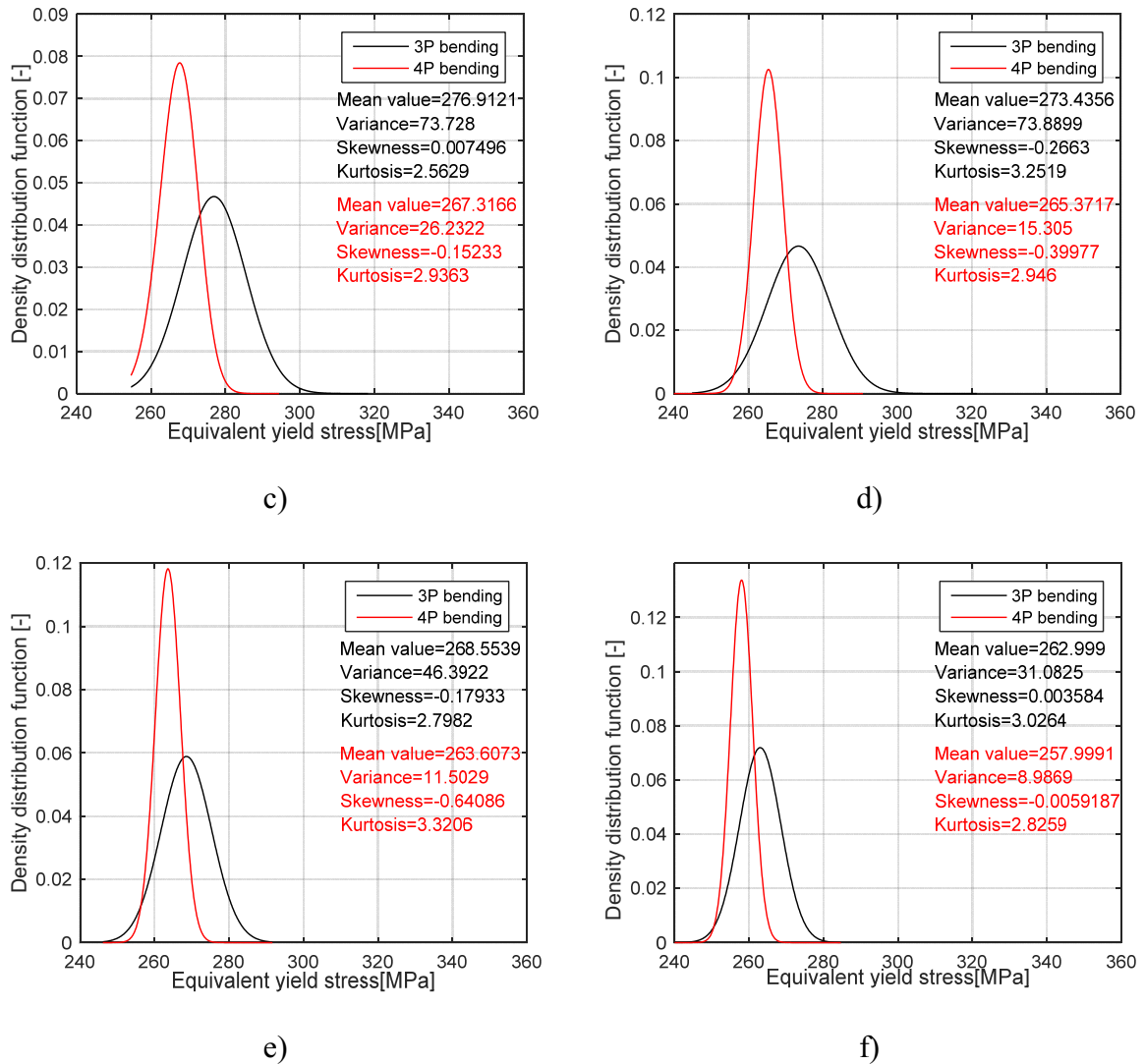


Figure 5.7: Evolution of strength probability density function for 3P and 4P flexural members, a) IPE100, b) IPE200, c) IPE300, d) IPE400, e) IPE500, f) IPE600

5.6 Influence of statistical size effect on the structural safety

For assessing the influence of statistical size effects on structural reliability, the reliability index β was calculated by 10^7 time MCS with IP according to the flowchart in Figure 5.4. Figure 5.8 shows the reliability indices obtained using the proposed method in which the limit state function is defined explicitly using the various probabilistic models of the ultimate strength of the flexural members with increasing sample sizes. The results represent that the influence of sample size on the reliability of the structure is negligible if the number of samples is equal to or greater than 150. Essentially, the sample size changes only the distribution function of the structural response obtained by the maximum entropy fitting method. In the present case, the sample size considered in the MEM has small effect on the calculated reliability index. This trend applies to different types and distribution function of load.

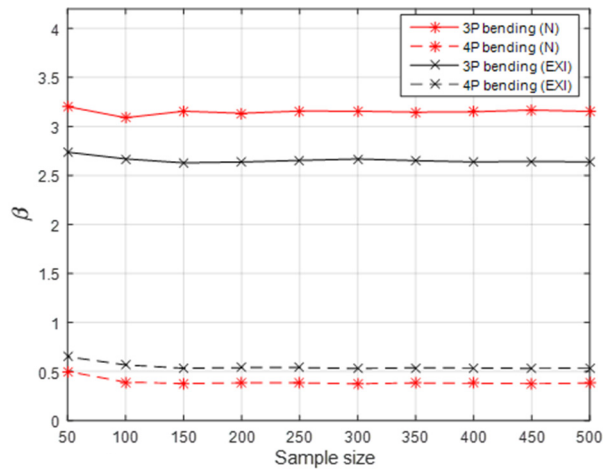


Figure 5.8: Reliability indices with increased sample sizes

Figure 5.9 shows the reliability indices β obtained by MCS with IP for 3P and 4P bending simulation with different specimen volume. The reliability indices of 3P and 4P bending beam have a relatively significant difference even if the structure is applied by the same bending moment. This is due to the statistical size effect caused by different yield volume under the ultimate bearing capacity. The M_l / W_{pl} in abscissa represents equivalent stress of the structure, where M_l is the mean value of the applied moment. For different sizes of beams, the reliability index of the 3P bending beam is always greater than the 4P bending beam with the same M_l / W_{pl} value. The relationship of the reliability index and the volume of structure cannot be simply summarized. For example, in the case of three-point bending the structural reliability index increases with the enlarged volume of the structure, while in the case of four-point bending it decreases. Therefore, the reliability analysis for flexural members considering the statistical size effect needs to be calculated separately for each structure, because the reliability index is significantly influenced by the structural volume and stress gradient of the structure.

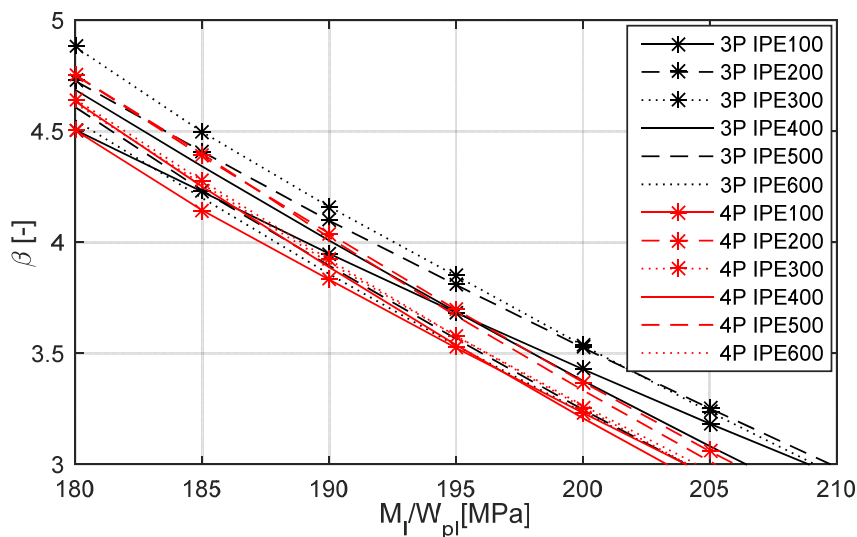
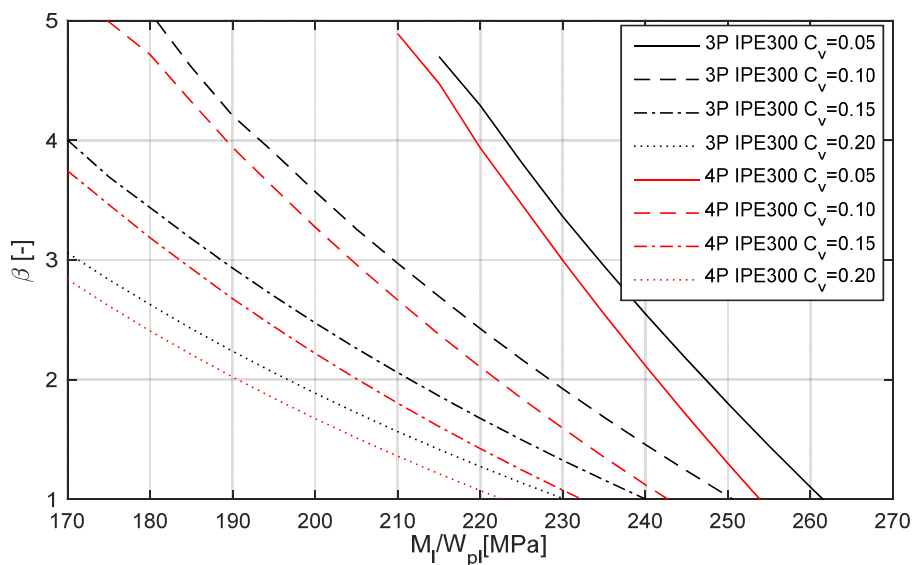


Figure 5.9: Fluctuation of reliability indices considering statistical size effect

In general, there is a pre-defined target reliability index in the design code. Eurocode [118] has defined the target reliability index β for limit state of ultimate in 50 years as 3.8 for Class RC2 of structural members. According to Figure 5.9, the mean value of the allowable stress for 3P bending IPE100 specimen is 195 MPa, but for 4P bending IPE600 beam, it is less or equal to 190 MPa, when target $\beta \leq 3.8$. This means that the yield stress, which is obtained by the experiment with the small specimen in laboratory based on the traditional statistical theory, is no more suitable for large structures. The reliability of structures with relatively large effective volume is smaller than the small structures with the conventional design method, even if the material of the different structure is same.

The reliability of the structure depends not only on the distribution of the resistance but also the statistical distribution of applied load. To demonstrate the effect of the load distribution in the reliability analysis considering the statistical size effect, the reliability assessment was implemented for different distributions of applied load with the various coefficient of variation C_v and distribution types.

The results in Figure 5.10 a) show that the reliability index β of the structure decreases as the coefficient of variation of the applied moment increases. For the same load, the structure with the load obeyed by Weibull distribution always has a lower reliability in Figure 5.10 b). However, the effect of the load distribution on the reliability is not equivalent to the 3P and 4P bending beam with different effective volumes. Therefore, for each structure, the particular applied load are required to be analyzed separately in the study of structural reliability considering the statistical size effect.



a)

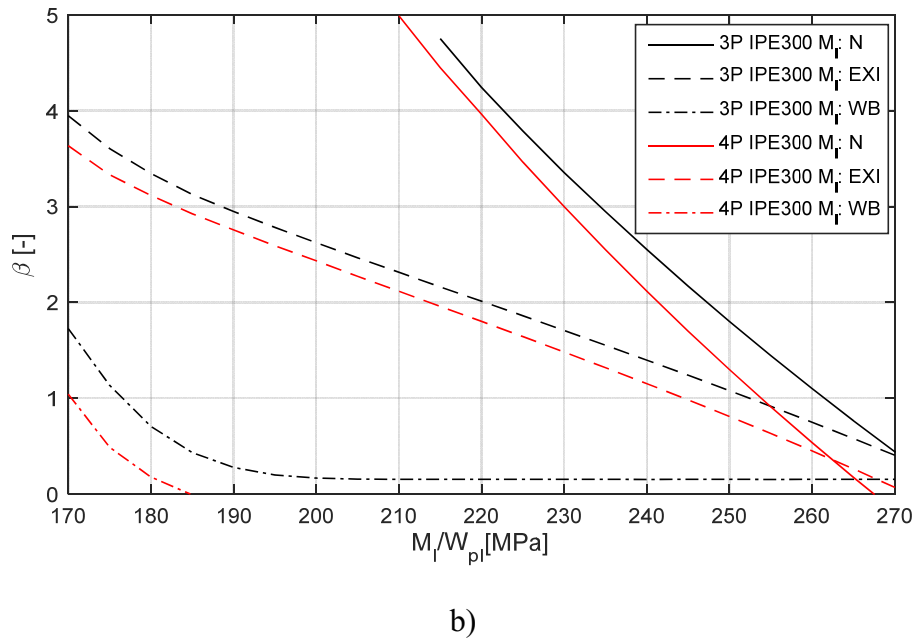


Figure 5.10: Influence of applied load distribution on the reliability analysis considering the statistical size effect, a) coefficient of variation of load distribution, b) distribution types of load

5.7 Conclusions

In this chapter, an approach for structural reliability analysis was proposed considering statistical size effect. This method combined the maximum entropy fitting method for resistance moment of responses and the reliability evaluation. The reliability index was obtained with a small sample by this approach, thereby effectively avoiding the unacceptable computational cost problem caused by the direct Monte Carlo simulation.

Firstly, the maximum entropy fitting method, which is based on information entropy under the constraints supplied by the available information, was briefly introduced. Besides, the fitting of the existing distribution proved that the maximum Entropy fitting method could be employed to obtain the optimal distribution under known information. It can be demonstrated that the maximum Entropy fitting method obtained accurate probabilistic descriptions of the response due to the flexibility of fitting function. Then, the Monte Carlo simulation with the important sampling technique was applied to obtain the structural reliability, since this approach can be achieved the most accurate results through a large number of repeated calculations. Finally, the K-S test was used in all steps of the analysis process that can be improved if necessary by increasing the sample size from the results of stochastic FEM.

The 3- and 4-point bending simulations for the I-section beam considering the statistical size effect are performed in ABAQUS with stochastic FEM and the probability density function of the structural response and corresponding reliability indices β are calculated with the proposed

method. The evolution of strength probability density function was consistent with the description of the stochastic material model. Furthermore, the results of the 3- and 4-point bending simulations show that the reliability index β was changing with the applied load types and the specimen sizes. The maximum allowable stress was different for the various specimens with same target reliability index. This means that the yield strength obtained by the small specimens can lead to a smaller reliability index for a large steel structures.

The proposed approach provides a probabilistic description of the structural responses under considering statistical size effect in an efficient way. Although the proposed approach requires lots of nonlinear numerical analysis, the response modeling employing the maximum entropy fitting method has advantages in versatility as well as universality for probabilistic analysis of complex structures.

6 Overall conclusions

This thesis presents a contribution to investigating the statistical size effect and confirms the existence of this effect in steel made of S235JR and S355J2+N. The main research is studying the influence of material uncertainty on the strength of a structural component under considering different structural volume and stress gradient in steel structures. The stochastic material properties were directly embedded in numerical calculations to account for statistical size effect with two different approaches. The first is to develop the stochastic material model for elasto-plastic material properties by mathematical analysis. The second way is to implement the stochastic FEM with direct Monte Carlo simulation for the steel structures by interactively applying FEM program ABAQUS and mathematical program MATLAB with the random field of nonlinear materials. Besides, the uniaxial tensile tests with different specimen sizes, namely max. specimen diameter up to 32 mm, and different materials confirmed the existence of statistical size effect in steel structures. The results of the 3- and 4-point bending tests demonstrate once again the statistical size effect in flexural members, and it shows that the relationship between the sizes and the specimen strength can be analyzed through the probability and reliability theory. Finally, the investigation clarifies the influence of statistical size effect on structural reliability by the efficient method based on the stochastic FEM for response variability and reliability analysis.

In chapter 2, a treatment of connections between fiber bundle model and Weibull weakest link model was presented. According to the classical material models, the mechanism of statistical size effect of steel structures has been clarified and analytical formulas for the equivalent mean strength and the probability density function of strength have been derived and proposed. This model has two separate scaling structures governing two different statistical distributions of the strength. The proposed stochastic material model provides a potential to study the evolution process of the probability density function of equivalent yield strength over the volume domain. Therefore, this model can theoretically be used in all imperfect materials. By employing the developed model, it requires only one time FEM analysis utilizing the statistical size effect coefficient to obtain the equivalent mean yield strength, so the necessity of time-consuming statistical simulation is avoided. The other achievement is mainly that the proposed model is extended to the multi-axial stress state with the combination of the von Mises yield criterion. Besides, the developed model is integrated into the commercial FEM software ABAQUS by user subroutine and applied to structural components with non-uniform stress distribution.

In chapter 3, the stochastic FEM was implemented and the important achievement is the development of specialized stochastic FEM to analyze the response of the 3D structures in a general purpose simulation software. The discretization of the random field was realized by the Karhunen-Loève expansion with Galerkin finite element techniques. To reduce the computing costs of solving the homogeneous Fredholm integral equation, a 3D eigenfunction problem was decomposed in orthogonal coordinate axes. Afterward, the eigenvalue matrixes of the 3D random field were composed again with the coordinates of elements. In particular, issues on the separation of random field mesh from finite element mesh have been addressed by suggesting a general mapping-interpolation method for stochastic finite element simulation with the 3D random field. Because this method completely separates the two different meshes, different criteria for these two different meshes can flexibly be applied. The proposed approach is not only applied in different criteria for two different meshes, but also could be employed for different element types. According to the error estimation studies, the errors are strongly depended on the Karhunen-Loève expansion. The global error can be reduced as the truncated terms are added. It was found by the interpolation error studies that an unacceptable deviation was not generated by the mapping interpolation method with a coarse mesh of random field and the smaller finite elements. The distortion of the random field from mapping and interpolation can be theoretically avoided. Simultaneously, with the development of computer technology, the stochastic FEM could be applied to treat the complicated problems, in which nonlinear materials are involved in the 3D random field, with the Monte Carlo simulation at the expense of computing resources.

In chapter 4, the experimental investigation was carried out to verify the statistical size effect in steel structures. Besides, the stochastic material model was embedded in the FEM software for comparative analysis of the bending tests. The results shown that the statistical size effect also exists in the flexural members and the equivalent yield stress is closely related to the stress distribution and volume of the structural components. According to the experimental results and simulations with the stochastic material model and stochastic FEM, it is evident that the two proposed simulation methods can efficiently simulate the statistical size effect for the tensile and flexural components in steel structures. For this reason, it is essential to consider the statistical size effect in the structural design, since the distribution and variance of the strength vary with the effective volume of the specimens.

In chapter 5, the influence of statistical size effect on structural reliability was studied. The focus was on the techniques that provide the probabilistic description of response quantities

obtained by the stochastic FEM. After that, it was used in the reliability assessment. This approach was implemented by the combination of the maximum Entropy fitting method for resistance moment of responses and the reliability evaluation. The statistical moments of the response and the reliability index were obtained with small sample size. Besides, this proposed method was applied to obtain the structural response of the 3- and 4-point bending simulations with I-section profile for different specimen sizes. The corresponding results show that the strength, which has been obtained from small specimens through statistical analysis in the laboratory, is no more accurately applicable to large structural components, because the statistical size effect changed the structural safety in the reliability analysis. Simultaneously, the reliability index was closely related to the effective volume and stress gradient of the structures.

The stochastic modeling framework has been used for derivation of the statistical size effect for the considered randomness of material properties in this thesis. The results show that the changing rates and variation coefficients of the strengths decrease with increasing structural component sizes. The statistical distribution of the material strength will be varied due to the change of the coefficient of variation. Therefore, the influence of the statistical size effect on structural safety must be noted by structural engineers. The structural safety and reliability theory which exists over the decades can be compared and validated (or improved) with the simulation by the stochastic FEM with the random fields of material properties and boundary conditions. Moreover, the approach for solving the structural optimization problem, which considers the randomness of material and boundary conditions with finite element analysis, is expected to become a popular research topic for future investigations.

7 Recommendations for future works

This thesis shows that the statistical size effect presents in steel structures due to the uncertain microscopic structure of the material properties. The numerical studies exhibit the great potential of the embedding uncertainty directly into the structural analysis. Furthermore, the influence of statistical size effect on the reliability of the structure is not negligible. Therefore, it is necessary to perform the following studies in the future:

- The statistical size effect in steel structural components requires further verification through experiments with thicker and larger specimens. For example, the tensile tests using a specimen with a diameter up to 100 mm need to be performed and the effect of delamination of a thick steel plate should be excluded.
- The elastic and plastic moments of resistance of steel structures are redefined based on the reliability theory with the stochastic FEM considering the statistical size effect. Such as, the bearing capacity of the existing rolled steel sections could be modified with a reduction factor so that the structural safety factor is guaranteed and consistent.
- The statistical size effects need to be applied to other constructions such as beams, columns and plates of steel structures.
- The influence of the statistical size effect on the structural reliability also needs to be discussed for the different cross-section types and various load types.

Based on the obtained results, the other possible directions of future work are summarized in the following text. According to the studies in this thesis, the statistical size effect caused by the randomness of the yield strength in steel structures can be essentially seen as the evolution of the probability density function of the material strength with different effective volumes. It has been shown that the evolution of probability density function of the material strength influences the maximum bearing capacity and the stress response. The stochastic material model has a great advantage regarding computational efficiency and it also has the potential to consider the evolution of the strength probability density function directly. The future works for the stochastic material model are recommended as following direction. Firstly, the proposed stochastic material model needs to be developed combined with the evolution process of the strength probability density function so that it can be more efficiently used to analyze the statistical size effect in the structural design. Then, the material constants of the stochastic material model need to be accurately measured through more experimental investigation for different materials.

Although the simulation of the random field in 3D was solved and applied to the analysis in steel structures, this discretization is still limited to the research area since the number of the discrete element can only reach 10^5 levels. As the direct stochastic FEM to nonlinear problems with the elasto-plastic material is at the expense of a prohibitive computational cost, the efficient application remains a challenge. The following future works are recommended and indicated. Firstly, the discrete efficiency of the 3D random field needs to be improved with the orthogonal decomposition technique based on the Cartesian coordinate system. Secondly, the stochastic finite element method for the treatment of elasto-plastic materials can be improved by some alternative formulations for stochastic FEM analysis or the more efficient sampling techniques. Then, a user-friendly specialized software has to be developed, and it needs to be able to provide strong interaction with powerful general commercial FEM software, thereby reducing the use threshold of the stochastic FEM for structural engineers. Finally, the parameters of the uncertainty of material properties, such as the correlation length and the statistical distribution parameters, need to be obtained with plenty of numerical simulations based on the structural response inverse analysis or through experiments in the laboratory for different materials.

References

- [1] Deutsche Norm, DIN EN 1993-1-1 Eurocode 3: Design of steel structures- Part 1-1: General rules and rules for buildings, (2010).
- [2] E. Saibel, Size effect in structural safety, in: Mater. Sci. Eng., Southampton, 1969: pp. 125–130.
- [3] C. Petersen, Überlegungen zur Einführung des neuen Sicherheitskonzeptes im Stahlbau, in: Arbeitsberichte zur Sicherheitstheorie der Bauwerke, Munich, 1974: pp. 27–57.
- [4] Q. Yu, Size effect and design safety in concrete structures under shear., Northwestern University, 2007.
- [5] J.L. Le, Size effect on reliability indices and safety factors of quasibrittle structures, Struct. Saf. 52 (2015) 20–28.
- [6] M. Shinozuka, Probabilistic Modeling of Concrete Structures, J. Eng. Mech. Div. Proc. ASCE. 98 (1972) 1433–1451.
- [7] Z.P. Bažant, J. Planas, Fracture and Size Effect in Concrete and other Quasibrittle Materials, CRC press, 1998.
- [8] C. Petersen, Stahlbau-Grundlagern der Berechnung und baulichen Ausbildung von Stahlbauten, 3., überarbeitete und erweiterte Auflage, Vieweg, Munich, 1993.
- [9] P.G. Kossakowski, Microstructural failure criteria for S235JR steel subjected to spatial stress states, Arch. Civ. Mech. Eng. 15 (2015) 195–205.
- [10] Z. Li, H. Pasternak, Development of a stochastic material model at constant stress distribution in steel construction, in: XVI Int. Sci. Conf. VSU, Sofia, 2016: pp. 193–198.
- [11] Z. Li, Statistical size effect in steel structures, in: YOUNG Eng. Colloq., BOCHUM, 2017: pp. 52–53.
- [12] W. Weibull, A Statistical Theory of the Strength of Materials, R. Swedish Inst. Eng. Res. 151 (1939).
- [13] W. Weibull, A Statistical Distribution Function of Wide Applicability, J. Appl. Mech. (1951) 293–297.
- [14] F. Colling, Einfluss des Volumens und der Spannungsverteilung auf die Festigkeit eines Rechtecktraegers, Holz Als Roh- Und Werkst. 44 (1986) 121–125.
- [15] Z.P. Bažant, Y. Xi, S.G. Reid, Statistical size effect in quasi-brittle structures: I. Is Weibull theory applicable?, J. Eng. Mech. 117 (1991) 2609–2622.

- [16] Z.P. Bažant, Y. Xi, Statistical Size Effect in Quasi-Brittle Structures: II. Nonlocal Theory, *J. Eng. Mech.* 117 (1991) 2623–2640.
- [17] Z.P. Bažant, Probability distribution of energetic-statistical size effect in quasibrittle fracture, *Probabilistic Eng. Mech.* 19 (2004) 307–319.
- [18] Z.P. Bažant, N. Drahomír, Probabilistic nonlocal theory for quasibrittle fracture initiation and size effect. I: Theory, *J. Eng. Mech.* 126 (2000) 166–174.
- [19] Z.P. Bažant, Probabilistic modeling of quasibrittle fracture and size effect, in: *Proc., 8th Int. Conf., Struct. Saf. Reliab., Swets & Zeitinger, Newport Beach, 2001*: pp. 1–23.
- [20] Z.P. Bažant, S.D. Pang, M. Vorechovsky, D. Novak, R. Pukl, Statistical size effect in quasibrittle materials: Computation and extreme value theory, *Fract. Mech. Concr. Struct.* 1 (2004) 189–196.
- [21] M. Vorechovsky, Stochastic fracture mechanics and size effect-Doctor thesis, Brno university of technology, 2004.
- [22] R.A. Fisher, L.H.C. Tippett, Limiting forms of the frequency distribution of the largest or smallest member of a sample, *Math. Proc. Cambridge Philos. Soc.* 24 (1928) 180.
- [23] A.M. Freudenthal, E.J. Gumbel, Physical and Statistical Aspects of Fatigue, *Adv. Appl. Mech.* 4 (1956) 117–158.
- [24] H.E. Daniels, The statistical theory of the strength of bundles and threads, *Proc. R. Soc. A Math. Phys. Eng. Sci.* A183 (1945) 405–435.
- [25] S.L. Phoenix, Stochastic strength and fatigue of fiber bundles, *Int. J. Fract.* 14 (1978) 327–344.
- [26] R.L. Smith, The asymptotic distribution of the strength of a series-parallel system with equal load sharing, *Ann. Probab.* 10 (1982) 137–171.
- [27] L.N. McCartney, R.L. Smith, Statistical Theory of the Strength of Fiber Bundles, 50 (1983) 601–608.
- [28] S.L. Phoenix, M. Ibnabdeljalil, C.Y. Hui, Size effects in the distribution for strength of brittle matrix fibrous composites, *International J. Solids Struct.* 34 (1997) 545–568.
- [29] E. Plate, *Statistik und angewandte Wahrscheinlichkeitslehre für Bauingenieure*, Ernst & Sohn, Berlin, 1993.
- [30] E. Vanmarcke, *Random Fields: Analysis and Synthesis*, World Scientific, 2010.
- [31] E.H. Vanmarcke, Probabilistic Modeling of Soil Profiles, *J. Geotech. Eng. Div.* 103 (1977) 1227–1246.

-
- [32] M. Shinozuka, Probabilistic Modeling of Concrete Structures, *J. Eng. Mech. Div.* 98 (1972) 1433–1451.
- [33] L.S. Katafygiotis, A. Zerva, A. A. Malyarenko, Simulation of Homogeneous and Partially Isotropic Random Fields, *J. Eng. Mech.* 125 (1999) 1180–1189.
- [34] C. Schwab, R.A. Todor, Karhunen–Loève approximation of random fields by generalized fast multipole methods, *J. Comput. Phys.* 217 (2006) 100–122.
- [35] S. Sakamoto, R. Ghanem, Simulation of multi-dimensional non-gaussian non-stationary random fields, *Probabilistic Eng. Mech.* 17 (2002) 167–176.
- [36] P. Bocchini, G. Deodatis, Critical review and latest developments of a class of simulation algorithms for strongly non-Gaussian random fields, *Probabilistic Eng. Mech.* 23 (2008) 393–407.
- [37] K.R. Gurley, A. Kareem, M.A. Tognarelli, Simulation of a class of non-normal random processes, *Int. J. Non. Linear. Mech.* 31 (1996) 601–617.
- [38] R. Popescu, G. Deodatis, A. Nobahar, Effects of random heterogeneity of soil properties on bearing capacity, *Probabilistic Eng. Mech.* 20 (2005) 324–341.
- [39] A.D. Kiureghian, J.-B. Ke, The stochastic finite element method in structural reliability, *Probabilistic Eng. Mech.* 3 (1988) 83–91.
- [40] W.K. Liu, T. Belytschko, A. Man, Random Field Finite Elements, *Int. J. Numer. Methods Eng.* 23 (1986) 1831–1845.
- [41] P.D. Spanos, R. Ghanem, Stochastic Finite element Expansion for Random Media, *J. Eng. Mech.* 115 (1989) 1035–1053.
- [42] M. Shinozuka, G. Deodatis, Simulation of stochastic processes by spectral representation, *Appl. Mech. Rev.* 44 (1991) 191–204.
- [43] M. Shinozuka, G. Deodatis, Simulation of multi-dimensional Gaussian stochastic fields by spectral representation, *Appl. Mech. Rev.* 49 (1996) 29–53.
- [44] F. Poirion, B. Puig, A unified approach for generating Gaussian random field simulation methods, in: *Proc. Ninth Int. Conf. Struct. Saf. Reliab.*, Roma, Italy, 2005: pp. 2453–2458.
- [45] B.N. Khoromskij, A. Litvinenko, H.G. Matthies, Application of hierarchical matrices for computing the Karhunen–Loève expansion, *Computing.* 84 (2009) 49–67.
- [46] G. Stefanou, The stochastic finite element method: Past, present and future, *Comput. Methods Appl. Mech. Eng.* 198 (2009) 1031–1051.
- [47] C.J. Astill, S.B. Nossier, M. Shinozuka, Impact Loading on Structures with Random

- Properties, *J. Struct. Mech.* 1 (1972) 63–77.
- [48] M. Shinozuka, E. Lenoé, A probabilistic model for spatial distribution of material properties, *Eng. Fract. Mech.* 8 (1976) 217–227.
- [49] F. Yamazaki, M. Shinozuka, G. Dasgupta, Neumann expansion for stochastic finite element analysis, *J. Eng. Mech.* 114 (1988) 1335–1354.
- [50] G. Stefanou, M. Papadrakakis, Stochastic finite element analysis of shells with combined random material and geometric properties, *Comput. Methods Appl. Mech. Eng.* 193 (2004) 139–160.
- [51] M. Zheng, G. Chen, An efficient 3D stochastic finite element method for failure probability analysis of high temperature components, *Comput. Math. with Appl.* 62 (2011) 333–341.
- [52] M. Kamiński, P. Świta, Structural stability and reliability of the underground steel tanks with the Stochastic Finite Element Method, *Arch. Civ. Mech. Eng.* 15 (2015) 593–602.
- [53] B. Cambou, Application of the first-order uncertainty analysis in the finite element method in linear elasticity, in: *Proc. Second Int. Conf. Appl. Stat. Probab. Soil Struct. Eng.*, 1975: pp. 67–87.
- [54] G.B. Beacher, Thomas S. Ingra, Stochastic FEM in settlement predictions, *J. Geotech. Eng. Div.* 107 (1981) 449–463.
- [55] T. Hisada, S. Nakagiri, Stochastic finite element method developed for structural safety and reliability, in: *Third Int. Conf. Struct. Saf. Reliab.*, 1981: pp. 395–408.
- [56] R.G. Ghanem, P.D. Spanos, *Stochastic Finite Elements: A Spectral Approach*, Springer-Verlag, New York, 1991.
- [57] L. Huyse, M.A. Maes, Random Field Modeling of Elastic Properties Using Homogenization, *J. Eng. Mech.* 2 (2001) 27–36.
- [58] S. Shang, G.J. Yun, Stochastic finite element with material uncertainties: Implementation in a general purpose simulation program, *Finite Elem. Anal. Des.* 64 (2013) 65–78.
- [59] M. Anders, M. Hori, Stochastic finite element method for elasto-plastic body, *Int. J. Numer. Methods Eng.* 1916 (1999) 1897–1916.
- [60] M. Anders, M. Hori, Three-dimensional stochastic finite element method for elasto-plastic bodies, *Int. J. Numer. Methods Eng.* 51 (2001) 449–478.
- [61] C. Methods, A. Mech, K. Sett, B. Jeremic, Stochastic elastic – plastic finite elements,

- Comput. Methods Appl. Mech. Eng. 200 (2011) 997–1007.
- [62] K. Karapiperis, K. Sett, M.L. Kavvas, B. Jeremi, Direct Fokker – Planck linearization for non-Gaussian stochastic elastoplastic finite elements, *Comput. Methods Appl. Mech. Eng.* 307 (2016) 451–469.
- [63] B. V. Rosic, H.G. Matthies, Stochastic Galerkin Method for the Elastoplasticity Problem with Uncertain Parameters, *Recent Dev. Innov. Appl. Comput. Mech.* (2011) 303–310.
- [64] M.F. Pellissetti, G.I. Schuëller, On general purpose software in structural reliability - An overview, *Struct. Saf.* 28 (2006) 3–16.
- [65] A.H.-S. Ang, C.A. Cornell, Reliability Bases of Structural Safety and Design, *J. Struct. Div.* 100 (1974) 1755–1769.
- [66] Deutsche Norm, Eurocode: Basis of structural design, (2010).
- [67] Y. Ciupack, H. Pasternak, Kalibrierung von Bemessungskonzepten gemäß Eurocode am Beispiel von Klebverbindungen, *Bauingenieur.* 87 (2012) 116–123.
- [68] M. Ouyang, L. Dueñas-osorio, X. Min, A three-stage resilience analysis framework for urban infrastructure systems, *Struct. Saf.* 36–37 (2012) 23–31.
- [69] M. Loebjinski, W. Rug, H. Pasternak, Zuverlässigkeitsbewertung von Holzbauteilen im Bestand, *Bauingenieur.* 92 (2017) 65–73.
- [70] M. Ghosn, M. Asce, D.M. Frangopol, D.M. Asce, T.P. Mcallister, M. Asce, M. Shah, F. Asce, S.M.C. Diniz, M. Asce, B.R. Ellingwood, D.M. Asce, L. Manuel, M. Asce, F. Biondini, M. Asce, N. Catbas, F. Asce, A. Strauss, M. Asce, X.L. Zhao, F. Asce, Reliability-Based Performance Indicators for Structural Members, *J. Struct. Eng.* 142 (2016) 1–13.
- [71] H. Pasternak, B. Launert, T. Kannengießer, M. Rhode, Advanced Residual Stress Assessment of Plate Girders Through Welding Simulation, *Procedia Eng.* 172 (2017) 23–30.
- [72] P.E. Hess, D. Bruchman, I.A. Assakkaf, B.M. Ayyub, Uncertainties in Material Strength , Geometric , and Load Variables, *Nav. Eng. J.* 114 (2002) 139–166.
- [73] E.T. Jaynes, Information Theory and Statistical Mechanics, *Phys. Rev.* 106 (1957) 620–630.
- [74] M.D. Pandey, Direct estimation of quantile functions using the maximum entropy principle, *Struct. Saf.* 22 (2000) 61–79.
- [75] E. V. Volpe, D. Baganoff, Maximum entropy pdfs and the moment problem under near-

- Gaussian conditions, *Probabilistic Eng. Mech.* 18 (2003) 17–29.
- [76] J. Ching, Y. Hsieh, Local estimation of failure probability function and its confidence interval with maximum entropy principle, *Probabilistic Eng. Mech.* 22 (2007) 39–49.
- [77] J. Deng, M.D. Pandey, Estimation of minimum cross-entropy quantile function using fractional probability weighted moments, *Probabilistic Eng. Mech.* 24 (2009) 43–50.
- [78] S. Lee, I. Vonta, A. Karagrigoriou, A maximum entropy type test of fit, *Comput. Stat. Data Anal.* 55 (2011) 2635–2643.
- [79] D.W. Liu, G. Soares, Return Value Estimation of Significant Wave Heights With Maximum Entropy Distribution, *J. Offshore Mech. Arct. Eng.* 135 (2013). doi:10.1115/1.4023248.
- [80] X. Shi, A.P. Teixeira, J. Zhang, C.G. Soares, Structural reliability analysis based on probabilistic response modelling using the Maximum Entropy Method, *Eng. Struct.* 70 (2014) 106–116.
- [81] K.H. Thoma, *Stochastische Betrachtung von Modellen für vorgespannte Zuelemente*, Eidgenössische Technische Hochschule Zürich, 2004.
- [82] M. Hohenbichler, R. Rackwitz, Reliability of Parallel Systems under Imposed Uniform Strain, *J. Eng. Mech.* 109 (1983) 896–907.
- [83] Z.P. Bažant, S.-D. Pang, Activation energy based extreme value statistics and size effect in brittle and quasibrittle fracture, *J. Mech. Phys. Solids.* 55 (2007) 91–131.
- [84] A.H.-S. Ang, W.H. Tang, *Probability concepts in engineering planning and design*, Wiley, New York, 1990.
- [85] R. V. Mises, *Mechanik der festen Körper im plastisch deformablen Zustand*, *Nachrichten von Der Gesellschaft Der Wissenschaften Zu Göttingen, Math. Klasse.* (1913) 582–592.
- [86] G. Wilhelm, *PC-Fotran Handbuch*, Carl Hanser Verlag, München, 1988.
- [87] H.R. Schwarz, N. Köckler, *Numerische Mathematik*, Vieweg+ Teubner Verlag, 2011.
- [88] W.H. Press, S.A. Teukolsky, W.T. Vetterling, B.P. Flannery, *Numerical Recipe-The Art of Scientific Computing*, Cambridge University Press, Cambridge, 2007.
- [89] W. Betz, I. Papaioannou, D. Straub, Numerical methods for the discretization of random fields by means of the Karhunen–Loève expansion, *Comput. Methods Appl. Mech. Eng.* 271 (2014) 109–129.
- [90] B. Sudret, A.D. Kiureghian, *Stochastic Finite Element Methods and Reliability: A State-of-the-Art Report*, 2000.

- [91] C.-C. Li, A.D. Kiureghian, Optimal Discretization of Random Fields, *J. Eng. Mech.* 119 (1993) 1136–1154.
- [92] M. Grigoriu, Crossings of non-gaussian translation processes, *J. Eng. Mech.* 110 (1984) 610–620.
- [93] A.D. Kiureghian, P.-L. Liu, Structural Reliability under Incomplete Probability Information, *J. Eng. Mech.* 112 (1986) 85–104.
- [94] K.K. Phoon, Reliability-based design in geotechnical engineering - Computation and applications, 2008.
- [95] J. Zhang, B. Ellingwood, Orthogonal Series Expansions of Random Fields in Reliability Analysis, *J. Eng. Mech.* 120 (1994) 2660–2677.
- [96] O.C. Zienkiewicz, R.L. Taylor, *The Finite Element Method Volume 1 : The Basis*, Butterworth-Heinemann, Oxford, 2000.
- [97] D.E. Huntington, C.S. Lyrintzist, Improvements to and limitations of Latin hypercube sampling, *Prob. Engng. Mech.* 13 (1998) 245–253.
- [98] M. Vořechovský, D. Novák, Simulation of random fields for stochastic finite element analysis, *Icosar 2005*. (2005) 2545–2552.
- [99] D.L. Allaix, V.I. Carbone, Discretization of 2D random fields: A genetic algorithm approach, *Eng. Struct.* 31 (2009) 1111–1119.
- [100] Y. Perl, A. Itai, H. Avni, Interpolation Search A Log LogN Search, *Commun. ACM.* 21 (1978) 550–553.
- [101] M.R. Rajashekhar, B.R. Ellingwood, A new look at the response surface approach, *Struct. Saf.* 12 (1993) 205–220.
- [102] S. Jiang, D. Li, C. Zhou, L. Zhang, Capabilities of stochastic response surface method and response surface method in reliability analysis, 49 (2014) 111–128.
- [103] G.I. Schuëller, Developments in stochastic structural mechanics, *Arch. Appl. Mech.* 75 (2006) 755–773.
- [104] Deutsche Norm, DIN 50125: Testing of metallic materials – Tensile test pieces, (2009).
- [105] Deutsche Norm, DIN EN ISO 6892-1: Metallic materials – Tensile testing – Part 1: Method of test at room temperature, (2009).
- [106] W. Urban, Über des Verhalten eines Trägers mit I-Profil im plastischen Bereich unter Berücksichtigung der Eigenspannungen und der unterschiedlichen Fließgrenze nach Theorie und Versuch, TU Berlin, 1974.

- [107] Joint Committee on Structural Safety, Probabilistic Model Code, PART III - Resistance models, Static Properties of Structural Steel, 2001.
- [108] C. Petersen, Stahlbau-Grundlagen der Berechnung und baulichen Ausbildung von Stahlbauten-4., vollständig überarbeitete und aktualisierte Auflage, Springer Vieweg, München, 2013.
- [109] J. Scheer, H. Nölke, Anmerkungen zur Fließgelenk- Rotation in Stabtragwerken, Stahlbau. 72 (2003) 517–526.
- [110] C.E. Shannon, A Mathematical Theory of Communication, Bell Syst. Tech. J. 27 (1948) 379–423.
- [111] A. Mohammad-Djafari, A Matlab Program to Calculate the Maximum Entropy Distributions, Maximum Entropy and Bayesian Methods. 221 (1992) 221–33.
- [112] A.L. Berger, S.A. Della Pietra, V.J. Della Pietra, A Maximum Entropy Approach to Natural Language Processing, Comput Linguist 1996;22(1)39–71. 22 (1996) 39–71.
- [113] R.V. Abramov, An improved algorithm for the multidimensional moment-constrained maximum entropy problem, J. Comput. Phys. 226 (2007) 621–644.
- [114] O. Ditlevsen, H.O. Madsen, Structural Reliability Methods, Chichester, 2007.
- [115] C.A. Cornell, A Probability-Based Structural Code, J. Proc. 66 (1969) 974–985.
- [116] A.D. Kiureghian, M. Asce, H. Lin, S. Hwang, Second-order reliability approximations, J. Eng. Mech. 113 (1987) 1208–1225.
- [117] K. Breitung, Asymptotic approximations for probability integrals, Probabilistic Eng. Mech. 4 (1989) 187–190.
- [118] British Standard, BS EN 1990 Eurocode — Basis of structural design, (2002).